WORKSHOP ON EVOLUTION OF IGNEOUS ASTEROIDS: FOCUS ON VESTA AND THE HED METEORITES

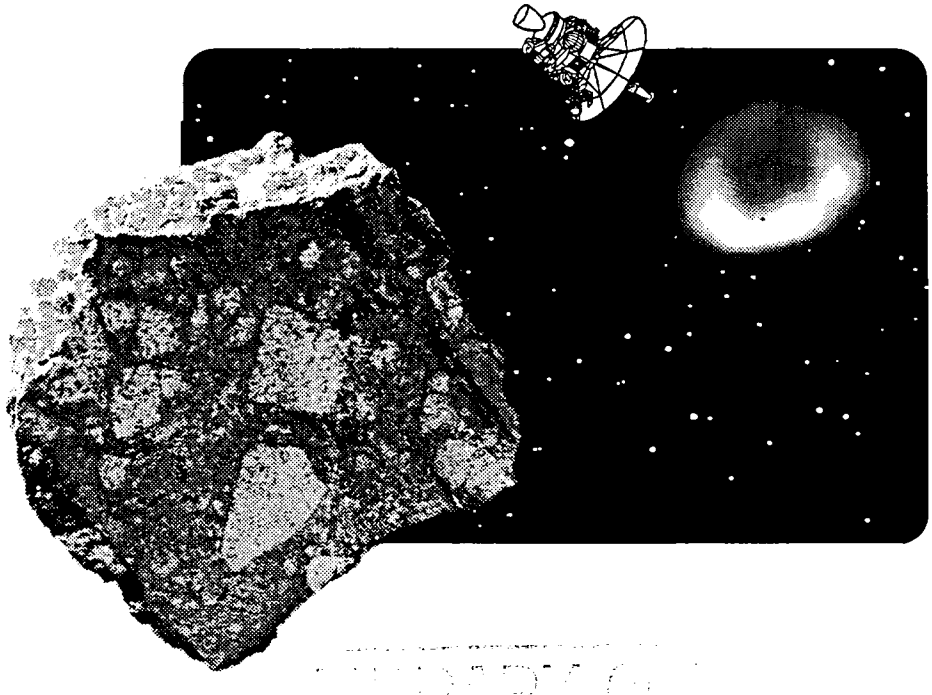

LPI Technical Report Number 96-02, Part 1

Lunar and Planetary Institute 3600 Bay Area Boulevard Houston TX 77058-1113
LPI/TR--96-02, Part 1

ENTER:

DISPLAY 97N25363/2

97N25363*# ISSUE 1 CATEGORY 90

RPT#: NASA-CR-204832 NAS 1.26:204832 LPI-96-02, PART 1 NIPS-97-32331

CNT#: NASW-4574 96/01/01 52 PAGES UNCLASSIFIED DOCUMENT

UTTL: Workshop on Evolution of Igneous Asteroids: Focus on Vesta and the HED Meteorites

AUTH: A/MITTLEFEHLDT, D. W.; B/PAPIKE, J. J. PAT: A/ed.; B/ed.

CORP: Lunar and Planetary Inst., Houston, TX.

SAP: Avail: CASI HC A04/MF A01; Abstract Only

CIO: UNITED STATES Presented at Workshop on Igneous Asteroids, Houston, TX, United States, 16-18 Oct. 1996; Sponsored by Lunar and Planetary Inst.,

MAJS: /*ASTEROIDS/*ASTRONOMY/*CONFERENCES/*GEOLOGICAL SURVEYS/*MAPPING/* SPECTROSCOPY/*VESTA ASTEROID

MINS: / COLLISIONS/ HEATING/ HUBBLE SPACE TELESCOPE/ METEORITES/ MINERALOGY/ RADIOACTIVE ISOTOPES/ SPACE MISSIONS

ABA: Derived from text

19970025927

ABS: This volume contains papers that have been accepted for presentation at the Workshop. Topics considered include: On the sample return from Vesta by low-thrust spacecraft; Astronomical evidence linking Vesta to the HED meteorites; Geologic mapping of Vesta with the Hubble Space Telescope; A space mission to Vesta; Asteroid spectroscopy; The thermal history of asteroid 4 Vesta, based on radionuclide and collision heating; Mineralogical records of early planetary processes on Vesta.

ENTER:

WORKSHOP ON

EVOLUTION OF IGNEOUS ASTEROIDS: FOCUS ON VESTA AND THE HED METEORITES

Edited by

D. W. Mittlefehldt and J. J. Papike

Held at
Houston, Texas

October 16–18, 1996

Sponsored by
Lunar and Planetary Institute

Lunar and Planetary Institute 3600 Bay Area Boulevard Houston TX 77058-1113

LPI Technical Report Number 96-02, Part 1
LPI/TR--96-02, Part 1

Compiled in 1996 by
LUNAR AND PLANETARY INSTITUTE

The Institute is operated by the Universities Space Research Association under Contract No. NASW-4574 with the National Aeronautics and Space Administration.

This report may be cited as

Mittlefehldt D. W. and Papike J. J., eds. (1996) *Workshop on Igneous Asteroids: Focus on Vesta and the HED Meteorites*. LPI Tech. Rpt. 96-02, Part 1, Lunar and Planetary Institute, Houston. 44 pp.

This report is distributed by

ORDER DEPARTMENT
Lunar and Planetary Institute
3600 Bay Area Boulevard
Houston TX 77058-1113

Mail order requestors will be invoiced for the cost of shipping and handling.

Preface

This volume contains papers that have been accepted for presentation at the Workshop on Evolution of Igneous Asteroids: Focus on Vesta and the HED Meteorites, October 16–18, 1996, in Houston, Texas. The organizers for this workshop were David Mittlefehldt from NASA Johnson Space Center, and James Papike from the University of New Mexico.

Logistics and administrative and publications support were provided by the Publications and Program Services Department staff at the Lunar and Planetary Institute.

Contents

Abstracts

ON THE SAMPLE RETURN FROM VESTA BY LOW-THRUST SPACECRAFT. R. Z. Akhmetshin, T. M. Eneev, and G. B. Efimov, Keldysh Institute of Applied Mathematics, Miuskaya Street 4, Moscow 125047, Russia.

It is well known that there would be tremendous scientific value in a sample-return mission to a main-belt asteroid such as Vesta. The sample return from Vesta by traditional high-thrust vehicles is impossible at the present time. Combining high- and low-thrust propulsion (electric propulsion with energy supply by solar arrays) would permit the solution of this problem. At first, the spacecraft would be boosted by the high-thrust engine to the hyperbolic velocity. The rendezvous with the asteroid would then be performed using the low-thrust engine. Flight time to asteroids such as Vesta or Fortune is 2–3 yr. The resulting payload would prove sufficient to solve the problem of the sample return (depending essentially on the parameters of the rocket and the space systems).

After the rendezvous with the asteroid, in the case of return with the high-thrust engine, the landing module could land on the asteroid and then return to Earth. In the case of the low-thrust return, the distant sample grab is used. The hyperbolic velocity surplus of returning capsules can be diminished by means of an appropriate entrance into the Earth's atmosphere.

If the Soyuz rocket is used, the payload mass near Vesta is equal to 700 kg (except EP and solar array mass). In this case the return with high thrust is possible. For a conversional rocket, there would be 400 kg of payload mass. This would allow landing of the scientific apparatus on the surface or to make a distant grab, with its low thrust returning to the Earth.

The total expedition time depends on the combination of dates of the rendezvous with the asteroid and the return to Earth, and would be 4–5 yr for an asteroid such as Vesta. These mission variants suppose use of the new technology, in large part tested during flight, such as EP SPT, ESA-XX, "Super ULP" solar arrays, etc.

VESTA: THE BIG QUESTIONS. J. F. Bell, Hawai'i Institute of Geophysics and Planetology, University of Hawai'i at Mānoa, 2525 Correa Road, Honolulu HI 96822, USA.

Is Vesta Unique? There is no doubt that Vesta is unique today as the sole *intact* asteroid that has undergone complete planetary-style differentiation—all other basaltic (class V) asteroids can be explained as ejected fragments of Vesta's crust. However, its uniqueness may be limited to having escaped catastrophic removal of its outer crust by major impacts. There are three other classes of asteroids that might represent objects with similar igneous histories that have undergone more extensive collisional evolution. Several dunite (class A) asteroids could represent mantle fragments from large vestoids now disrupted, or smaller ones with crusts eroded away and cores still concealed within. Some metal (class M) asteroids probably are surviving cores of vestoids from which both cores and mantles have been eroded. 16 Psyche is a good candidate for a surviving core of a near-twin to Vesta. However, many other supposed M asteroids may be hydrated clay-rich objects not related to igneous processes. Finally, 349 Dembowska (class R) is a doubtful case. It has a peridotite-like composition that could represent either a vestoid that has been stripped down to the upper mantle, or less complete differentiation.

At a guess, there may survive large fragments of 6–12 proto-asteroids that looked more or less like the modern Vesta after igneous differentiation. It is possible that others may have been completely reduced to subkilometer fragments (e.g., magmatic iron meteorites) or may have even completely vanished. Vesta is really a "living fossil," giving us a valuable glimpse of a very ancient type of surface that has otherwise vanished from the solar system.

Is Vesta Typical? Inherent in the title of this workshop is the concept that one learns something in general about the evolution of igneous asteroids from Vesta and the HED meteorites. Actually, the howardite clan represents an extreme end member of igneous activity in meteorites. Most melted meteorites (nonmagmatic irons, silicate-rich irons, stony-irons, primitive achondrites) represent less-extreme cases of melting and segregation of components. These meteorites probably come from the more common class-S asteroids that dominate the inner, igneously evolved part of the asteroid belt, and that probably never had the distinct core/mantle/crust structure we see in Vesta. The large number of surviving S asteroids relative to the possible surviving vestoids listed above suggests that Vesta-like total differentiation was relatively rare in the asteroid belt. Meteoritical evidence is consistent with this picture, although confused by a large number of irons that do not fall into recognized Ga-Ge groups.

Is the Vesta Family Unique? Another feature of Vesta commonly considered unique is the large family of small basaltic asteroids extending from Vesta to the 3:1 resonant zone. This discovery solves the classical problem of how the HED meteorites are transported to Earth, but raises more problems. Direct injection of these objects into their present orbits would require large ejection velocities, previously thought impossible. All other well-defined families are much more concentrated in orbital element space. (Indeed, dynamical workers who originally identified the Vesta family gave it a much smaller extent than that later discovered by spectroscopy.) Special circumstances such as antipodal spalling or highly oblique impacts have been invoked to explain this family as yet another unique, freakish event in Vesta's history. If these interpretations are correct, the delivery of the HED meteorites to Earth from an "inaccessible" region of the belt is a rare event, and the classical picture in which most meteorites come from narrow resonance zones remains essentially intact. However, another interpretation is possible. The traditional dynamical families are examples of complete collisional disruption of parent asteroids, whereas the Vesta family was formed in a cratering event in which the target remained essentially intact. Dynamicists have generally not considered such conditions in their models. Furthermore, spectroscopic surveys would probably not have detected other such families. Class V asteroids have a distinctive spectral signature in the visible that stands out from the background population, but most similar families would consist of S or C objects that would be lost in the clutter of many unrelated S and C asteroids. With current information, it is not possible to rule out the possibility that high-velocity ejection of fragments is common in asteroid collisions. If so, the entire asteroid

belt is communicating with Earth, rather than a few narrow zones—and much of the conventional wisdom is wrong.

Should We Visit Vesta? A variety of spacecraft missions to Vesta have been proposed in the past, and this object will undoubtedly remain a seductive candidate for Discovery-class missions. Arguments in favor of Vesta include its large size, its unambiguous association with a well-studied meteorite class, and known complex mineralogical variations on its surface (which probably could be easily correlated with the various components of howardites). Indeed, one can argue that Vesta is a uniquely satisfying candidate for a remote-sensing asteroid mission, since the results would be far more understandable than the ambiguous results obtained to date from the Galileo observations of the class-S asteroids Gaspra and Ida. However, all these arguments boil down to the fact that we already understand Vesta so well that we can accurately predict the results of a mission. In terms of the huge variation in current properties and past history represented in the asteroid/meteorite complex, Vesta and the HEDs are the most conventional and Earth-like of all. At our current state of understanding, it appears more sensible to send the first asteroid missions to those classes of objects that are still truly mysterious, rather than the fifth terrestrial planet.

ASTRONOMICAL EVIDENCE LINKING VESTA TO THE HED METEORITES: A REVIEW.

R. P. Binzel, Department of Earth, Atmospheric, and Planetary Sciences, Massachusetts Institute of Technology, Cambridge MA 02139, USA.

While the reflectance spectrum of Vesta has been known to match that of HED meteorites since the 1970s [1], establishment of a definitive link has long been the subject of debate [2,3]. The principal obstacles have been establishment of the dynamical mechanisms by which (1) substantial material can be excavated from the surface of Vesta in light of its 360 m/s escape velocity, and (2) dispersal of Vesta material from its orbital location to dynamical escape hatches capable of delivery to the inner solar system (such as the 3:1 and ν_6 resonances). Required ejection velocities from Vesta to the resonances are on the order of 1000 m/s.

Recent astronomical measurements [4] have shown evidence that appears to overcome the dynamical obstacles. More than 20 small asteroids (5–10-km diameters) having Vesta-like spectroscopic properties have been found in the vicinity of Vesta. Such main-belt asteroids having Vesta-like spectral properties have been found only in the vicinity of Vesta, despite thorough sampling [5]. The orbital distribution of these Vesta-like objects is consistent with their being ejected from Vesta through one or more major impacts. Hubble Space Telescope images of Vesta confirm the presence of a probable large impact basin [6]. Perhaps most importantly, the distribution of the main-belt Vesta-like asteroids extends from Vesta to the 3:1 (and possibly ν_6) resonances, thus demonstrating a dynamically viable route for samples from Vesta to reach the inner solar system and the Earth as meteorites. While the new astronomical evidence appears to demonstrate that Vesta *can* supply the HED meteorites, it naturally does not prove such a link. Current limitations for the model will also be discussed.

References: [1] McCord T. B. et al. (1970) *Science, 168*, 1445. [2] Consolmagno G. J. and Drake M. J. (1977) *GCA, 41*, 1271. [3] Wetherill G. W. (1987) *Philos. Trans. R. Soc. London, A323*, 323. [4] Binzel R. P. and Xu S. (1993) *Science, 260*, 1–36. [5] Xu S. et al. (1995) *Icarus, 115*, 1. [6] Binzel R. P. et al. (1996) *Icarus*, submitted.

GEOLOGIC MAPPING OF VESTA WITH THE HUBBLE SPACE TELESCOPE.

R. P. Binzel[1], M. J. Gaffey[2], P. C. Thomas[3], B. H. Zellner[4], A. D. Storrs[5], and E. N. Wells[6], [1]Department of Earth, Atmospheric, and Planetary Sciences, Massachusetts Institute of Technology, Cambridge MA 02139, USA, [2]Department of Earth and Environmental Sciences, Rensselaer Polytechnic Institute, Troy NY 12181, USA, [3]Center for Radiophysics and Space Research, Cornell University, Ithaca NY 14853, USA, [4]Department of Physics, Georgia Southern University, Statesboro GA 30460, USA, [5]Space Telescope Science Institute, 3700 San Martin Drive, Baltimore MD 21218, USA, [6]Astronomy Programs, Computer Sciences Corporation, Space Telescope Science Institute, 3700 San Martin Drive, Baltimore MD 21218, USA.

The Wide Field Planetary Camera (WFPC2) and Hubble Space Telescope (HST) are outstanding tools for obtaining resolved images of the surface of Vesta at multiple wavelengths. We have used WFPC2 and HST to obtain rotationally resolved images of Vesta during its 1994 and 1996 apparitions [1–3]. From multiple-filter imaging we have constructed geologic maps of Vesta's surface. We find Vesta to be geologically diverse and dichotomous at hemispheric scales. We find the eastern hemisphere to be dominated by units interpreted to be impact excavated plutonic material composed of Mg-rich and Ca-rich pyroxene. The mineralogy of this region appears to be most analogous to diogenite meteorites. Eastern hemisphere units that have the deepest and broadest 1-μm absorption bands may contain a substantial olivine component. The locations of these units are consistent with previous maps based on rotationally resolved groundbased spectroscopy [4]. We find that the western hemisphere is dominated by units interpreted to consist of a single component of Mg-rich pyroxene, analogous to surface basalts such as eucrite meteorites. In investigating the spectral properties of various surface regions, we find a correlation between the 1-μm absorption band depth and albedo, where the units with lower albedos have shallower band depths. Our interpretation is that such a relationship could arise from differences in lithologies, differences in surface particle sizes, or from a weathering effect that decreases albedo and band depth over time. In examining Vesta's geologic diversity and hemispheric dichotomy, it is apparent that any major impact events, such as those possibly related to the formation of the Vesta family [5], did not globally resurface the planet. Units that appear to be remnants of a basaltic crust most likely date back to the time of their emplacement, ~4.5 b.y. ago. If a weathering process exists that alters the albedo, then the lowest-albedo units such as the feature with the proposed name "Olbers" most likely represent the oldest remnants of Vesta's original basaltic crust.

References: [1] Zellner B. et al. (1996) *Icarus*, submitted. [2] Thomas P. C. et al. (1996) *Icarus*, submitted. [3] Binzel R. P. et al. (1996) *Icarus*, submitted. [4] Gaffey M. J. (1996) *Icarus*, in press. [5] Binzel R. P. and Xu S. (1993) *Science, 260*, 186–191.

EARLY ENERGETIC PARTICLE IRRADIATION OF THE HED PARENT BODY REGOLITH.

D. D. Bogard[1], D. H.

Garrison[1,2], and M. N. Rao[1,3], [1]Mail Code SN4, NASA Johnson Space Center, Houston TX 77058, USA, [2]Lockheed Martin Engineering and Space Sciences, Houston TX 77058, USA, [3]Chemistry Department, Texas A&M University, College Station TX 77843, USA.

Early Work: Previous studies have shown that many individual grains within the dark phase of the Kapoeta howardite were irradiated with energetic particles while residing on the surface of the early HED regolith. Particle tracks in these grains vary in density by more than an order of magnitude and undoubtedly were formed by energetic heavy (~Fe) ions associated with early solar flares [1–3]. Many grains in Kapoeta's dark phase also contain excess cosmogenic Ne produced in the early parent body regolith [4,5], whereas the light phase contains neither solar particle tracks nor excess Ne. Neon present in the light phase was entirely formed by galactic protons during the ~3-m.y. recent space exposure of the Kapoeta meteorite. Excess Ne in the dark phase represents early production within the HED regolith by either galactic (GCR) protons or energetic (>10 MeV/nucleon) solar flare protons. Given the recent flux of solar protons, however, it would require ~200 m.y. or longer to make the excess ^{21}Ne observed in highly-solar-irradiated grains of Kapoeta [4,5]. Some authors concluded that the excess Ne was made by a much higher flux (compared to the recent past) of energetic protons from the early Sun [4,5]. This explanation also has been invoked for excess Ne observed in solar-irradiated grains of some carbonaceous chondrites [6]. On the other hand, other workers [7] have argued that the excess ^{21}Ne in the dark phase of some meteorites, possibly including Kapoeta, could have been produced by an early GCR irradiation of the parent body regoliths for time periods of no more than ~10–20 m.y., and that solar-produced, or SCR, Ne was not required.

Early Irradiation of HED Regolith: Concentrations of excess Ne alone are not sufficient to decide between competing galactic and solar irradiation models. However, from recent studies of depth samples of oriented lunar rocks, we have shown that the cosmogenic ^{21}Ne/^{22}Ne ratio produced in feldspar differs substantially between GCR and solar protons, and that this difference is exactly that predicted from cross-section data [8]. Using Ne literature data and new isotopic data we obtained on acid-etched, separated feldspar from both the light and dark phases of Kapoeta, we derive ^{21}Ne/^{22}Ne = 0.80 for the recent GCR irradiation and ^{21}Ne/^{22}Ne = 0.68 for the early (precompaction) regolith irradiation. This derived ratio indicates that the early Ne production in the regolith occurred by both galactic and solar protons. If we adopt a likely one-component regolith model in which all grains were exposed to galactic protons but individual grains had variable exposure to solar protons, we estimate that this early GCR irradiation lasted for ~3–6 m.y. More complex two-component regolith models involving separate solar and galactic irradiation would permit this GCR age to be longer. Higher-energy solar protons would permit the GCR age to be shorter. Further, cosmogenic ^{126}Xe in Kapoeta dark is no more than a factor of ~2 higher than that observed in Kapoeta light. Because ^{126}Xe can only be formed by galactic protons and not solar protons, these data support a short GCR irradiation for the HED regolith. This would also be the maximum time period for the solar irradiation. Various asteroidal regolith models, based on Monte Carlo modeling of impact rates as a function of size and on irradiation features of meteorites, predict surface exposure times of ~0.1–10 m.y., and depend on such factors as gravity, rock mechanical properties, and micrometeoroid flux [2,7,9]. Because the depth at which solar Fe tracks are produced ($\ll$1 mm) is much less than the depth at which SCR Ne is produced (~1 cm), for a reasonably well-stirred HED regolith [1] the "surface exposure time" for SCR ^{21}Ne production should be significantly longer than that for solar tracks and some other surface irradiation features.

Enhanced Solar Proton Irradiation: For bulk samples of Kapoeta dark feldspar and a one-component regolith model, the derived ratio of ^{21}Ne/^{22}Ne = 0.68 implies that the early production ratio of SCR ^{21}Ne to GCR ^{21}Ne was ~0.5–1.5. This ratio is independent of any assumptions about the fraction of dark grains that are irradiated or of the variability in the degree of solar irradiation among grains. The ^{21}Ne SCR/GCR ratio indirectly derived from bulk Kapoeta pyroxene is somewhat larger, as is the ratio derived for simple two-component regolith models. Individual feldspar grains that were extensively solar irradiated [4,5] would require even larger ^{21}Ne SCR/GCR production ratios. In contrast, the theoretical SCR/GCR production ratio for lunar feldspar with 0 g/cm^2 shielding is $\leq$2, and the lowest ratio observed in near-surface samples of lunar anorthosites is $\leq$1. Considering the greater solar distance of Vesta (compared to the Moon), the likelihood that SCR ^{21}Ne was acquired under some shielding where production rates are lower, and the likelihood that the exposure time to galactic protons exceeded the exposure time to solar protons because of their very different penetration depths, the ^{21}Ne SCR/GCR production ratio on the HED parent body was probably <0.1. The relatively large difference between the derived ^{21}Ne SCR/GCR ratio in Kapoeta dark feldspar and the estimated production ratio strongly indicates that the early solar irradiation involved a flux ~20–50× the recent solar flux. This enhanced proton flux was probably associated with an overall greater solar activity in the first ~10^7–10^8 yr of solar history.

References: [1] Rajan S. (1974) *GCA, 38*, 777–788. [2] Goswami J. N. et al. (1984) *Space Sci. Rev., 37*, 111–159. [3] Lal D. (1980) *Proc. Intl. School Physics LXXIII*, pp. 219–238. [4] Caffee M. W. et al. (1987) *Astropyhs. J. Lett., 313*, L31–L35. [5] Olinger C. T. et al. (1988) *LPS XIX*, p. 889. [6] Hohenberg C. M. et al. (1990) *GCA, 54*, 2133–2140. [7] Wieler R. et al. (1989) *GCA, 53*, 1441–1448. [8] Rao M. N. et al. (1993) *JGR, 98*, 7827–7835. [9] Housen K. R. et al. (1979) *Annu. Rev. Earth Planet. Sci., 10*, 355–376.

AUTOMATED SEM MODAL ANALYSIS APPLIED TO THE DIOGENITES.

L. E. Bowman, M. N. Spilde, and J. J. Papike, Department of Earth and Planetary Sciences, Institute of Meteoritics, University of New Mexico, Albuquerque NM 87131, USA.

Introduction: Analysis of volume proportions of minerals, or modal analysis, is routinely accomplished by point counting on an optical microscope, but the process, particularly on brecciated samples such as the diogenite meteorites, is tedious and prone to error by misidentification of very small fragments, which may make up a significant volume of the sample. Precise volume percentage data can be gathered on a scanning electron microscope (SEM) utilizing digital imaging and an energy dispersive spectrometer (EDS). This form of automated phase analysis reduces error (and tedium), and

at the same time provides more information than could be gathered using simple point counting alone, such as particle morphology statistics and chemical analyses.

We have previously studied major-, minor-, and trace-element chemistry of orthopyroxene from a suite of diogenites [1,2]. This abstract describes the method applied to determine the modes on this same suite of meteorites and the results of that research. The modal abundances thus determined add additional information on the petrogenesis of the diogenites. In addition, low-abundance phases such as spinels were located for further analysis by this method [3].

Methods: We have employed Featurescan and Phase Distribution Analysis (PDA) software on an Oxford/Link eXL II system integrated to a JEOL JXA 733 Superprobe. The Featurescan system defines discrete features based on gray-level intensity in a backscattered electron (BSE) image. The system then applies short-duration EDS analysis to determine the chemical composition of each feature and classifies it according to operator-defined chemical criteria, shown in Table 1. Since discrete features are analyzed and typed with the Featurescan system, the xyz coordinates of phases that fit certain criteria (e.g., spinels) can be stored for follow-up detailed analysis. Similar to Featurescan, the PDA system performs the same chemical typing over a grid of points within a BSE image but without first defining features. However, gray-level thresholds may be used to define conditions over which the analysis takes place, thereby avoiding epoxy within void spaces in the thin section. A system of primary grid points is first established on each thin section, and at each point on the grid, a BSE image collected. The number, magnification, and spacing of fields of view must provide

TABLE 1. Phase criteria given in normalized, integrated peak areas (not actual element concentrations in a given mineral).

Phase	Element	Criteria
Chromite	Cr	10–100%
	Si	0–10%
Troilite	S	40–100%
	Fe	15–50%
Glass/quartz	Si	65–100%
Plagioclase	Al	30–100%
	Ca	5–100%
Clinopyroxene	Ca	5–100%
	Mg	5–40%
Orthopyroxene	Mg	5–40%
	Si	45–60%
Olivine	Mg	40–100%
	Si	5–45%
Gold	Au	5–100%
Phosphate	P	5–100%
Fe-metal/oxide	Fe	70–100%

*Residual Au coat from SIMS analysis.

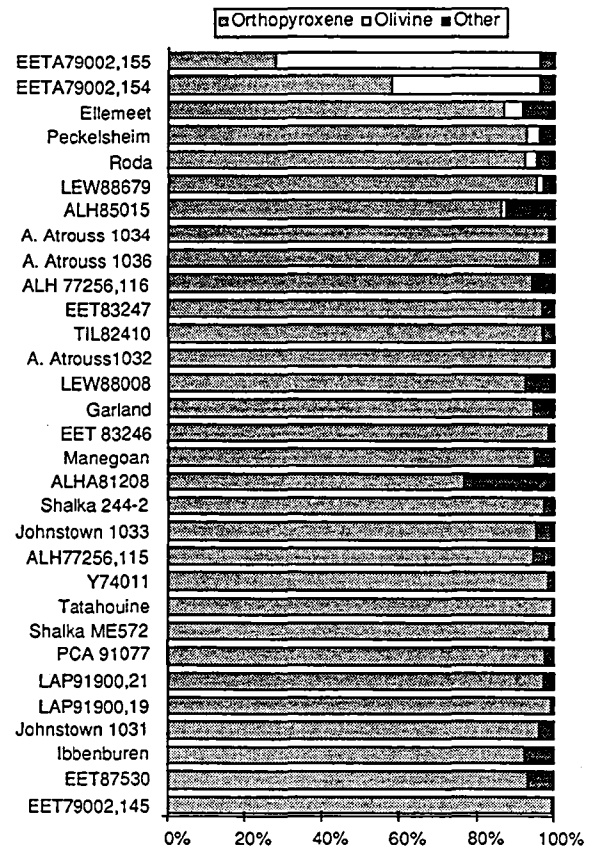

Fig. 1a. Diogenite major components. "Other" components are shown in detail in Fig. 1b.

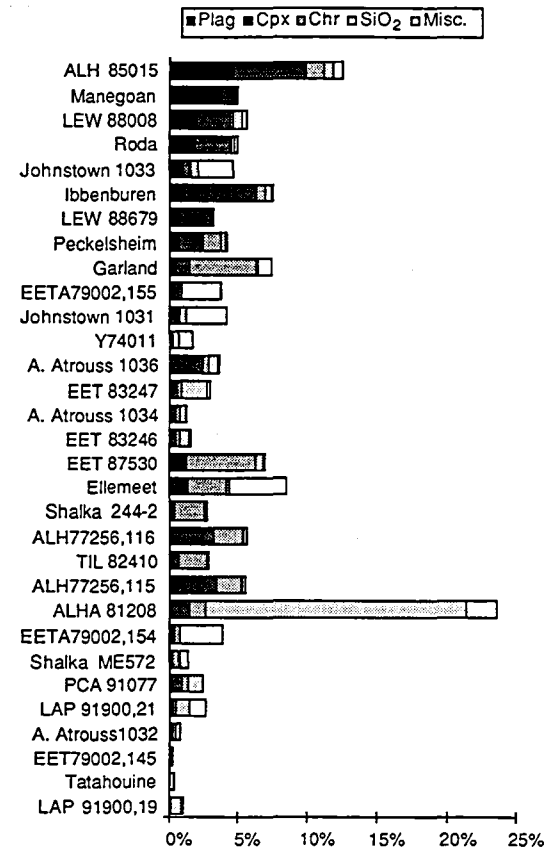

Fig. 1b. Diogenite "other" components from Fig. 1a.

good statistical coverage of each thin section; on average, ~135 individual fields of view were analyzed per thin section. Within each field of view, the PDA software analyses a 15 × 15 grid of points. This provided over 800,000 analytical points across the suite of diogenite samples.

Results and Discussion: This method of modal analysis has been validated by Higgins et al. [4]. However, to determine how closely the modes determined by SEM automated phase analysis compared to optical modes, especially for brecciated samples, optical point counts were done on 10 of the samples for comparison. Good agreement exists in most cases, except for the more brecciated samples, where the methods tend to deviate. This is probably because of the problems noted above with optical modes conducted in brecciated samples.

Modal analysis has been accomplished on 23 of the 24 known diogenites; the results are shown in Figs. 1a and 1b. This study confirms that the volume percent of plagioclase in the diogenites is extremely low (<5%), which is consistent with a scenario that diogenite melts originate from a eucrite-depleted source [2,5]. These analyses also document a generally low abundance of olivine, except for the two of the three samples from EETA 79002. Sack et al. [6] had reported a high modal olivine content in EETA 79002 and ALHA 77256. The extreme variability of olivine in our three EETA 79002 samples and near lack of olivine in our samples of ALHA 77256 indicate that high modal abundance of olivine in the olivine diogenites may simply be the result of sampling bias.

Acknowledgments: This research was funded by a NASA National Space Grant Fellowship, by NASA grant NAGW-3347 (J. J. Papike), and by the Institute of Meteoritics.

References: [1] Fowler G. W. et al. (1994) *GCA, 58,* 3921–3929. [2] Fowler G. W. et al. (1995) *GCA, 59,* 3071–3084. [3] Papike J. J. et al., this volume. [4] Higgins S. J. et al. (1996) *Meteoritics & Planet. Sci., 31,* 356–361. [5] Stolper E. (1977) *GCA, 41,* 587–611. [6] Sack R. et al. (1991) *GCA, 55,* 1111–1120.

A SPACE MISSION TO VESTA: GENERAL CONSIDERATIONS.

L. Bussolino[1], R. Sommat[1], C. Casaccit[1], V. Zappalà[2], A. Cellino[2], and M. Di Martino[2], [1]Alenia Spazio S.p.A., corso Marche 41, Torino, Italy, [2]Osservatorio Astronomico di Torino, strada Osservatorio 20, 10025 Pino Torinese (TO), Italy.

The large asteroid 4 Vesta appears today as the most interesting target for a possible space mission devoted to main-belt asteroids. There are several reasons for this conclusion. First, this asteroid is known to exhibit a rare mineralogic composition. Its surface is basaltic and indicates a differentiated composition, implying a complex thermal history. The fact that Vesta experienced an early phase of melting during its history has strong implications for the present understanding of the history of the solar system. In spite of its relatively large size compared to the bulk of the asteroid population, it is not easy to explain an early melting of Vesta as the consequence of the decay of radioactive isotopes, since the expected amount of such elements in a body of this size seems insufficient to cause a global melting. An alternative theory is based on electromagnetic heating during an episode of strong solar wind from the early proto-Sun when our star experienced a T Tauri phase, as predicted by modern stellar astrophysics. In any case, a close approach by a space probe could provide essential observational constraints in order to better understand the thermal history of this body. On the other hand, Vesta is very interesting from the point of view of the physics of collisions and the overall process of collisional evolution of the main belt. It is known that Vesta suffered a very important collision in the past. This collision created a hemispheric-sized crater whose existence has been detected through photometric and polarimetric studies [1,2]. Moreover, this collision is expected to be related to the formation of the dynamical family associated to Vesta. This big family (including more than 200 small members) has been first identified by means of statistical analyses of the distribution of orbital proper elements [3]. Subsequently, its real nature, that it is physically associated with objects derived from a common collisional origin, has been confirmed by spectroscopic observations, showing that the small family members share a basaltic composition with Vesta [4]. The high ejection velocities imparted to the fragments from this event can have allowed a fraction of them to reach both the ν_6 secular resonance and the 3:1 mean-motion resonance with Jupiter. These resonances are known to be efficient dynamical routes leading to the inner zones of the solar system. As a consequence, we believe today that both the known V-type (basaltic) near-Earth asteroids (NEAs) and the basaltic achondritic meteorites (eucrites) found on Earth can derive from Vesta. In this sense, a comparison between the mineralogical properties of eucrites and those of V-type asteroids could provide invaluable information about the mineralogical variations induced by the exposure to solar wind and by the impact with the Earth atmosphere in the case of eucritic meteorites. For these reasons, an analysis of the Vesta surface as could be performed by means of direct observations from a space probe should be of the highest importance, and could also provide information about the probable age of the Vesta family.

On the basis of the body of scientific evidence explained above, we suggest that a mission devoted to a low-velocity rendezvous with Vesta should deserve high priority in the planning of space activity in the next few years. Several possible mission scenarios are currently under scrutiny. A simple approach would consist of a simple rendezvous by a probe equipped to analyze the surface structure and the chemical composition of the asteroid (imaging system, mass spectrometer, etc.). A much more sophisticated and expensive mission could be planned, based on a spacecraft carrying one or more landers. In this way, one or more interesting regions on Vesta could be investigated in detail by performing a carroting of the surface and complete *in situ* chemical analysis. In this scenario, at least one region within the big hemispheric-sized crater on the Vesta surface, which should be very interesting from a mineralogical point of view, could be analyzed. In general, the mission requirements can be fulfilled by a small spacecraft with high-level onboard technologies presently in development, such as miniaturization of electronics (MMIC) or electrical/ion propulsion for low-velocity rendezvous associated with an overall mission strategy based on a possible "fuzzy boundary" approach for the phase of interplanetary navigation. We plan to analyze the overall preliminary spacecraft configuration in the framework of a possible feasibility study to be carried out by Italian industry, with the support of the Italian Space Agency (ASI).

References: [1] Cellino A. et al. (1987) *Icarus, 70,* 546. [2] Dollfus A. et al. (1989) *Asteroids II,* pp. 594–616, Univ. of Arizona, Tucson. [3] Zappalà V. et al. (1990) *Astrophys. J., 100,* 2030. [4] Binzel R. P. and Xu S. (1993) *Science, 260,* 186.

COSMOGONIC IMPLICATIONS OF THE HED-VESTA CONNECTION. G. J. Consolmagno SJ, Specola Vaticana, V-00120, Vatican City State, and Vatican Observatory Research Group, Steward Observatory, University of Arizona, Tucson AZ 85721, USA.

The simplest model for the genesis of the HED meteorites involves a series of partial melting and crystallization events [1] of a small parent body whose bulk composition is more or less consistent with cosmic abundances but is depleted in the moderately volatile elements Na and K [2]. The connection between the HED parent body and asteroid Vesta was first suggested on spectral reflectance grounds more than 25 years ago [3]; 20 years ago it was first noted that the predominance of surface basalts among the differentiated rocky meteorites, and the dearth of olivine meteorites or asteroids representing the parent body interior, argued that the HED parent body was still intact and thus Vesta was the only plausible candidate [4]. Though serious challenges remain, this is still a useful and powerful model.

However, if this model is true, it raises several significant questions about our understanding of the origin and evolution of the solar system. Among them:

1. Why should both Vesta and the Moon be rich in oxidized Fe but depleted in Na and K? The condensation temperature of Na and K under nebula conditions is around 1000 K. The depletion of these elements in the HED parent body might imply that the material from which it accreted was equilibrated with the nebula near or above this temperature. However, at this temperature Fe should be almost entirely metallic, yet the petrogenic model demands a source region rich in oxidized Fe. A similar Na-depleted, FeO-rich source region puzzle exists for the Moon. The lunar problem might be solved by the giant impact hypothesis for its formation: At that time the more volatile elements could be vaporized, while FeO in the absence of nebular H would remain stable. However, if Vesta also has a similar pattern, does this argue against such a solution? Or is Vesta also the product of a giant impact?

2. How did Vesta melt? Why was it only partially molten? And why didn't other asteroids melt? Everyone's favorite extinct radionuclide, ^{26}Al, faces two almost insurmountable problems in being the Vesta heat source. First, because of its small size, Vesta is less able to use the methods that larger planets use to regulate their internal temperature (such as convection), and so it would have needed an improbably precise amount of ^{26}Al (or any other short-lived nuclide) to be only partially melted: If there were too little, no melting would occur, but too much and the body would be totally melted in spite of vigorous internal convection. Second, and more damning, it is precisely in Al-rich, Mg-poor minerals such as eucrite plagioclase that excess ^{26}Mg daughter isotopes from ^{26}Al decay should be most obvious. They were among the first places searched in the 1970s, and no such anomalies were found. Other heat sources dependent on early solar system conditions, like solar wind heating or impacts, should have melted any asteroid in Vesta's neighborhood to the same degree as Vesta, but Vesta is unique.

3. How did the HEDs get here from Vesta? The discovery of a string of Vesta-like asteroids in orbits linking Vesta to nearby orbital resonances [5] has shown that earlier arguments on the difficulty for material originating at Vesta to reach Earth-crossing orbits are not valid. Nonetheless, Vesta itself is still in an unlikely position to be a source of meteorites. So where did those earlier arguments go wrong? Why isn't phase space filled with chains of vestoids going in all possible directions, including all the wrong directions, away from Vesta? Did Vesta experience an unusual kind of impact, or is it generally characteristic of energetic collisions that fragments are perturbed into resonance-approaching orbits without substantially changing their orbital inclinations? If so, should we expect to see a disproportionate number of meteoroids from other bodies large enough to sustain energetic impacts?

4. Why is Vesta unique? If Vesta is merely the last survivor of a class of differentiated asteroids, where are fragments of the others, the dunite meteorites and olivine-rich small asteroids? And where are the parent bodies (or the complementary remains) of the angrites, the pallasites, and the igneously processed irons? If only the strongest (metal-rich) pieces of those other parent bodies have survived to the present, this would imply that the collisional lifetime and clearing-out time for rocky debris in the asteroid belt is significantly shorter than the age of the solar system. But if this were true, then why should any rocky asteroids at all (including ordinary chondrite sources and, even weaker, the carbonaceous chondrite parent bodies) have survived until today? Such a short clearing time is also incompatible with the observed partial segregation of C- and S-type asteroids, unless one concludes that these groups—and by extension, all asteroid types—only reflect recent surface-alteration effects, and are not diagnostic of fundamental compositional differences. Though possible, this seems unlikely.

None of these questions are new. But taken together, as a whole, they suggest that Vesta may have experienced a unique history, shaped by one or more low probability events. Thus it may be misleading to treat Vesta as a model for the source body of differentiated meteorites in general.

References: [1] Stolper E. (1977) *GCA, 41*, 587–611; Stolper E. et al. (1979) *GCA, 43*, 589–602. [2] Morgan J. W. et al. (1978) *GCA, 42*, 27–38; Drake M. J. (1979) in *Asteroids*, Univ. of Arizona, Tucson. [3] McCord T. B. et al. (1970) *Science, 168*, 1445–1447. [4] Consolmagno G. J. and Drake M. J. (1977) *GCA, 41*, 1271–1282. [5] Binzel R. P. and Xu S. (1993) *Science, 260*, 186–191.

DISRUPTING AND DESTROYING FAMILIES FROM DIFFERENTIATED PARENT BODIES. D. R. Davis[1], P. Farinella[2], F. Marzari[3], and E. Ryan[1], [1]Planetary Science Institute, 620 N. 6th Avenue, Tucson AZ 85705, USA, [2]Universita di Pisa, Via Buonarroti 2, I-56127, Pisa, Italy, [3]Universita di Padova, Dipartimento di Fisica, Via Marzolo 8, I-35131, Padova, Italy.

One of the major dilemmas with our current understanding of the formation and evolution of asteroids is associated with the differentiated asteroids. Meteoritical, spectroscopic, and radar evidence strongly support the idea that iron meteorites are derived from asteroidal parent bodies that are to be found among the M-type asteroids. A subset of the M asteroids are thought to be the collisionally exposed cores of differentiated parent bodies; asteroid 16 Psyche is the largest and best-studied example of such a body. The dilemma posed by this model is that there is little evidence left for any mantle or crustal material from the parent body(ies); essentially only the metallic cores have survived. So what has happened to remove the volumetrically dominant material from the parent body?

The favored explanation to account for the near absence of olivine-rich and basaltic small asteroids (the Vesta case excepted) is that collisions have ground down the mantle and crustal material

to sizes smaller than can be observed today [1,2]. Recently, Burbine et al. [3] have affirmed this interpretation using data from the SMASS survey [4], where they find no evidence for a significant population of olivine-rich asteroids down to 5–10 km in diameter. Furthermore, the interpretation that some M asteroids are collisionally exposed cores means that there should have been an extensive dynamical family formed as the core was being stripped of overlying material. Yet there are no families associated with the large M-type asteroids. So, either all evidence of the collisional stripping process has been removed by subsequent collisional evolution or our understanding of how iron asteroids and meteorites form is totally wrong.

We have explored the plausibility of collisionally grinding the mantle and crustal material produced while exposing the core of a differentiated parent body from the perspective of asteroid collisional evolution models. The asteroid collisional evolution code, used extensively over the past two decades to explore the collisional evolution of asteroids [5,6], has the capability of treating the simultaneous collisional evolution of two distinct but interacting populations. We have exploited this capability to study the evolution of a family formed by the collisional disruption of a large differentiated asteroidal parent body.

The parent body of asteroid 16 Psyche (hereafter referred to as PPB) was chosen as an example of a very large parent body. Since Psyche is ~260 km in diameter, its parent body would have been somewhat smaller than 4 Vesta. We assume that a catastrophically disruptive impact occurred that produced a family having Psyche as the largest member. The size distribution of the remaining family is derived based on results from laboratory impact experiments of simulated differentiated bodies [7] and from numerical hydrocode calculations on the fragmented size distributions from disruptive collisions [8]. The time of the PPB breakup was varied, reflecting our uncertainty as to when Psyche was formed as an exposed core. We then calculated the subsequent collisional evolution of the PPB family, treating both collisions with the general asteroid population and collisions from other family members.

We will present results from a variety of simulations on the efficacy of collisional grinding at removing mantle and crustal material from the observed population of asteroids and will offer predictions as to the sizes at which such material might still exist in the present asteroid belt.

References: [1] Chapman C. R. (1986) *Mem. S. A. It., 57*, 103–122. [2] Bell J. F. et al. (1989) in *Asteroids II* (R. P. Binzel et al., eds.), Univ. of Arizona, Tucson. [3] Burbine T. H. (1996) in *Asteroids, Comets, Meteors*, COSPAR Colloquium 10. [4] Binzel R. P. (1996) in *Asteroids, Comets, Meteors*, COSPAR Colloquium 10. [5] Davis D. R. et al. (1989) in *Asteroids II* (R. P. Binzel et al., eds.), Univ. of Arizona, Tucson. [6] Davis D. R. et al. (1994) *Planet. Space Sci., 42*, 599–610. [7] Davis D. R. and Ryan E. V. (1990) *Icarus, 83*, 156–182. [8] Ryan E. V. and Melosh H. J. (1996) *Icarus*, in press.

MAPPING VESTA IN THE VISIBLE AND NEAR-INFRARED: THE 1994 AND 1996 OPPOSITIONS AS VIEWED FROM THE GROUND.

C. Dumas and O. R. Hainaut, Institute for Astronomy, 2680 Woodlawn Drive, Honolulu HI 96822, USA.

Until recently it was not possible to directly image and resolve any asteroids from the ground. This situation was mainly due to the limitation imposed by the atmospheric turbulences to resolve any subarcsecond object. High-resolution observations of asteroid surfaces were then obtained from speckle interferometry [1] and radar imaging [2] as well as direct imaging from space: The Galileo spacecraft [3] made two successful flybys of asteroids 951 Gaspra and 243 Ida and Hubble Space Telescope [4] observed 4 Vesta during the 1994 opposition.

Adaptive optics (AO) is radically changing this situation: Correcting the effects of the atmospheric turbulences, it restores the full theoretical resolving power of a telescope. Details on the surface of the largest asteroids can be imaged from the ground in the near-infrared and visible; these are the optimal wavelength ranges because the gain in resolution obtained with AO is maximal and they contain most of the spectral signatures of the minerals.

Vesta is certainly the most interesting asteroid to be observed with AO since it is the only large minor planet showing substantial hemispherical albedo variations [5]. Its surface spectrum is typical of pyroxene and feldspar mixtures at some rotational phases, which would correspond to regions containing remnants of the original basaltic flows, while other rotational phases show more pyroxene and olivine-rich regions, which would have formed through impact excavation of geological units from below the basalt crust [6]. We therefore expect to detect a strong albedo contrast over the surface of Vesta.

We will present the results of the two last Vesta oppositions observed using telescopes equipped with AO. We obtained during these two campaigns some data in the near-infrared with the 3.6-m telescopes at the European Southern Observatory in Chile and the Mauna Kea Observatory in Hawai'i, in addition to some visible data obtained with the 100-in telescope at Mount Wilson Observatory and the 1.5-m telescope at the Observatoire de Haute-Provence in France.

December 1994 Opposition: We observed Vesta with the Come-On-Plus AO system at the ESO 3.6-m telescope from December 9–13, 1994 [7]. The images were obtained on the Nicmos SHARP II camera through a Continuously Variable Filter ($\lambda/\Delta\lambda \simeq 60$) at 12 wavelengths along the 2.0-μm pyroxene band. The geometry of the opposition was such that 80% of Vesta's surface was visible over a rotation period. With an angular diameter of 0.44", Vesta covered 10 resolution elements. The plate-scale was 50 millarcsec/pixel. To restore the optimal resolution of our images, we applied different techniques: Wiener filtering, Richardson-Lucy deconvolution, and wavelet transform. The results of these three independent restorations are in excellent agreement, confirming that the albedo variations detected are real and correspond to some changes in the nature of the minerals over the surface. Unfortunately we were not able to obtain a complete longitudinal coverage of Vesta and our dataset is roughly centered on two opposite Vesta longitudes. The next step was to extract a mineralogical map from these images. We obtained two maps: one from the images recorded at the bottom of the pyroxene band and the other with the images recorded at the top of the band. These two maps show the presence of a hemisphere dominated by pyroxene as well as some smaller high- and low-albedo regions in each hemisphere. The ratio of the maps obtained at the top and bottom of the band give some additional information on the spatial distribution of the strength of the pyroxene band over Vesta's surface.

May 1996 Opposition: The geometry of this opposition was particularly favorable since Vesta's angular diameter was 0.65" and more than 99% of its surface was visible. The primary goals were not only to image Vesta along the two pyroxene bands centered at

0.94 μm and 2.0 μm but also to scan the 1.0–1.5-μm range by using narrow-band filters in order to discriminate between feldspar-, pyroxene-, and olivine-rich regions. We always oversampled our images in order to respect the Shannon criterium, and the plate scale was such that we had more than three physical pixels per resolution element. We imaged Vesta from June 11–14, 1996, using the 100-in telescope at Mount Wilson Observatory. This telescope is equipped with a powerful AO system. We obtained diffraction limited images of Vesta at 0.7, 0.83, and 0.94 μm (i.e., outside) at midband depth and at the bottom of the first pyroxene band. Some images were also obtained during three nights early in June with the 1.5-m telescope at the Observatoire de Haute-Provence in France, equipped with an AO system built by ONERA. Here also the first pyroxene band was scanned using a set of 50-nm-wide narrow band filters centered at 0.7, 0.85, and 0.95 μm. The program planned with the Canada-France-Hawai'i telescope at Mauna Kea was the most ambitious since it was originally scheduled to image Vesta during two consecutive nights, simultaneously on a CCD using a narrow-band filter centered at 0.9 μm and on an infrared camera at diverse wavelengths between 1.0 and 2.5 μm. Unfortunately, some technical problems with the filter wheels occurred at the last minute and we could not image Vesta through our set of narrow-band filters but only through a broad-band H filter, thereby losing most of the mineralogical information since this filter integrates the flux coming from a range of wavelengths that contains the second band of pyroxene as well as the continuum. These infrared images will nevertheless be used as a comparison with the set of visible images in order to confirm the main albedo features present on the surface of Vesta and the rotational variation of the asteroid shape. The images recorded through the three narrow-band filters across the 0.9-μm pyroxene band show a dramatic contrast between the region dominated by pyroxene and feldspar. From the entire set of data we will be able to estimate with extremely high resolution the pyroxene distribution over the surface of Vesta, as well as the shape and dimensions of the asteroid and its rotation parameters. We will also discuss the extension of this high-resolution mapping project to other main-belt asteroids and our prospects concerning the mineralogical mapping of Vesta for the next opposition of October 1997.

References: [1] Drummond J. D. et al. (1989) in *Asteroids II* (Binzel et al., eds.), pp. 171–191, Univ. of Arizona, Tucson. [2] Ostro S. J. (1993) *Rev. Mod. Phys., 65*, 1235–1277. [3] See review in *Icarus, 120*, March 1996. [4] Zellner B. et al. (1995) Presentation at DPS meeting. [5] Degewij J. et al. (1979) *Icarus, 40*, 364. [6] Gaffey M. J. (1996) *Icarus*, submitted. [7] Dumas C. et al. (1995) Presentation at DPS meeting.

ASTEROID SPECTROSCOPY: VESTA, THE BASALTIC ACHONDRITES, AND OTHER DIFFERENTIATED ASTEROIDS. M. J. Gaffey[1,2,3], [1]Department of Earth and Environmental Sciences, West Hall, Rensselaer Polytechnic Institute, Troy NY 12180-3590, USA, [2]Sabbatical Address: Department of Geological Sciences, 253 Science I, Iowa State University, Ames IA 50011, USA, [3]Visiting Astronomer at the Infrared Telescope Facility, University of Hawai'i, Honolulu HI 96822, USA.

Reflectance spectroscopy, thermal infrared radiometry, optical polarimetry, speckle interferometry, and high-resolution imagery are among the remote sensing techniques applied to Vesta, producing a sophisticated characterization of this object. Reflectance spectroscopy has provided relatively detailed descriptions of the surface mineralogy of Vesta and has provided critical evidence linking Vesta to the basaltic achondrite meteorites (see [1] for a detailed review).

Vesta exhibits a unique reflectance spectrum and taxonomic type (V), indicating that it is either the parent body of the basaltic achondrites or has undergone an evolutionary history very similar to that parent body [2–5]. No other asteroid larger than 25 km shares Vesta's characteristic spectral reflectance curve, albedo, and polarimetric properties [6–8]. On compositional grounds, it's plausible that Vesta is indeed the basaltic achondrite parent body, and as such would represent one of only five known solar system bodies for which actual rock samples are available in terrestrial laboratories.

However, Vesta is poorly situated to directly provide any significant flux of meteorites [e.g., 3,9], although its large size may compensate for its distance from the resonant "escape hatches" in the asteroid belt, potentially allowing it to contribute a few percent of the asteroidal fragments reaching Earth [10]. A family of small (<10 km) V-type asteroids extends from Vesta to the edge of the 3:1 resonance [11]. These objects were interpreted as ejecta from a large impact onto Vesta that extends into the chaotic region around the 3:1 resonance where fragments can be rapidly transferred to Earth-crossing orbits [e.g., 12]. There are thus convincing observational and dynamical cases that Vesta is indeed the actual parent body of the basaltic achondrites.

Recently, high-precision spectrophotometry of Vesta was used to refine its surface composition and to investigate mineralogical variations across its surface [1]. The average surface of Vesta is analogous to howardite and/or polymict eucrite assemblages, regolith-derived meteorites consisting of a eucrite matrix with a diogenite component. Studies of Vesta dating back to 1929 exhibit a consistent relationship of color and/or spectral changes to rotational phase. These rotational changes arise from hemispheric variations in surface lithology. The background surface of Vesta is a relatively dark howardite or polymict eucrite assemblage with several compositionally distinct bright regions clustered in one hemisphere. These include an olivine-bearing unit located near Vesta's equator that probably represents the ejecta of an impact basin that penetrated through the basaltic crust. Other high-albedo units include several diogenite regions, perhaps smaller, shallower impact basins.

By analogy to the HED meteorites, the low-albedo howardite or polymict eucrite units represent a regolith-gardened ancient surface of Vesta that was darkened by space weathering similar to that inferred from the Galileo images of Gaspra and Ida [13]. On this old dark surface, several impacts in one hemisphere have exposed fresher brighter diogenite and olivine-bearing material. A generalized lithologic map of Vesta was produced based on qualitative analysis of the mineralogical variations as a function of rotation [1].

Hubble Space Telescope observations at four wavelengths have produced spatially resolved multicolor images of the equatorial region of Vesta [14]. The color ratio images indicate that Vesta is geologically diverse. The eastern hemisphere is dominated by high-albedo units interpreted to be impact-excavated plutonic material, perhaps analogous to diogenites. Several eastern units with deep and broad 1-μm absorption bands may contain a substantial olivine component. The locations of these units are consistent with the previous map based on rotational spectroscopy [1]. The western

hemisphere is dominated by low-albedo units analogous to surface eucritic basalts. The correlation between absorption band depth and albedo indicates a space-weathering effect that decreases albedo and band depth over time.

Vesta's apparently intact basaltic crust provides significant constraints on the collisional processes in the asteroid belt [e.g., 15,16]. Given the abundance of differentiated asteroids in the inner belt [17], why are basaltic asteroids so rare? Vesta may have survived by virtue of its large size, or it may have undergone efficient segregation of basaltic liquids from a "basalt-rich" (e.g., H-chondrite) precursor to produce an exceptionally thick basaltic crust [e.g., 17]. It is likely that basaltic crusts were originally common in the inner belt, but only Vesta survived into the present epoch. Clast 4 in the Antarctic polymict eucrite ALHA 76005 may be a fragment of one of those other basaltic crusts [18].

Acknowledgments: Various portions of this analysis effort were supported by NASA Planetary Geology and Geophysics grant NAGW-642 and by NSF Solar System Astronomy grant AST-9012180. The Infrared Telescope Facility is operated by the University of Hawai'i under contract to the National Aeronautics and Space Administration.

References: [1] Gaffey M. J. (1996) *Icarus*, in press. [2] McCord T. B. et al. (1970) *Science, 168*, 1445–1447. [3] Drake M. J. (1979) in *Asteroids* (T. Gehrels and M. S. Matthews, eds.), pp. 765–782, Univ. of Arizona, Tucson. [4] Feierberg M. A. and Drake M. J. (1980) *Science, 209*, 805–807. [5] Feierberg M. A. et al. (1980) *GCA, 44*, 513–524. [6] Bowell E. et al. (1978) *Icarus, 35*, 313–335. [7] Zellner B. (1979) in *Asteroids* (T. Gehrels and M. S. Matthews, eds.), pp. 783–806, Univ. of Arizona, Tucson. [8] Tholen D. J. (1984) Ph.D. dissertation, Univ. of Arizona, Tucson. [9] Wetherill G. W. (1987) *Philos. Trans. R. Soc. London, A323*, 323–337. [10] Farinella P. et al. (1993) *Icarus, 101*, 174–187. [11] Binzel R. P. and Xu S. (1993) *Science, 260*, 186–191. [12] Wisdom J. (1985) *Icarus, 63*, 272–289. [13] Chapman C. R. et al. (1995) *Nature, 374*, 783–785. [14] Binzel R. P. et al. (1996) *Icarus*, submitted. [15] Davis D. R. et al. (1985) *Icarus, 62*, 30–53. [16] Davis D. R. et al. (1994) *Planet. Space Sci., 42*, 599–610. [17] Gaffey M. J. et al. (1993) *Icarus, 106*, 573–602. [18] Grossman L. et al. (1981) *GCA, 45*, 1267–1279.

THE THERMAL HISTORY OF ASTEROID 4 VESTA, BASED ON RADIONUCLIDE AND COLLISIONAL HEATING.

A. Ghosh and H. Y. McSween Jr., Department of Geological Sciences, University of Tennessee, Knoxville TN 37996-1410, USA.

We have simulated the thermal evolution of asteroid 4 Vesta through its complex history of growth, core separation, crust formation, and cooling by radiation. The model takes into account the latent heat of fusion and the increased specific heat capacity of melts, and considers the effects of collisional heating and redistribution of radioactive nuclides (^{26}Al and ^{60}Fe) during differentiation.

Eucrites and diogenites provide chronological constraints on the onset and duration of volcanism [1,2] and evidence for core formation [3] on the HED parent body. The discovery of a cluster of small V-class asteroids extending from Vesta to the 3:1 mean motion resonance [4] has provided new evidence linking Vesta to HED meteorites. This association allows several additional constraints when simulating the thermal evolution of the HED parent body, the most important of which are radius (270 km) and heliocentric distance (2.36 AU).

In our finite-element model [5], Vesta is assumed to grow from the accretion of 10-km-radius planetesimals according to a formulation of [6]. The energy balance is given by the heat transfer equation, and heat loss from the surface of the body is governed by a radiation boundary condition. Thermal diffusivity and specific heat capacities are recalculated for each temperature. The body is heated primarily by the decay of ^{26}Al and ^{60}Fe. The latter is included to assess whether it causes significant heating when Fe is sequestered to form the core. The collisional heat generated during accretion is estimated according to [7]. The initial composition of Vesta varies between H and LL chondrite.

Chronologically, the thermal model can be divided into four stages: Stage 1 (accretion) ends when the growth of Vesta is complete. During stage 2, the homogeneous asteroid undergoes heating until core separation (beginning at ~980°C, based on chondrite melting experiments [8]). We observed that the near-surface layers never attain high temperatures because of heat loss by radiation. Hence, in our thermal model we approximate core formation to take place when Fe-Ni-S eutectic melting occurs in the whole asteroid except for the outer few kilometers. Instantaneous core separation takes place at the end of stage 2. In stage 3, further heating of the mantle continues until silicate partial melting (beginning at 1190°C, the eucrite solidus [9]). The temperature of the mantle increases, but as in stage 2, the near-surface layers do not experience silicate melting. We induce instantaneous crust formation when 25% partial melting has occurred below a depth of 30 km. Stage 4 involves further heating and subsequent cooling of the core, mantle, and crust. The thermal evolution of Vesta through the begining of stage 4 is summarized in Fig. 1.

Results from the thermal model are: (1) Vesta must have accreted within a time frame of 2.85 ± 0.05 Ma. If it accreted earlier, there would have been whole-mantle melting; conversely, if it accreted later, core formation would not have been possible. (2) The process of accretion causes cooling during stage 1 [10], which offsets the effect of radiogenic and collisional heating during the accretion interval. (3) We constrain the time for partial melting on Vesta to be between 6 and 8 Ma relative to formation of Allende CAIs. The first-formed volcanics should thus have an ^{26}Al/^{27}Al ratio of ~10^{-8}, which matches the analytical upper limits of $<5 \times 10^{-8}$ in noncumulate

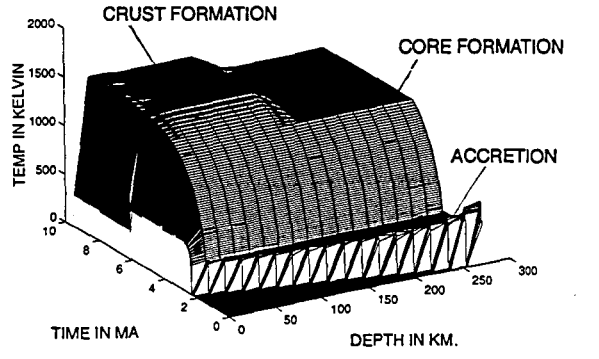

Fig. 1. Temperature-time-radius profiles of Vesta through its complex history of accretion, core separation, and crust formation. Subsequent cooling through 100 Ma is illustrated in [10].

eucrites [11]. (4) It is possible to maintain high temperatures, and even eucritic liquids, inside Vesta for 100 Ma after the onset of volcanism. This results from redistribution of ^{26}Al in the mantle and crust during core- and crust-forming events respectively. These episodes cause an "anomalous" thermal gradient in the asteroid with temperature *decreasing* with depth. This may explain the apparent time interval of ~100 Ma between cumulate and non-cumulate eucrites [1,2], and dismantles a major argument against the ^{26}Al heating hypothesis [12]. (5) Neither decay of ^{60}Fe sequestered in the core nor collisional heating make a marked difference in the whole-body thermal history of Vesta. (6) The outer layers of proto-Vesta before crust formation did not melt due to the powerful radiation boundary condition at the surface. The heat generated in these layers by radionuclide decay was efficiently radiated away. It is conceivable that the olivine-rich spot on Vesta inferred from spectra [13] may not be mantle exposed in a crater but a surviving portion of the outer, chondritic layer of proto-Vesta that survived the asteroid's differentiation. (7) Thermal metamorphism of eucrites can be explained by eruption and subsequent burial of lava flows, but not by heating from a subjacent mantle as implied by the model of [14].

References: [1] Jacobsen S. B. and Wasserburg G. J. (1984) *GCA, 67*, 137. [2] Carlson R. W. et al. (1988) *LPS XIX*, p. 166. [3] Newsom H. E. (1985) *Proc. LPSC 15th*, in *JGR, 90*, C613. [4] Binzel R. P. and Xu S. (1993) *Science, 260*, 186. [5] Ghosh A. and McSween H. Y. (1996) *LPS XXVII*, p. 407. [6] Wetherill G. W. (1990) *Annu. Rev. Earth Planet. Sci., 18*, 205. [7] Melosh H. J. (1991) *Origin of the Earth*, p. 69, Oxford, New York. [8] McSween H. Y. et al. (1977) *Proc. LPSC 9th*, p. 1437. [9] Stolper E. (1977) *GCA, 41*, 587. [10] Ghosh A. and McSween H. Y. (1996) *Meteoritics & Planet. Sci.*, in press. [11] Schramm D. N. et al. (1970) *EPSL, 10*, 44. [12] Wood J. A. and Pellas P. (1988) *The Sun in Time*, p. 74. [13] Gaffey M. J. (1983) *LPS XIV*, p. 231. [14] Yamaguchi A. et al. (1995) *Meteoritics, 30*, 603.

THE CONTENT AND ISOTOPIC COMPOSITION OF CARBON IN HED BASALTIC ACHONDRITES.

M. M. Grady[1,2], I. P. Wright[2], and C. T. Pillinger[2], [1]Department of Mineralogy, The Natural History Museum, Cromwell Road, London SW7 5BD, UK, [2]Planetary Science Research Institute, The Open University, Walton Hall, Milton Keynes MK7 6AA, UK.

Howardites, eucrites, and diogenites make up a suite of rock types (HED) known to be related through O isotope systematics and by complex processes of partial melting, fractional crystallization, thermal metamorphism, brecciation, and mechanical mixing. The HEDs crystallized *in vacuo*, and thus are presumably degassed of volatiles. Notwithstanding, C is present and has played an active role in influencing the redox conditions prevailing during formation. The actual form in which C occurs in this suite of meteorites is unknown, but by analogy with terrestrial basalts, may be present as a coating of free C along grain boundaries, and possibly as dissolved $CO/CO_2/CO_3^{2-}$ in silicate minerals [1]. We have measured the content and isotopic composition of C in three eucrites, four diogenites, and two howardites by stepped combustion in order to comprehend the role that C plays during the melting and differentiation of solar system materials; preliminary data were given by [2].

TABLE 1. Carbon in HED meteorites.

		Total		T > 600°C	
Sample	Type	C (ppm)	$\delta^{13}C$ (‰)	C (ppm)	$\delta^{13}C$ (‰)
ALHA 76005	Eucrite	252	–26	11	–26
Juvinas	Eucrite	603	–21	18	–24
Pasamonte	Eucrite	213	–28	8	–28
EETA 79002	Diogenite	88	–23	11	–19
Johnstown	Diogenite	270	–25	27	–27
Shalka	Diogenite	107	–23	19	–25
Tatahouine	Diogenite	159	–28	54	–27
EETA 79006	Howardite	149	–24	16	–22
Kapoeta (dark)	Howardite	597	–15	94	–6

The release of C by incremental oxidation enables biological contaminants to be combusted selectively at low temperatures, giving a more accurate assessment of indigenous C content [3]. A temperature of 600°C generally defines the region at which indigenous components become observable over any "tail" from contamination; this value is therefore taken as the cutoff in distinguishing between indigenous and terrestrial species. Previously reported bulk C measurements of HED meteorites [4] are in error because of a high degree of terrestrial contamination swamping the indigenous C, and literature values for bulk C in HEDs are thus a factor of 10–100 higher than the true indigenous C component of these meteorites. Once the effects of contaminant C have been removed from the HED meteorites, it is apparent that there is very little indigenous C present in these samples. Eucrites and diogenites contain ~10–70 ppm of indigenous C. The more mafic diogenites contain a discrete carbonaceous component that combusts across an extended temperature range, from 900°C to 1100°C, and has an isotopic composition ~ –30‰. This material is presumably primitive elemental C trapped (or possibly C as the carbonate anion dissolved) within silicate grains, and therefore not available for release until the minerals soften at high temperatures. The Pasamonte eucrite also evidences this material in low abundance, presumably contained in clasts of diogenitic material. The range in $\delta^{13}C$ of HEDs (–28‰ to –19‰) is similar to that of magmatic C from lunar samples (–25‰ to –15‰ [5]) and SNC meteorites (–30‰ to –20‰ [6]). All these groups have more ^{12}C-enriched C than the Earth's mantle (–10‰ to 0‰), an observation that might relate to the precursor materials that formed the Earth, Moon, Mars, and asteroids. Alternatively, it is known that the Moon and the asteroids underwent extensive melting early in their history and thus the differences in $\delta^{13}C$ between these entities may be the results of planetary-scale processes.

The low abundance of C in HEDs is a reflection of their igneous history. It has been proposed [7,8] that eucrites and diogenites were derived from a single source of primitive undifferentiated material through episodes of partial melting and remelting, followed by subsequent thermal annealing and brecciation. Eucrites are products of open-system melting of the source region at an early stage in its differentiation, whereas diogenites are late-stage, slowly cooled plutonic cumulates. It is possible to rationalize C chemistry in the framework of this model of eucrite-diogenite development: The higher abundance and lighter isotopic composition of C in dioge-

nites implies that greater quantities of primitive C were assimilated into the mafic material than into the more rapidly quenched eucrites. This is in keeping with the different mineralogy of the eucrites and diogenites. Equilibrated eucrites that have been annealed (e.g., Juvinas) have heavier $\delta^{13}C$ values than the unequilibrated (ALHA 76005, Pasamonte), a result of isotopic fractionation during open-system metamorphism, leading to loss of ^{12}C-enriched C. If the annealing temperature rose above ~1000°C for extended periods of time, then the primitive C component seen in diogenites and Pasamonte with $\delta^{13}C \sim -30‰$ would readily be lost. Pasamonte has clearly not experienced this second stage of thermal annealing.

Carbon in the Kapoeta howardite is dominated by components from clasts of CM-related material: The meteorite contains ^{13}C-enriched carbonate minerals ($\delta^{13}C$ ~20‰). Below 600°C, although the effects of terrestrial contamination cannot be distinguished from the presence of chondritic macromolecular material, the carbonate C to total C ratio falls within the range of CM chondrites. The fragment studied is not totally chondritic, since its overall C content is too low and the sample also shows relict primitive C combusting at high temperatures, in keeping with the occurrence of diogenitic clasts.

References: [1] Mattey D. P. et al. (1989) *GCA, 53,* 2377–2386. [2] Grady M. M. and Pillinger C. T. (1985) *LPS XVI,* pp. 286–287. [3] Swart P. K. et al. (1983) *Meteoritics, 18,* 137–154. [4] Gibson E. K. et al. (1971) *Meteoritics, 6,* 87–92. [5] Des Marais D. J. (1983) *GCA, 47,* 1769–1781. [6] Wright I. P. et al. (1990) *JGR, 95,* 14789–14794. [7] Longhi J. and Pan V. (1988) *Proc. LPSC 18th,* pp. 459–470. [8] Stolper E. (1977) *GCA, 41,* 587–611.

NONCUMULATE VS. CUMULATE EUCRITES: HETEROGENEITY OF 4 VESTA.

W. Hsu and G. Crozaz, Department of Earth and Planetary Sciences and McDonnell Center for the Space Sciences, Washington University, St. Louis MO 63130, USA.

Eucrites, diogenites, and howardites are generally believed to have been derived from the same source. Although the parent body of these meteorites has not been identified, a strong argument was made in favor of the asteroid 4 Vesta [1–3]. Noncumulate eucrites are thought to be near-surface basalts, and cumulate eucrites plutonic dikes. Despite the debate of whether eucrites are the products of either fractional crystallization of more magnesian liquids [4] or low-pressure partial melting of an olivine + pyroxene + plagioclase assemblage [5], most investigators believe that noncumulate and cumulate eucrites are closely related. This concept was first challenged by the Schmitt group, who argued that the magmas with which cumulate eucrites may have equilibrated were LREE-rich and that such melts could not be related to noncumulate eucrites by fractional crystallization [6,7]. Unfortunately, their plagioclase separates were contaminated by pyroxene; furthermore, pyroxene was not included in their study. As cumulate eucrites experienced extensive thermal metamorphism, it is legitimate to ask whether their results truly reflect cumulate eucrite characteristics or whether they are the consequence of subsolidus equilibration. Here we studied individual grains of pyroxene and plagioclase, the first two minerals to crystallize from a eucritic melt, in an attempt to derive independent information about the nature of the parent melts they grew in contact with. We made more than 400 *in situ* ion microprobe measurements of plagioclase and pyroxene in 12 eucrites representing all the chemical groups previously defined (Stannern and Ibitira from the Stannern trend, Nuevo Laredo and Lakangaon from the Nuevo Laredo trend, Chervony Kut and Sioux County from the main group, the Moore County and Moama cumulate eucrites, the mainly unequilibrated eucrites Pasamonte and ALHA 76005, and the anomalous eucrites Peramiho and Pomozdino). We evaluate the effects of subsolidus equilibration and examine the relationships between noncumulate and cumulate eucrites. Our study supports the suggestion that noncumulate and cumulate eucrites are not genetically related.

Figure 1 shows average LREE (La or Sm) and HREE (Y or Yb) concentrations in pyroxene and plagioclase of the eucrites studied. ALHA 76005 is excluded from this figure because of weathering effects. Except for Ibitira, which is a highly equilibrated eucrite, all noncumulate eucrites plot on the same trends, indicating that they may have been derived from the same source. In addition, the La/Y ratio recorded in noncumulate plagioclases is consistent with the crystallization of this mineral from melts with REE abundances in chondritic proportions. Pyroxene and plagioclase in Ibitira have higher LREE/HREE ratios than in other noncumulate eucrites. We attribute these higher ratios to REE redistribution between phosphates and silicates. Phosphate, the major REE-carrier in eucrites, is LREE-rich, and merrillite in Ibitira has significantly lower REE concentrations than in Stannern, Lakangaon, and Sioux County (a factor of 3–5) [8].

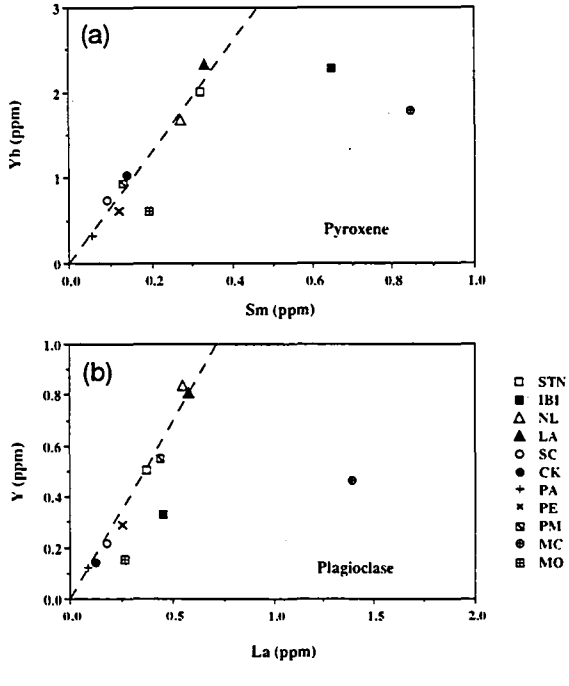

Fig. 1. LREE (La or Sm) and HREE (Y or Yb) concentrations in (a) pyroxene and (b) plagioclase of noncumulate eucrites (STN, Stannern; IBI, Ibitira; NL, Nuevo Laredo; LA, Lakangaon; SC, Sioux County; CK, Chervony Kut; PA, Pasamonte; PE, Peramiho; PM, Pomozdino) and cumulate eucrites (MC, Moore County; MO, Moama). Except for Ibitira, noncumulate eucrites fall on the same trends. Pyroxene and plagioclase of cumulate eucrites have higher LREE/HREE ratios than those phases in noncumulate eucrites.

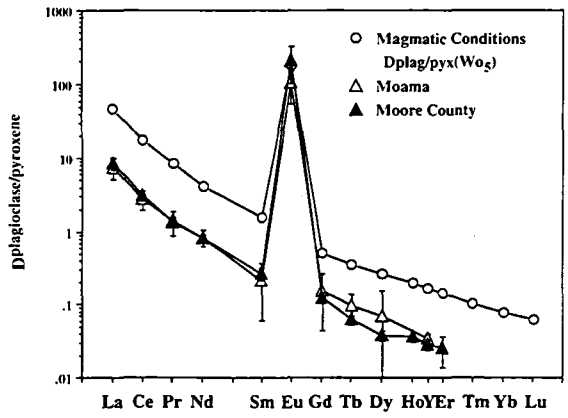

Fig. 2. Mineral/melt plagioclase/pyroxene (Wo_5) REE partition coefficient ratios and plagioclase/pyroxene REE abundance ratios in Moama and Moore County.

Pyroxene and plagioclase in cumulate eucrites have much higher LREE/HREE ratios than in noncumulate eucrites (Fig. 1). It is clear that cumulate eucrites experienced extensive reequilibration as their minerals are essentially homogeneous in major, minor, and trace elements. The question then is whether or not, in cumulate eucrites, the REEs were redistributed between the various minerals. Phosphates were not observed in cumulate eucrites and there is no other known LREE carrier. Therefore, the high LREE/HREE ratios (even higher than those of Ibitira) in silicates of cumulate eucrites cannot be due to the addition of REE from LREE-rich phases. Could they be the results of REE redistribution between pyroxene and plagioclase? In Fig. 2, we compare the expected REE partitioning between plagioclase and pyroxene crystallizing from a melt with the plagioclase/pyroxene elemental abundance ratios in Moama and Moore County. They define three parallel curves whose slopes are in agreement. Values for Moama and Moore County plot essentially on top of each other but are lower than predicted. This difference is easily explained because pyroxene REE partition coefficients increase as crystallization proceeds and the melt composition becomes more Ca-rich [9], whereas plagioclase REE partition coefficients are essentially invariant [10]. Therefore, plagioclase and pyroxene of cumulate eucrites probably retained their magmatic REE partitioning. Even if there were any REE redistribution between these two minerals, it is hard to envision how such a process could simultaneously raise the LREE/HREE ratios in *both* minerals. Thus, we suggest that cumulate eucrites were most likely derived from melts enriched in LREEs.

A LREE-rich melt cannot easily form by fractional crystallization of a primary eucritic melt with REEs in chondritic proportions. Calculations show that LREE/HREE ratios in residual melts remain almost constant: up to ~95% fractional crystallization of orthopyroxene or orthopyroxene and plagioclase in peritectic proportions [11]. Extensive reactions between cumulate eucrites and LREE-rich infiltrating liquids (whose origin, in turn, would have to be explained) could raise their LREE/HREE ratios. Although we cannot exclude this possibility, we have serious problems with it. There are no late-stage minerals in cumulate eucrites; furthermore, why would all cumulate eucrites have experienced this process but noncumulate eucrites did not? Therefore, we conclude that cumulate eucrites formed from different sources than those of noncumulate eucrites. This is consistent with the conclusion of [12], who observed that cumulate and noncumulate eucrites have distinct initial $^{87}Sr/^{86}Sr$ ratios.

In summary, our data support the suggestion that noncumulate eucrites were derived from a source with REEs in chondritic proportions. Cumulate eucrites most probably crystallized from melts with fractionated REE patterns. Thus cumulate and noncumulate eucrites do not seem to be related.

References: [1] McCord T. B. et al. (1970) *Science, 168*, 1445–1447. [2] Consolmagno and Drake (1977) *GCA, 41*, 1271–1282. [3] Binzel and Xu (1993) *Science, 260*, 186–191. [4] Mason B. (1962) *Meteorites*, pp. 116–119, Wiley. [5] Stolper E. (1977) *GCA, 41*, 587–611. [6] Fukuoda et al. (1977) *Proc. LSC 8th*, pp. 187–210. [7] Ma and Schmitt (1979) *Meteoritics, 14*, 81–89. [8] Hsu and Crozaz (1996) *GCA*, in press. [9] McKay et al. (1986) *GCA, 50*, 927–937. [10] Drake and Weill (1975) *GCA, 39*, 689–712. [11] Hsu and Crozaz (1996) *GCA*, submitted. [12] Smoliar M. I. (1993) *Meteoritics, 28*, 105–113.

ISOTOPIC CONSTRAINTS ON THE ORIGIN OF EUCRITES.

M. Humayun[1] and R. N. Clayton[2], [1]Department of Terrestrial Magnetism, Carnegie Institution of Washington, Washington DC 20015, USA, [2]Department of the Geophysical Sciences, Department of Chemistry, and the Enrico Fermi Institute, The University of Chicago, Chicago IL 60637, USA.

We present cosmochemical arguments for the origin of eucrites, and by inference the HED parent body (Vesta or otherwise), indicating that these formed from distinct nebular materials, unrelated to any known type of chondrite. We find this result to be generally true for all the known planetary compositions: the Earth, Moon, SNC meteorites (Mars), and HED meteorites. Two isotopic constraints prove to be important here: O isotopes ($^{17}O/^{16}O$ and $^{18}O/^{16}O$), which fingerprint various nebular reservoirs, and K isotopes ($^{41}K/^{39}K$), which are diagnostic of nebular vs. planetary formational processes related to the mechanisms of volatile-element depletion. Planetary compositions are to first-order chondritic [e.g., 1,2] in their abundances of major elements, but differ from known chondrites in having a larger degree of volatile element depletion in all elements with condensation temperatures lower than those of Mg and Si, e.g., Mn, K, P, Rb, Cs, S, Pb, Tl, etc. The relative order of depletion for K (values in parentheses) for various planetary compositions is

SNC (0.27) < Earth (0.19) < HED (0.05) < Moon (0.03)

Condensation from the nebula or partial loss of volatile elements during heating accompanying differentiation can both affect the K/La ratios, but partial loss by heating of condensed materials results in mass fractionation of the isotopes of various volatile elements, of which the best estimate can be made using stable K isotopes ($^{41}K/^{39}K$).

Potassium isotopic analysis of Juvinas (2.2 g) and Ibitira (0.058 g) were carried out [3]. A small fractionation in Ibitira is not regarded as particularly significant, in view of the absence of any effect in Juvinas and the less-than-optimal sample amount for analysis. Results on vesicular lunar mare basalts [3] showed that planetary materials exposed to high vacuum at magmatic temperatures does not

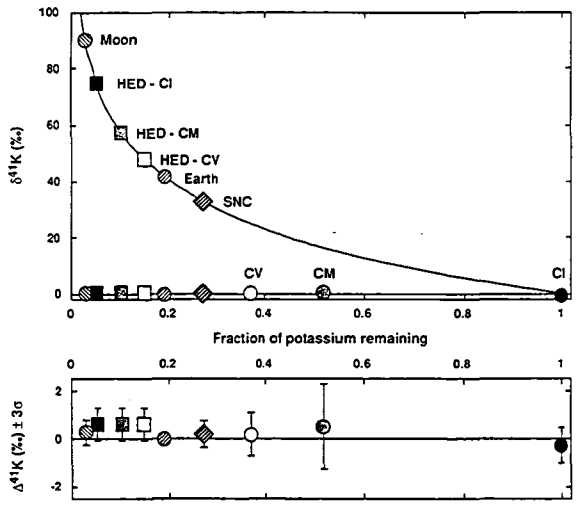

Fig. 1. Potassium isotopic data of HEDs, SNCs, the Earth, and the Moon compared with the observed depletion of K, assuming Rayleigh fractionation from a CI initial composition. The result does not significantly change by assuming an initial starting composition of CM or CV chondrite, as shown for HEDs.

result in measurable K loss. A limit of a few percent relative loss is set by the $^{41}K/^{39}K$ ratio, confirming the absence of large losses in K/La and other elemental correlations [4]. Accordingly, the presently observed depletion of volatile elements must be a feature intrinsic to the nebular constituents of the eucrite parent body, and as such distinguish it from CM or other types of chondrites thought to be possible parental materials [5,6].

Oxygen isotope studies of chondrites and achondrites show that the HED meteorites are not related to any single group of chondrites [7]. Furthermore, K isotopic data indicate that all possible mixtures of the known chondrite classes cannot account for the compositions of HED meteorites, SNC meteorites, the Earth, and the Moon, since such mixtures have significantly higher volatile-element abundances [3,7]. The Earth and Moon are similar to enstatite chondrites in O isotopes, but lack any of the chemical properties of the E chondrites: low Mg/Si, highly reduced mineralogy, and high volatile elements. Likewise, the Moon cannot be derived from the terrestrial mantle by volatile fractionation [8].

In conclusion, the HEDs are better understood to be an example of volatile-depleted planetary building blocks [9] that inherited their characteristic compositional features from the inner solar nebula. Global high temperatures in the inner solar nebula are indicated by such depletions [10], and the chemical patterns were established during nebular cooling and accretion of condensates [11].

The relationship between the HEDs and Vesta proposed by Binzel and Xu [12] cannot be evaluated from compositional data, with the exception of O isotopes. The O isotopic composition of HEDs is shared by silicates from main group pallasites, mesosiderites, and IIIAB iron meteorites; this can be taken to imply a common parent body [7]. The absence of distinctive reflection spectra of Fe metal from Vesta implies that the surface of Vesta is not the source of some or all of these meteorites. Either a basaltic veneer resurfaced the asteroidal rubble pile from which the HED-pallasite (main group)-mesosiderite-IIIAB iron association was derived, or there are other differentiated asteroidal bodies from which some or all of these meteorites were derived.

References: [1] Dreibus G. et al. (1977) *Proc. LSC 8th*, pp. 211–227. [2] Morgan J. W. et al. (1978) *GCA, 42*, 27–38. [3] Humayun M. and Clayton R. N. (1995) *GCA, 59*, 2131–2148. [4] Jochum K. P. and Palme H. (1990) *Meteoritics, 25*, 373–374. [5] Jurewicz A. J. G. et al. (1993) *GCA, 57*, 2123–2139. [6] Zolensky M. E. et al. (1996) *Meteoritics & Planet. Sci., 31*, 518–537. [7] Clayton R. N. and Mayeda T. K. (1996) *GCA, 60*, 1999–2017. [8] Humayun M. and Clayton R. N. (1994) *LPS XXV*, pp. 579–580. [9] Taylor S. R. and Norman M. D. (1990) in *Origin of the Earth* (H. E. Newsom and J. H. Jones, eds.), pp. 29–43, Oxford, New York. [10] Boss A. P. (1993) *Astrophys. J., 417*, 351–367. [11] Cassen P. (1996) *Meteoritics & Planet. Sci.*, in press. [12] Binzel R. P. and Xu S. (1993) *Science, 260*, 186–191.

MULTISPECTRAL LIGHT CURVES OF VESTA.

R. Jaumann, A. Nathues, S. Mottola, and H. Hoffmann, German Aerospace Research Establishment, Institute of Planetary Exploration, 12484 Berlin, Rudower Chaussee 5, Germany.

In order to characterize its compositional heterogeneity we have carried out time-resolved CCD spectrophotometry of 4 Vesta during its last apparition in 1996.

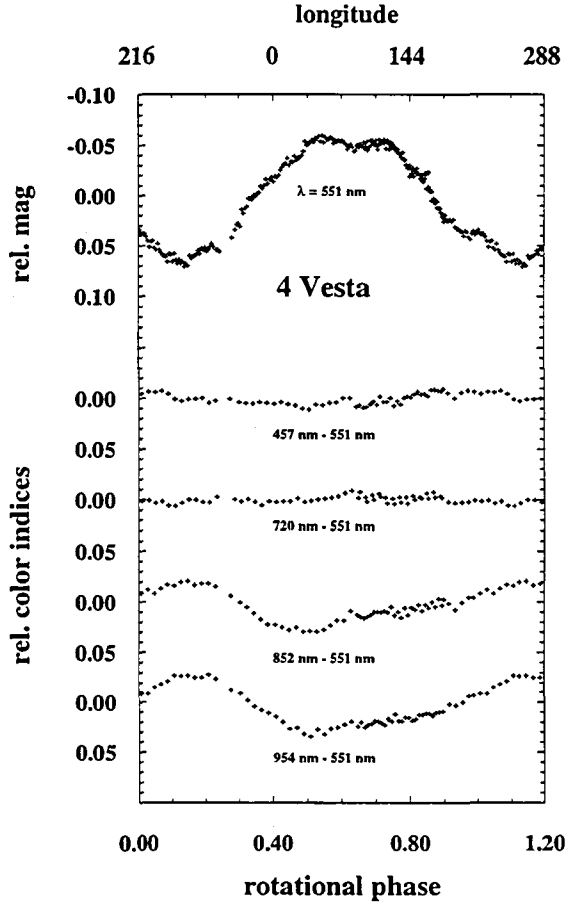

Fig. 1. Light curve at 551 nm and color indexes.

The observations have been performed from the European Southern Observatory (La Silla, Chile), with the DLR CCD camera attached at the Bochum 24" telescope using a set of five interference filters covering the spectral range 0.45–0.95 μm. In order to obtain the high photometric accuracy necessary to reveal subtle color variations, we have performed on-chip differential photometry against a field star, which allows effective correction for short-term atmospheric extinction fluctuations. The observations were therefore carefully planned and scheduled for one night when 4 Vesta was passing close to a bright star (SAO 140637). Measurements in each filter were automatically cycled over about 5 hr, in order to fully cover an asteroid's rotational period. Only the small portion of the CCD actually containing 4 Vesta and the comparison star was read out, which allowed us to have a very fast duty cycle of about 90 s. A G0-type star (BS 5779) located less than 2° from the Vesta field was acquired during its passage at meridian, in order to provide reflectance calibration. The resulting dataset of ~1000 frames was preprocessed using bias frames and twilight sky flat fields, while photometry was computed by using ASTPHOT, a synthetic aperture program developed at DLR. Extinction correction was derived directly by dividing the flux of the asteroid by the on-field comparison star, while higher-order, differential extinction coefficients were neglected due to the comparatively narrow bandwidth of the filters used.

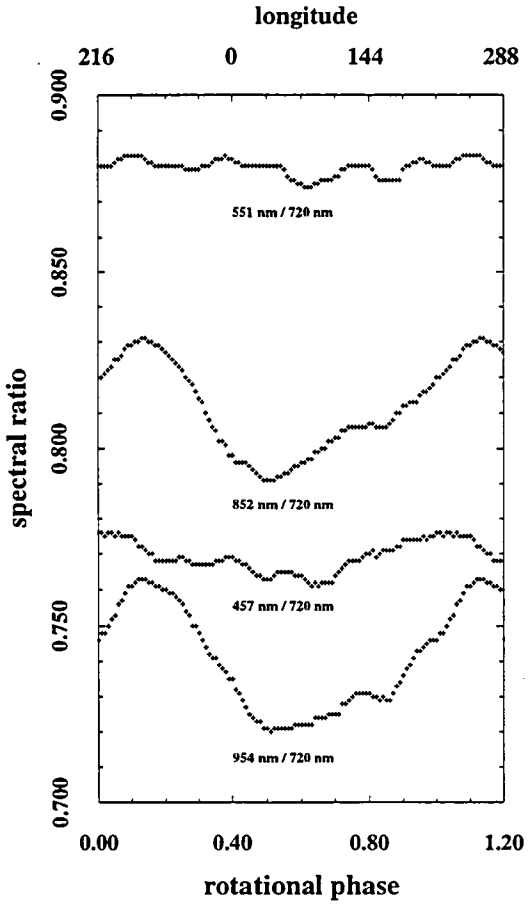

Fig. 2. Time-resolved spectral ratios relative to 720 nm.

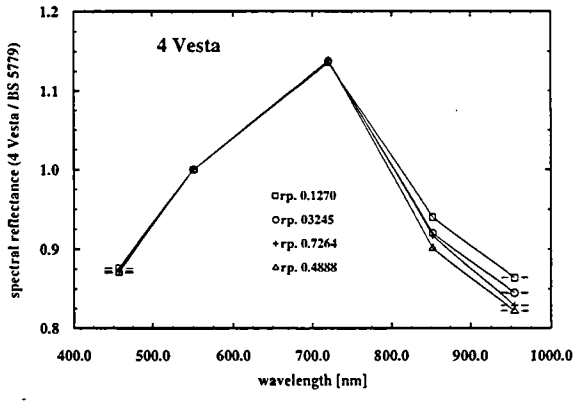

Fig. 3. Spectra at different rotational phases.

The resulting light curves (Fig. 1) have an RMS error of ~0.003 mag, and the absolute flux calibration against the reference star results in errors of ~0.01 mag.

In order to detect rotation-induced spectral variations, we have computed color indexes relative to the 550-nm filter, which is taken as a reference. Since the measurements in the different spectral channels, although very close in time, were not acquired strictly simultaneously, we have interpolated the reference light curve with a high-order Fourier polynomial, and subtracted this from each individual data point in the other spectral channels. This assures that no light-curve-induced shift produces spurious effects in the color light curves. The resulting time-resolved color indexes are shown in Fig. 1. In order to reduce the number of data points displayed in the graph, four adjacent measurements were averaged, resulting in about 50 data points per light curve.

The time-resolved spectral variability of Vesta has been estimated by calculating the spectral ratios relative to the 720-nm filter (Fig. 1). Spectral variations that occur at distinct positions of the rotation phase correspond to compositional heterogeneities on Vesta's surface. The strongest variations are found between 0.4 and 0.8 rotation phases in the near-infrared wavelength range. The spectral signatures at different rotational phases (Fig. 3) indicate that the spectral variations are correlated with the 1-μm absorption band of Fe-bearing silicates. Statistically, at least three types of spectrally different materials can be separated based on a principal component analysis:

1. Materials showing the weakest absorption in the NIR spectral range cover the rotation phases <0.35 and >0.9 (215° to 320° longitude). These materials may reflect Vesta's ancient crust of surface lava, which is expected to be eucritic in composition.

2. Materials that exhibit strong absorptions in the 852-nm to 954-nm spectral range. These materials occur on Vesta's surface from ~0.35 to 0.9 rotation phases (320° to 215° longitude) and are interpreted as relatively pyroxene-rich subsurface materials that have been mixed up with surface lava by impact processes.

3. Embedded in the above mentioned surface unit, a further increase of the absorption at 852 nm and less pronounced at 954 nm can be observed near 0.5 rotation phases. Due to the restricted spectral coverage of our observation, it cannot be decided whether this feature is caused by orthopyroxene-rich or olivine-rich materials. However, this feature is closely related to a dark circular area called Olbers that was observed in the Hubble Space Telescope images and is interpreted as deep impact that reveals mantle mate-

rial [1]. A dunite-rich feature on Vesta was already reported by [2] based on telescopic observations with high spectral resolution.

4. Weak spectral variation in the visible spectral range may reflect spectral reddening, which is caused by alterations of the surface regolith due to "cosmic" weathering processes.

References: [1] Zellner B. et al. (1995) World-Wide Web pages of Hubble Space Telescope. [2] Gaffey M. (1983) *LPS XIV*, pp. 231–232.

THE ORIGIN OF EUCRITES: AN EXPERIMENTAL PERSPECTIVE. J. H. Jones[1], D. W. Mittlefehldt[2], A. J. G. Jurewicz[3], H. V. Lauer Jr.[2], B. Z. Hanson[1], C. R. Paslick[4], and G. A. McKay[1], [1]Mail Code SN4, NASA Johnson Space Center, Houston TX 77058, USA, [2]Mail Code C23, Lockheed Martin Engineering and Sciences Company, 2400 NASA Road 1, Houston TX 77058, USA, [3]3463 Barry Avenue, Los Angeles CA 90066, USA, [4]Physical Science Division, Rock Valley College, 3301 North Mulford Road, Rockford IL 61114, USA.

The origin of eucrites has been the subject of debate. At issue is whether high-Mg# eucrites such as Sioux County are primitive or evolved liquids. We believe that the problem of the origin of eucrites is essentially solved. Problems associated with the petrogenesis of other achondrite groups remain, but the eucrites, taken as a whole, seem to present a clear and understandable story that we will present using experiments, analyses, and calculations.

The two traditional eucrite groupings, the partial melting trend (a.k.a. Stannern trend) and the fractional crystallization trend (a.k.a. Nuevo Laredo trend) have both been reproduced experimentally. The partial melting trend culminates in Sioux County. Sioux County is also an acceptable starting point for the fractional crystallization trend. The implication of these experimental results is that it is extremely difficult to relate the eucrites to diogenites, a group of pyroxene cumulates that conceivably could have crystallized from eucrite parent magmas.

Chemical Signatures of Eucrites: 1. Most eucrites have Cr_2O_3 concentrations of 0.30–0.32 wt% [1], translating into Cr/La ratios that are distinctly low relative to chondritic. Experimentally, it has been determined that these Cr concentrations are the signature of chromite saturation at an fo_2 of IW-1, in the temperature range 1170°–1200°C [1]. This is perhaps the strongest evidence that most eucrites are actual liquids, not partial cumulates or impact melts.

2. Most eucrites that meet the Cr_2O_3 spinel-saturation criterion can be reasonably assigned to either a partial melting or fractional crystallization trend. Within the partial melting trend Mg# is essentially constant, but Al_2O_3 and V concentrations increase as melting proceeds. Conversely, REE concentrations, TiO_2 concentrations, and the magnitude of the negative Eu anomaly decrease as melting increases. At the degree of partial melting that produced Sioux County, the chondrite-normalized REE pattern is flat and the Eu anomaly has disappeared. Within the fractional crystallization trend, these chemical characteristics of the partial melting trend are replayed, in reverse order, as crystallization proceeds (except that Mg# decreases).

3. Most eucrites have approximately chondritic relative abundances of refractory-lithophile-incompatible elements. However, relative to other refractory lithophiles, Sc and V (in like manner to Cr) are quite depleted. This is because they are more compatible than elements such as La and U.

Experimental Reproduction of the Partial Melting Trend: Murchison partial melting experiments [1] mimic the partial melting trend of eucrites. These experiments were performed at 1160°–1200°C at 1-bar pressure and an fo_2 of IW-1. The 1180°C Murchison melt is almost indistinguishable from Sioux County in terms of its major-element composition. The only serious disagreement is for MnO, presumably because Murchison itself is depleted in MnO relative to the EPB. Vanadium analyses of the Murchison partial melts reinforce the conclusions from the major and minor elements. Thus, of the depletions in refractory lithophile elements observed in eucrites (i.e., Sc, V, Cr), two of these, V and Cr, have been reproduced experimentally.

Experimental Reproduction of the Fractional Crystallization Trend: Fractional crystallization experiments have not been performed on a primitive eucrite, but equilibrium crystallization experiments have [2]. And differences between equilibrium and fractional crystallization trends are thought to be small, as long as the degree of crystallization is not large. Major and minor elements in these experimental glasses track the eucrites of the fractional crystallization trend well. The fractional crystallization trend can be reproduced by ~40% crystallization of a Sioux County composition from ~1180°C to ~1140°C.

Experimental Partitioning of Sc and V: Several types of experiments and broadly eucritic experimental compositions have been used to study Sc and V partitioning and to relate these results to eucrites [3]. Systematics of partitioning with composition and temperature have been observed and have been used to define partition coefficients (D) for olivine, low-Ca pyroxene, and spinel at the 1180°C liquidus temperature of Sioux County. These Ds can be used to calculate the degree of partial melting and the mineralogy of the source region. The correctness of the partial melting model can be evaluated with hindsight, based on the ability of the model to reproduce the observed Sc and V depletions in Sioux County. Both the Sc and V calculations predict that Sioux County was produced by ~20% partial melting, leaving behind a residuum that contained 94% olivine, 6% low-Ca pyroxene, and a trace of chromite.

It is significant that the Sc and V calculations agree. Vanadium is compatible and Sc is incompatible during silicate partial melting. Therefore, any deviation of the model from that of the actual situation should cause the solutions for V and Sc to diverge. The most uncertain portion of this exercise is the V content of Sioux County. The most reliable V analysis [4] yielded 114 ppm, but this sample was slightly enriched in pyroxene, making this an upper limit. Our current best estimate of the Sioux County V content is 90–100 ppm.

We take confidence from the convergence of the Sc and V model results. Moreover, the results of the calculation agree with the modal mineralogy of our 1180°C Murchison experiment, whose partial melt greatly resembled Sioux County. We take this as evidence that high-Mg# eucrites such as Sioux County are produced by simple partial melting. The implication of this exercise is that the chemical signatures of partial melting trend eucrites are dominated by olivine/liquid equilibria and that diogenites and eucrites are not related by liquid-line-of-descent. This result is mineralogical in nature and should be independent of small changes in intensive variables such as pressure [e.g., 5].

References: [1] Jurewicz A. J. G. et al. (1993) *GCA, 57*, 2123–2139. [2] Stolper E. M. (1977) *GCA, 41*, 587–611. [3] Hanson B. Z. et al. (1995) *Meteoritics, 30*, 516–517. [4] Mittlefehldt D. W. (1979) *GCA, 43*, 1917–1935. [5] Bartles K. S. and Grove T. L. (1991) *Proc. LPS, Vol. 21*, pp. 351–365.

PRACTICAL EVALUATION OF REGOLITH MATURATION PROCESSES. L. Ksanfomality[1] and W. K. Hartmann[2], [1]Space Research Institute, 84/32 Profsoyuznaya Street, Moscow, 117810, Russia, [2]Planetary Science Institute, 620 N. 6th Avenue, Tucson AZ 85705, USA.

Observational understanding of the degree of differentiation on asteroid surfaces is clouded by questions of regolith evolution and hypothetical "space weathering." Recent debates about the existence of "space weathering," and whether it modifies S-type asteroids to look like chondrites, have not answered these questions [1]; nonetheless, it is clear that some maturation of airless surfaces occurs that suppresses spectral signatures.

Referring to this general process as "maturation" (to avoid the controversy about space weathering), we suggest that an important next step is direct study of surface materials and the maturation process *in situ*. A good opportunity to clarify regolith accumulation and maturation is offered by Phobos, because it is likely to be revisited in the next decade, and we can plan specific observations in advance. Phobos is not ideal in the context of understanding differentiated asteroids, because it is probably not differentiated and may have a "nonasteroidal" gardening regime by virtue of reabsorbing some of its own ejecta as well as debris from Mars; nonetheless, Phobos offers excellent opportunities to study aspects of the maturation process, with the advantage that we already know positions of relevant sites on its surface.

For example, the PHOBOS II spacecraft revealed examples of the maturation process through spectral differences between fresher Phobos craters and older background areas. A specific example is a crater about 300 m deep, at 25°N and 245°W on Phobos. The spectrum of its interior is much flatter (less red) than spectra of the surrounding area. The implication is that the background surface material is different from the freshly excavated material. Other known surface features (Stickney, crater chains, grooves, etc.) offer opportunities to clarify theories of regolith accumulation and impact processes on small bodies.

Knowing the location of such features in advance permits preplanning of observations to clarify the nature of the maturation process on future Mars orbital missions that involve close approaches to Phobos. These observations should, in turn, constrain theories of regolith maturation on all classes of asteroids.

References: [1] Binzel R. P. (1996) *Meteoritics & Planet. Sci., 31*, 165.

THE VESTA ASTEROID FAMILY: ORIGIN AND EVOLUTION. F. Marzari[1], A. Cellino[2], D. R. Davis[3], P. Farinella[4], V. Zappalà[2], and V. Vanzani[1], [1]Dipartimento di Fisica, Università di Padova, Via Marzolo 8, I-35131 Padova, Italy, [2]Osservatorio Astronomico di Torino, I-10025 Pino Torinese, Italy, [3]Planetary Science Institute/SJI, 620 N. Sixth Avenue, Tucson AZ 85705-8331, USA, [4]Gruppo di Meccanica Spaziale, Dipartimento di Matematica, Università di Pisa, Via Buonarroti 2, I-56127 Pisa, Italy.

In the latest family search by Zappalà et al. [1] with a 12,487-asteroid sample, the size of the Vesta family has increased to more than 200 objects. The large gap in size between Vesta and other family members strongly suggests that the Vesta family was generated by an energetic impact cratering event, ejecting a large number of fragments from Vesta's surface at speeds exceeding ≈350 m/s (Vesta's escape velocity). Recent images of Vesta obtained with the Hubble Space Telescope [2] have confirmed the presence of large-scale albedo and color variegation of the surface that can be interpreted as distinct impact basins product of giant impacts that exposed deeper strata on the asteroid surface. High-velocity ejecta from Vesta can be inserted into Earth-crossing orbits by the 3:1 jovian mean motion resonance and become near-Earth asteroids (NEAs) and meteorites. Howardite/eucrite/diogenite (HED) basaltic achondrite meteorites and several NEAs display reflectance spectra nearly identical to that of Vesta. This spectral relationship suggests that Vesta might be the parent body of these objects.

We have adopted a numerical approach to model the cratering event(s) on Vesta that generated the family, and to simulate the subsequent evolution of the family due to catastrophic collisions with "background" asteroids [3]. Comparing the size and orbital distribution of the model Vesta families with the observed family, we estimate the number and size of the projectile(s) that have impacted Vesta and the age of the family itself. Our model also keeps track of the orbital distribution of the small fragments generated by the cratering impacts in order to match the observed features of the family and to study the possible connection between Vesta's ejecta and the 3:1 resonance.

In our model the amount of mass excavated in the cratering process is computed with the scaling approach described in Holsapple [4] and the distribution of the number of fragments vs. size is described with a single-exponent power-law, in reasonable agreement with the results from laboratory-scale impact craters, nuclear explosion craters, and ejecta from large terrestrial and lunar impact craters. The three-dimensional velocity field of the fragments has been computed by assuming a conical distribution of the velocity vectors around the perpendicular to the impact site, as suggested by most small-scale experiments performed in a vacuum [5].

According to our numerical modeling, there are two possible scenarios for the formation of the Vesta family: (1) The family is the outcome of a major cratering event, resulting from the impact of an asteroid ≈40 km in diameter on the surface of Vesta ~1 G.y. ago, followed by another more recent lower-energy impact (by a projectile ≈20 km in diameter), producing the family's subgrouping close to the 3:1 mean motion jovian resonance. This is in agreement with Gaffey's [6,7] rotationally resolved spectroscopic observation of Vesta, suggesting that more than one large crater is present on its surface; moreover, impacts with projectiles some 20 km across should occur on Vesta every 0.5–1 G.y., according to the current estimates on the main belt population. (2) A single impact by an ≈40-km-sized projectile occurred ≈1 G.y. ago and formed the whole family at the same time. In this case we have to assume that the fragments were ejected isotropically over a hemispheric region of Vesta, whose axis is perpendicular to the surface at the impact site, instead of being concentrated near the surface of a cone, as suggested by laboratory impact experiments with planar targets. This different ejection geometry yields a more scattered orbital distribution of the fragments, resulting in better agreement with the observed family.

An interesting aspect of our numerical approach is the computation of the orbital element distribution of the family at different evolutionary stages. Comparing the family distribution with the location of the 3:1 jovian resonance, we can estimate how many fragments from the family-forming cratering event(s) could be in-

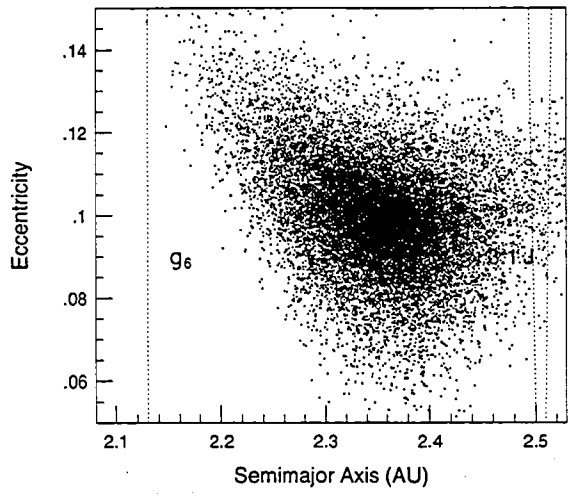

Fig. 1.

jected into this resonance and then inserted into Earth-crossing orbits, becoming V-type near-Earth asteroids and HED meteorites. As shown in Fig. 1, several tens of fragments a few kilometers in diameter (and many more smaller ones, according to the assumed power-law size distribution of the ejecta) were delivered to the 3:1 resonance. In other words, in its early stages the Vesta family extended enough in proper element space to reach (and overlap) the resonance and inject a significant number of kilometer-sized and smaller fragments into the 3:1 resonance, thus generating V-type near-Earth asteroids and HED meteorites. Later on, the collisional erosion process produced a shrinkage of the family, making the identification of the link with the resonance more difficult.

References: [1] Zappalà V. et al. (1995) *Icarus, 116*, 291. [2] Zellner B. et al. (1995) *LPS XXVI*, p. 1553. [3] Marzari F. et al. (1995) *Icarus, 113*, 168. [4] Holsapple K. A. (1993) *Annu. Rev. Earth Planet. Sci., 21*, 333. [5] Melosh H. J. (1989) *Impact Cratering*, Oxford Univ., New York. [6] Gaffey M. J. (1983) *LPS XIV*, p. 231. [7] Gaffey M. J. (1996) *Icarus*, submitted.

A DYNAMICAL STUDY OF VESTA-FAMILY FRAGMENTS.

F. Migliorini[1], V. Zappalà[2], A. Morbidelli[3], and A. Cellino[2], [1]Armagh Observatory, College Hill Armagh, BP61 9DG Northern Ireland, UK, [2]Osservatorio Astronomico di Torino, strada Osservatorio 20, 10025 Pino Torinese (TO), Italy, [3]OCA, Observatoire de Nice, BP 229, 06304 Nice Cedex 4, France.

We have for the first time performed an extensive numerical analysis of the orbital evolution of fragments possibly ejected from 4 Vesta as a consequence of the event that created the dynamical family associated with this asteroid. It was shown in the past [1] that V-type plausible fragments from 4 Vesta actually make a bridge between the location of the family and both the 3:1 mean-motion resonance with Jupiter and the ν_6 secular resonance. Moreover, three NEAs (3551 Verenia, 3908 1980 PA, and 4055 Magellan) have been found to exhibit reflectance spectra typical of V-type asteroids [2]. Using a procedure recently developed [3] in order to reconstruct the original velocity field of the fragments from family-forming events, we have derived the most plausible features of the original event. Accordingly, we have generated a number of fictitious fragments originating from this family. In particular, we considered 125 fragments ejected into the 3:1 resonance, and 55 ejected into the ν_6 secular resonance. The dynamical evolution of these objects has been computed through numerical integrations spanning about 4 m.y. Moreover, the orbits of the three V-type NEAs mentioned above, as well as five fictitious "clones" for each of them, have also been integrated over the same time span. In the case of 4055 Magellan and its five clones, the integration was carried out over 10^7 yr. In spite of the fact that the time span of our integrations is not very long, we find some interesting and surprising results, which are summarized as follows:

1. About 30% of the fragments located in both the 3:1 and the ν_6 resonances die as Sun grazers within a few million years.
2. The volume of the phase space covered by the known V-type NEAs is better fitted by the set of fictitious fragments put into the ν_6 secular resonance, rather than by those initially located in the 3:1 mean-motion resonance. The observed behavior strongly suggests that the presently known V-type NEAs come from Vesta through the ν_6.
3. The orbital evolution of 3551 Verenia is dominated by the ν_6 resonance and by Earth encounters. As a consequence, it has a high probability (66%) of dying within the next 4 m.y.
4. 3908 1980 PA has been found to be controlled by the influence of Earth, and has a 50% probability of dying within the period of integration inside the 3:1 resonance.
5. 4055 Magellan is the V-type NEA with the longest lifetime. Neither it nor any of its clones have been found to die within 10 m.y. However, three of its five clones become Earth crossers within the timescale of our integrations.
6. Some fragments are also found to be ejected from the solar system basically under the control of Jupiter or Saturn.

References: [1] Binzel R. P. and Xu S. (1993) *Science, 260*, 186. [2] Cruikshank D. P. et al. (1991) *Icarus, 89*, 1. [3] Zappalà V. et al. (1996) *Icarus*, in press.

CORE FORMATION IN THE HOWARDITE-EUCRITE-DIOGENITE PARENT BODY (VESTA).

H. E. Newsom, Institute of Meteoritics, Department of Earth and Planetary Sciences, University of New Mexico, Albuquerque NM 87131, USA.

Recent images of Vesta by the Hubble Space Telescope indicate that Vesta may be a surprisingly diverse world with an exposed mantle, basaltic crust, and impact basins. A large amount of evidence points to Vesta as being the source of the howardite-eucrite-diogenite (HED) clan of achondrite meteorites [e.g., 1]. The study of the differentiated meteorites provides clues to the origin and evolution of asteroid parent bodies and the heat sources that melted them [2–4]. Such bodies may have also represented planetary building blocks in the inner solar system [5]. This work describes problems involving core formation and the igneous evolution of the HED parent body as constrained by the abundances of the siderophile elements.

Detailed modeling of core formation in the HED parent body suggests a large Fe-rich core [2,3,6]. The relationship of the core formation event to the igneous differentiation that produced the HED clan is still uncertain. Recent work by Mittlefehldt [7] and Fowler et al. [8] suggests that the diogenites formed in the following

manner: An original chondritic source region first experienced partial melting and the removal of eucritic melts; subsequent melting of this residual source region produced the parental magmas from which the diogenites formed by fractional crystallization. This model is thus consistent with the partial melting model of Stolper [9] for the eucrites. Newsom and Drake [2] argued that siderophile-element abundances for the trend-A eucrites [10] was the same as for the main-group eucrites, with serious consequences for the core formation event. Basically, core formation must have occurred during the initial melting events, at a very low degree of partial melting, with all subsequent igneous fractionation occurring in the absence of metal. The test of this model is to determine if the normalized siderophile-element contents of the initial melts for different eucrites are similar or different. Limited siderophile-element data for the incompatible-rich trend-B-class meteorite Pomozdino [11] and Y 74450, Stannern, and Bouvante provide some constraints (Fig. 1, data referenced in [3] and [11]). The Pomozdino eucrite is an unusual, magnesian, yet incompatible-rich eucrite [12]. The few measured siderophile-element abundances for this meteorite are higher than the depletions observed in all other eucrites, and closer to the abundance in AdoR. The abundances of W, normalized to La, are also higher in Y 74450, Stannern, and Bouvante compared to most of the other eucrites, except for Ibitira. Thus the siderophile-element abundances support a partial melting model, although given the uncertainties in the bulk mineral/melt partition coefficients for elements such as W in the HED, we cannot exclude other models. There is also the problem of core formation at very low degrees of partial melting. The possibilities include very low degrees of partial melting consistent with the Stolper [9] model, or high degrees of partial melting implying a magma ocean model to explain the igneous fractionation trends. Metal segregation at low degrees of partial melting may not be possible [13,14], although studies by Herpfer and Larimer [15] and Jurewicz and Jones [16] challenge this premise. Understanding the physics of core formation will be important for the understanding the evolution of the HED parent body.

The Cameca 4f SIMS facility of the Institute of Meteoritics is being developed to determine the abundance of siderophile elements in metal phases present in HED materials. For example, eucrites contain ubiquitous metal with an abundance usually less than 1 wt%. The metal in eucrites and diogenites has only been studied by electron microprobe techniques [17,18]. The low Ni content of the eucrite metal suggests that this metal has formed by reduction, and we plan to see whether the metal quantitatively contains the siderophile elements in the rocks, and whether the formation of the metal contains clues to the origin of the magmas. Early work by Drake et al. [19] showed the promise of using the SIMS for metal analysis, and the Cameca 4f has many advantages over the older instruments, including O and Cs ion sources. A collection of meteoritic and NIST metal standards has been assembled that will allow the calibration for many siderophile elements to be thoroughly tested.

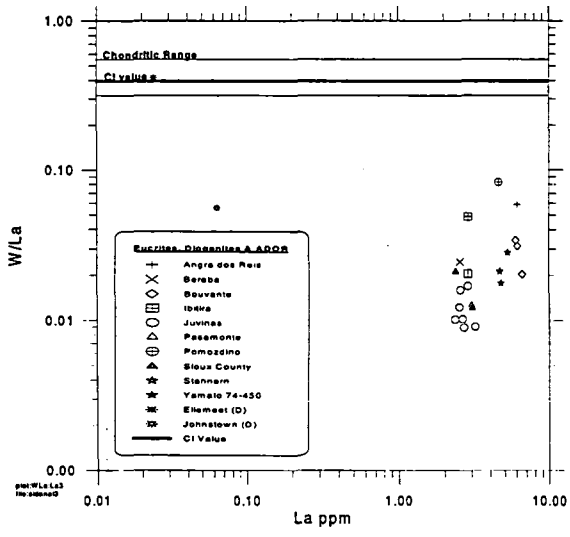

Fig. 1. La:W/La log-log plot of eucrites and diogenites.

References: [1] Binzel R. P. and Xu S. (1993) *Science, 260,* 186–191. [2] Newsom H. E. and Drake M. J (1982) *GCA, 46,* 2483–2489. [3] Hewins R. H. and Newsom H. E. (1988) (J. F. Kerridge and M. Matthews, eds.), pp. 73–101, Univ. of Arizona, Tucson. [4] Scott E. R. D. et al. (1989) in *Asteroids II,* pp. 701–739, Univ. of Arizona. [5] Taylor S. R. and Norman M. D. (1990) in *Origin of the Earth* (H. E. Newsom and J. H. Jones, eds.), pp. 29–44, Oxford, New York. [6] Newsom H. E. (1985) *Proc. LPSC 15th,* in *JGR, 90,* C613–C617. [7] Mittlefehldt D. W. (1994) *GCA, 58,* 1537–1552. [8] Fowler G. W. et al. (1995) *GCA, 58,* 3921–3929. [9] Stolper E. (1977) *GCA, 41,* 587–611. [10] Ikeda Y. and Takeda H. (1985) *Proc. LPSC 15th,* in *JGR, 90,* C649–C663. [11] Newsom H. E. et al. (1989) *Meteoritics, 24,* 308–309. [12] Warren P. H. and Jerde E. A. (1988) *LPS XIX,* pp. 1234–1235. [13] Taylor G. J. (1992) *JGR, 97,* 14717–14726. [14] Stevenson D. J. (1990) in *Origin of the Earth,* pp. 231–250, Oxford, New York. [15] Herpfer M. A. and Larimer J. W. (1993) *Meteoritics, 28,* 362. [16] Jurewicz S. R. and Jones J. H. (1994) *LPS XXV,* pp. 653–654. [17] Duke M. B. (1965) *JGR, 70,* 1523–1527. 118] Gooley R. and Moore C. B. (1976) *Am. Mineral., 61,* 373–378. [19] Drake M. J. et al. (1984) *GCA, 48,* 1609–1615.

PYROXENE HOMOGENIZATION AND THE ISOTOPIC SYSTEMATICS OF EUCRITES.

L. E. Nyquist and D. D. Bogard, Mail Code SN4, NASA Johnson Space Center, Houston TX 77058, USA.

The original Mg-Fe zoning of eucritic pyroxenes has in nearly all cases been partly homogenized, an observation that has been combined with other petrographic and compositional criteria to establish a scale of thermal "metamorphism" for eucrites [1]. To evaluate hypotheses explaining development of conditions on the HED parent body (Vesta?) leading to pyroxene homogenization against their chronological implications [e.g., 2,3], it is necessary to know whether pyroxene metamorphism was recorded in the isotopic systems. However, identifying the effects of the thermal metamorphism with specific effects in the isotopic systems has been difficult, due in part to a lack of correlated isotopic and mineralogical studies of the same eucrites. Furthermore, isotopic studies often place high demands on analytical capabilities, resulting in slow growth of the isotopic database. Additionally, some isotopic systems would not respond in a direct and sensitive way to pyroxene homogenization. Nevertheless, sufficient data exist to generalize some observations, and to identify directions of potentially fruitful investigations.

^{39}Ar-^{40}Ar System: The younger ^{39}Ar-^{40}Ar age of 3.98 ± 0.03 G.y. for metamorphic type 1 basalt clast Y 75011,84 [4], compared to Rb-Sr and Sm-Nd ages of 4.56 ± 0.06 G.y. and 4.52 ± 0.16 G.y. [5], establishes that the extensive Ar outgassing observed in many eucrites [6] accompanies thermally weaker events than those leading to pyroxene homogenization. Bogard and Garrison [7] determined that the type 5 thermal event observed in nonbrecciated Ibitiria predated its ^{39}Ar-^{40}Ar age of 4.495 ± 0.015 G.y. Yamaguchi et al. [2] concluded that pyroxene equilibration for eucrites of types 4–6 occurred at final temperatures of ~720°–880°C, was prolonged, and may have been global in scale.

Rb-Sr System: The Rb-Sr system presents a somewhat confused picture. Two eucrites of types 1 and 2 (Y 75011,84 [5] and EET 87513,18E [8] respectively) yield well-defined ages of 4.56 ± 0.06 G.y. [5] and 4.49 ± 0.08 G.y. [8]. The Rb-Sr isotopic data for pyroxenes are consistent with the isochrons from which these ages are derived. Alternatively, the Rb-Sr data for pyroxenes from two eucrites of types 5 and 6 (the Bholghati clast [9] and Y 792510,65 [10]) are consistent with younger ages in the range ~3.0–3.5 G.y., similar to the ^{39}Ar-^{40}Ar ages of the same samples. The Rb-Sr data for pyroxenes in many other eucrites are "disturbed." These observations suggest an indirect relationship between the Rb-Sr data and pyroxene homogenization. That is, the Rb-Sr system in pyroxenes of eucrites of high metamorphic grade seems to be nearly as susceptible to resetting as the ^{39}Ar-^{40}Ar systems, but the Rb-Sr system in pyroxenes of eucrites of low metamorphic grade seems to be more resistant to resetting.

Sm-Nd System: Conventional ^{147}Sm-^{143}Nd ages often seem "blind" to pyroxene metamorphic type. This is surprising because, in contrast to the other isotopic systems, the Sm-Nd ages are to a large extent determined by the isotopic data for pyroxene mineral separates. The implied conclusion is that either the thermal event(s) accompanying pyroxene homogenization are too mild to cause equilibration of the Nd isotopes, or they are too early to be resolved from initial crystallization of the eucritic basalt. Although either or both have usually been assumed to be the case, there is evidence that the ^{146}Sm-^{142}Nd system based on decay of short-lived ($t_{1/2}$ = 103 m.y.) may have responded to pyroxene homogenization. Recent data show a tendency for ^{146}Sm/^{144}Sm ratios determined for eucrites of high metamorphic grade to be systematically lower (^{146}Sm/^{144}Sm ~ 0.005) than for angrites and eucrites of lower metamorphic grade (^{146}Sm/^{144}Sm ~ 0.007–0.008). The difference in ^{146}Sm/^{144}Sm corresponds to a "formation" (equilibration?) interval of ~50–70 m.y., but is at the limit of analytical resolution of the current data. Interestingly, the ^{146}Sm-^{142}Nd "formation" intervals are comparable to those obtained by the ^{244}Pu-Xe method [11,12], where they can be compared and are similar to the age difference between ordinary and cumulate eucrites.

^{53}Mn-^{53}Cr System: The extinct radionuclide ^{53}Mn ($t_{1/2}$ = 3.7 m.y.) is shorter lived than ^{146}Sm, and in principle is capable of greater time resolution. Manganese-chromium data are still very sparse, and generalizations are tentative. Lugmair et al. [13] concluded from the inferred initial ^{53}Mn/^{55}Mn ratio of the type 5 eucrite Chervony Kut that it solidified ~6 m.y. before the angrite LEW 86010. Additionally, Wadwha and Lugmair [14] concluded that the unbrecciated eucrite Caldera formed ≥15 m.y. after Chervony Kut. We [10] found the Mn-Cr system of type 6 eucrite Y 792510,65 to be disturbed, with a strong indication that it had been reequilibrated subsequent to complete decay of ^{53}Mn, probably ≥15 m.y. after original crystallization. The Chervony Kut data suggests that either the Mn-Cr system was "blind" to pyroxene homogenization, or that homogenization took place very early in solar system history. The minerals for which Mn-Cr data were reported by [13] may not have responded to the pyroxene homogenization event, since the inferred ^{53}Mn/^{55}Mn ratio is greatly dependent on the Cr-isotopic data for chromite, which because of its high Cr concentration may not have equilibrated with Cr in pyroxene.

It is unclear whether these isotopic chronometers frequently applied to eucrites have responded to the events responsible for homogenization of their pyroxenes. However, the importance of determining the time of pyroxene homogenization to understanding the thermal history of the HED parent body (Vesta?) makes continued combined mineralogical and chronological investigations to HED meteorites a high priority.

References: [1] Takeda H. and Graham A. L. (1991) *Meteoritics, 26,* 129–134. [2] Yamaguchi A. et al. (1995) *LPS XXVI,* pp. 1531–1532. [3] Yamaguchi A. et al. (1996) *GRL,* preprint. [4] Takeda H. et al. (1994) *EPSL, 122,* 183–194. [5] Nyquist L. E. et al. (1986) *JGR, 91,* 8137–8150. [6] Bogard D. (1995) *Meteoritics, 30,* 244–268. [7] Bogard D. and Garrison D. (1995) *GCA, 59,* 4317–4322. [8] Nyquist L. E. et al. (1994) *LPS XXV,* pp. 1015–1016. [9] Nyquist L. E. et al. (1990) *GCA, 54,* 2195–2206. [10] Nyquist L. E. et al. (1996) *GCA,* submitted. [11] Shukolyukov A. and Begemann F. (1995) *LPS XXVI,* pp. 1299–1300. [12] Miura Y. N. (1995) Ph.D. dissertation, Univ. of Tokyo. [13] Lugmair G. W. et al. (1994) *LPS XXVI,* pp. 813–814. [14] Wadwha M. and Lugmair G. W. (1995) *Meteoritics, 30,* 592.

DIOGENITES: CUMULATES FROM ASTEROID 4 VESTA—INSIGHTS FROM ORTHOPYROXENE AND SPINEL CHEMISTRY.

J. J. Papike, L. E. Bowman, M. N. Spilde, G. W. Fowler, and C. K. Shearer, Institute of Meteoritics, Department of Earth and Planetary Sciences, University of New Mexico, Albuquerque NM 87131-1126, USA.

Introduction: Cumulate rocks are important planetary lithologies, but they can be difficult to interpret. Important clues to the nature of their parental melts may still be present in the interiors of cumulus phases. However, in some cases, even the cores of the cumulus grains may have been modified by postcrystallization reactions with trapped melt and other cumulus phases. We have previously studied the major-, minor-, and trace-element chemistry of orthopyroxene from a suite of diogenites [1,2] and concluded that their chemical attributes can best be explained by crystallization from parental melts that were derived from a depleted mantle source that had already experienced eucrite removal [3]. However, we and others [1,2,4] have had difficulty explaining the great range in concentration of minor elements (Al, Ti) and trace elements (REE, Y, Zr) if all diogenites were derived from a single magmatic system. Therefore, we have investigated the chemistry of diogenitic spinels to see if they still held clues to the diogenite parental melt compositions. Although spinel is low in abundance in diogenites (<5 vol% [5]) it still may hold clues to the magmatic and metamorphic history of these rocks.

Results and Discussion: Spinel grains are usually intact, unlike OPX in most diogenites where grains are usually brecciated and core-rim relations are difficult to establish. Thus, our first analytical task was to establish whether any spinel cores still held unmodified

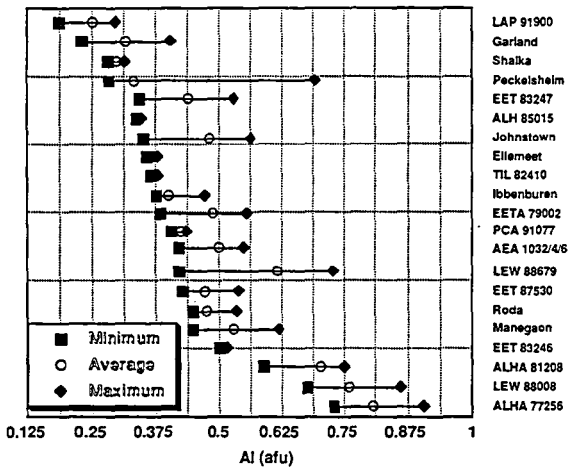

Fig. 1. Aluminum ranges of chromite in diogenites.

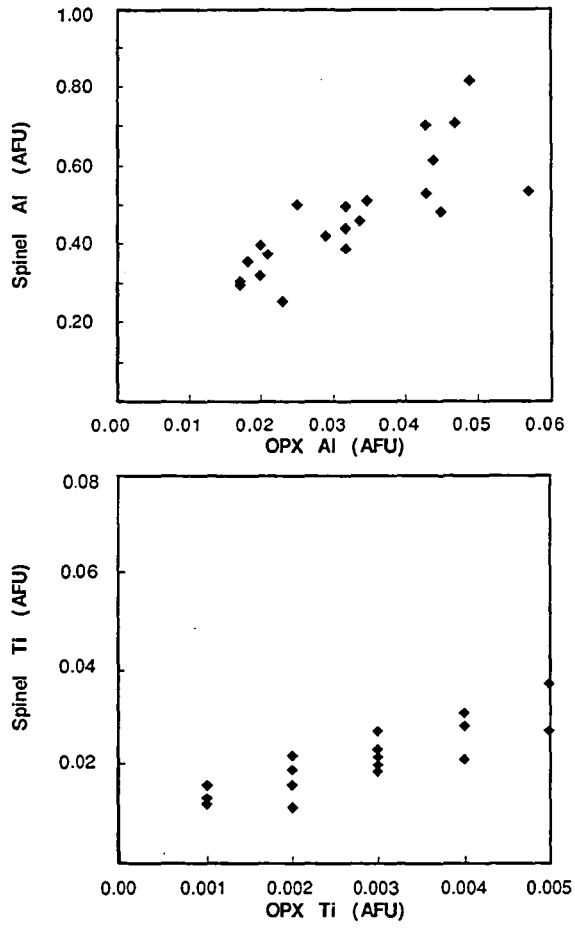

Fig. 2. Spinel vs. OPX.

igneous signatures. We conducted careful electron microprobe traverses, core to rim, on several grains in each sample from the suite of diogenites (Fig. 1). Within each grain, EMP traverses show homogeneous concentrations of Fe, Mg, Cr, and Al. Thus it appears as though spinel compositions have been reset by subsolidus reactions. In spinels from lunar mare basalts that also crystallized under conditions of low fO_2, the early crystallizing spinels are zoned with Cr decreasing and Al and Ti increasing from core to rim [6]. However, after plagioclase crystallizes, Al does not increase as dramatically in lunar spinels as in diogenetic spinels. This is because plagioclase is virtually absent in diogenites [5]. Although, apparently, diogenetic spinel grains lost their core-to-rim chemical systematics, it is possible that the modified Al, Cr, and Ti concentrations still hold clues to melt characteristics and the number of fractionation sequences involved. Before we can interpret our new spinel data further, we must determine the thermal histories of the various diogenite samples. We are in the process of doing this by using orthopyroxene-spinel and olivine-spinel geothermometry. Sack et al. [7] demonstrated that olivine-spinel geothermometry recorded temperatures as low as 700°C for two diogenites. Mittlefehldt [4] used both orthopyroxene-spinel and two-pyroxene geothermometry to show that these systems recorded temperatures from 1050° to 650°C. Mittlefehldt [4] also showed that there is a great range of Al and Cr concentrations in these spinels and that they are negatively correlated. The major solid solution involves the end members magnesio-chromite, chromite $(Mg,Fe^{2+})Cr_2O_4$, and hercynite $(Mg,Fe^{2+})Al_2O_4$. Our dataset shows that Cr varies from ~1.8 to 1.0 afu while Al varies inversely from 0.2 to 1.0 afu.

Figure 1 shows the range of Al found in spinel grains from each diogenite ordered in sequence of increasing Al. Because there is limited zoning within individual spinel grains, the variations reflect grain to grain differences that in turn reflect mixing by brecciation and "within grain" spinel vs. "grain boundary" spinel variability. In a general way, this sequence follows the sequence established for Al in OPX [1]; however, the correlation is far from perfect. Figure 2 plots average Al and Ti values for OPX [1] vs. spinel. There does appear to be a positive correlation between $Al)_{OPX}$ and $Al)_{spinel}$, but there is much scatter on this plot. There also appears to be a positive correlation between $Ti)_{OPX}$ and $Ti)_{spinel}$. Because of its high valence (probably $Ti^{4+} \geq Ti^{3+}$) and thus presumed lower diffusion rate, Ti may be the best of the spinel minor elements for retaining a record of the igneous history of these samples.

Conclusions: Although we are in the early stage of our diogenetic spinel data interpretation, there does appear to be some record of the igneous history in the Al and Ti concentrations. However, a quantitative inversion of these data to parental melt concentrations appears impossible, even if we had appropriate Ds, because the spinel compositions have been modified by postcrystallization reactions.

Acknowledgments: This research was funded by NASA grant NAGW-3347, the Institute of Meteoritics, and a NASA National Space Grant Fellowship to L. Bowman.

References: [1] Fowler G. W. et al. (1994) *GCA, 58*, 3921–3929. [2] Fowler G. W. et al. (1995) *GCA, 59*, 3071–3084. [3] Stolper E. (1977) *GCA, 41*, 587–611. [4] Mittlefehldt D. W. (1994) *GCA, 58*, 1537–1552. [5] Bowman L. E. et al. (1996) *LPS XXVII*, pp. 147–148. [6] Papike J. J. et al. (1976) *Rev. Geophys. Space Phys., 14*, 475–540. [7] Sack R. O. et al. (1991) *GCA, 55*, 1111–1120.

SHAPE AND ALBEDO VARIATIONS OF ASTEROID 4 VESTA. K. L. Reed[1], M. J. Gaffey[2], and L. A. Lebofsky[3], [1]Hawai'i Institute of Geophysics and Planetology, University of Hawai'i at Mānoa, 2525 Correa Road, Honolulu HI 96822, USA, [2]Department

of Earth and Environmental Sciences, Rensselaer Polytechnic Institute, 110 8th Street, Troy NY 12180-3590, USA, [3]Lunar and Planetary Laboratory, University of Arizona, Tucson AZ 85721, USA.

Near-infrared reflected and thermal emitted light curves were measured concurrently for asteroid 4 Vesta and were used to calculate relative projected area and relative albedo variations over its surface. The technique for calculating relative variations in projected area and albedo from simultaneously measured reflected and emitted light curves can be used to detect changes in shape and surface brightness of asteroids [1].

Near-infrared (0.55 μm, 0.575 μm, 0.60 μm) and thermal infrared (10.2 μm) photometric data (Fig. 1; only 0.575-μm near-infrared data are shown) were taken for asteroid 4 Vesta in December 1994 at the NASA Infrared Telescope Facility using the PRIMO2 near-infrared spectrophotometer and BOLO thermal infrared bolometer instruments. Light curves were generated for these data using a rotational period of 5.342 hr and a zero time of 0900 20 December 1994 UT. The data were taken with 4 Vesta showing southern latitudes sub-Earth (–17° to –50° latitude dependent upon pole position used).

Observing the three reflected flux light curves and the emitted flux light curve, the most obvious common feature is the sharp peak in relative flux at 0.61 rotational phase (rp). Other than this feature, there appears to be little similarity between the reflected flux and emitted flux light curves. This indicates that only a small portion of 4 Vesta's reflected light curve is dependent upon shape. Correlations between the reflected and emitted light curves include (1) a minimum in the thermal flux coinciding with the onset of the flat region (the "plateau") in the reflected flux at approximately 0.25 rp;

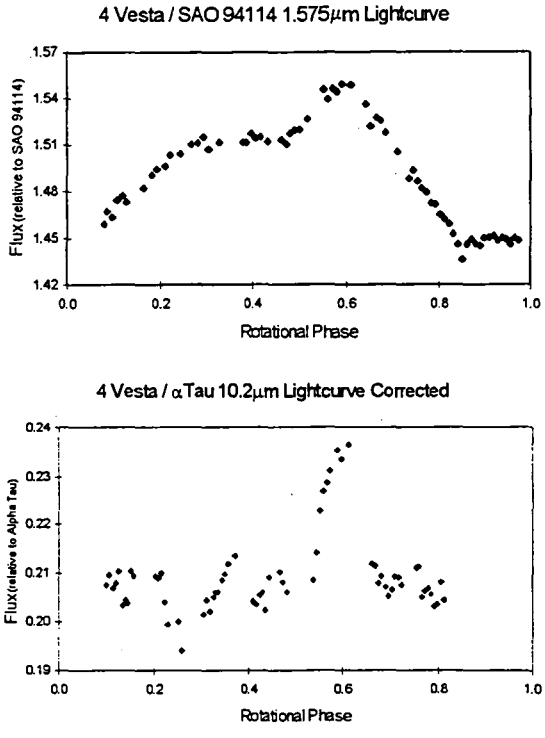

Fig. 1.

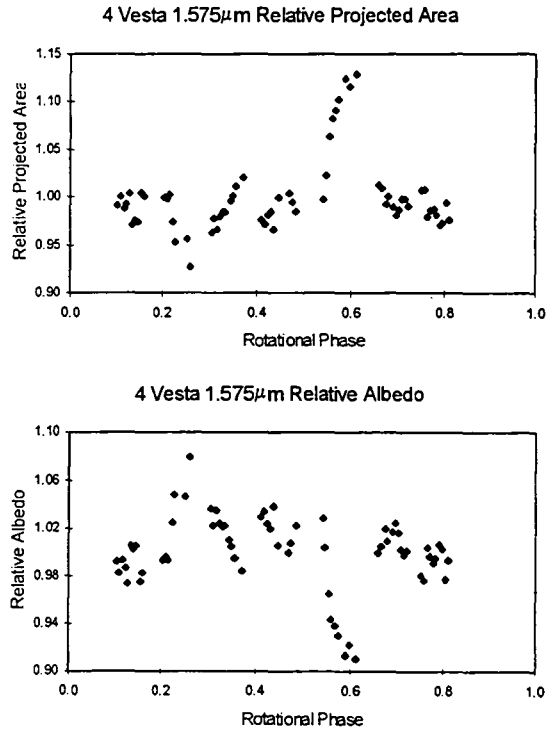

Fig. 2.

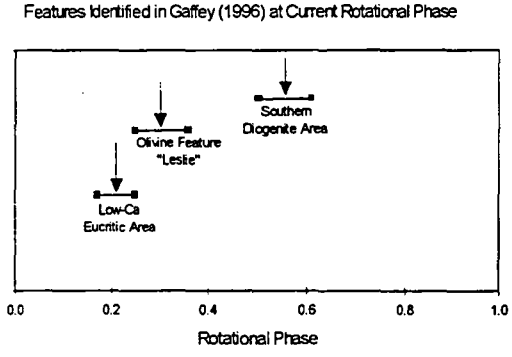

Fig. 3.

(2) a slightly varying thermal flux over the flat reflected light curve plateau region between 0.25 rp and 0.50 rp; and (3) the peaks in both reflected and emitted flux at 0.61 rp. The first two are indicative of albedo changes across this region while the last is characteristic of a change in projected area.

The reflected flux and emitted flux light curves were interpolated to a common set of rotational phase values and the paired reflected/emitted fluxes were used to calculate projected area and albedo for each given rotational phase. These area and albedo values were divided by the average value over a rotation, giving relative changes in projected area and albedo throughout a rotation. The projected area curves (Fig. 2; only data for the 0.575-μm light curve are shown) indicate the limb of 4 Vesta to have protrusions that vary the observed projected area as the asteroid rotates.

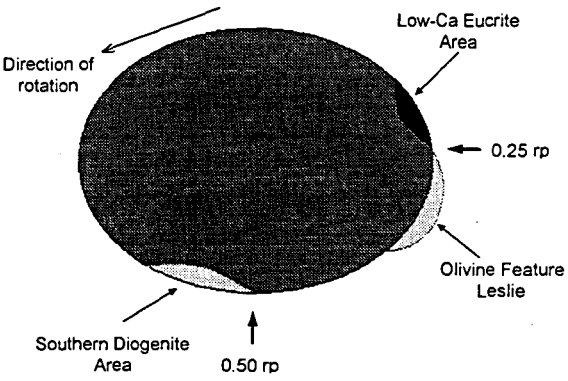

Fig. 4.

There are also indications of variations in surface albedo. A minimum in albedo is reached just after the southern diogenite area [2] transits the sub-Earth longitude. This may be correlated with the onset of the "dark region" as seen in [3], but the amplitude of the change in the current data may be artificially intensified due to a radius-of-curvature effect. A large portion of 4 Vesta's rotation has no projected area or albedo data due to nonoverlap of the two types of light curves.

Variations in relative projected area and relative surface albedo may be correlated with previous rotational spectral variations [2] (Fig. 3) in order to obtain new insights regarding the surface structure of 4 Vesta. The surface of asteroid 4 Vesta appears very heterogeneous and shows evidence of a complex history. The low-Ca eucrite area, southern diogenite area, and olivine feature "Leslie" observed spectrally [2] are confirmed through their coincidence with area/albedo features in this nonspectral data. Leslie appears to be associated with a topographic high, which is interesting given that it is possibly composed of mantle material [2]. The low-Ca eucrite area appears to be transiting just prior and physically adjacent to Leslie. The southern diogenite area, associated with a topographic low, follows approximately 90° after Leslie in 4 Vesta's rotation. There is evidence for a slight elongation in the shape of 4 Vesta with other minor protrusions and indentations. The remainder of the surface of 4 Vesta appears to be covered in a low-albedo, possibly space-weathered material.

The thermal infrared light curve and calculated projected area are highly correlated, indicating a small variation in surface thermophysical properties (e.g., thermal inertia, conductivity), i.e., the thermal flux varies as the projected area. Figure 4 shows a diagram of the relative positions of the observed features given the current data.

References: [1] Reed K. L. et al. (1996) *Icarus*, submitted. [2] Gaffey M. J. (1996) *Icarus*, submitted. [3] Zellner et al. (1995) *LPS XXVI*, pp. 1553–1554.

CORE FORMATION IN VESTA. K. Righter and M. J. Drake, Lunar and Planetary Laboratory, University of Arizona, Tucson AZ 85721-0092, USA.

Asteroid 4 Vesta is a small object with a radius of 275 km and a central pressure of about 4 kbar. We have not conducted sample return missions to Vesta. However, recent astronomical studies of Binzel and Xu [1] confirm earlier conclusions of Consolmagno and Drake [2] and Drake [3] that the howardite-eucrite-diogenite (HED) clan of meteorites are samples of Vesta. Chemical analysis of these meteorites permits the determination of the abundances of metal-seeking (siderophile) elements in their mantles. These siderophile elements may represent a chemical "fingerprint" of core formation, having been differentially extracted into Vesta's core according to their metal/silicate partitioning behavior during accretion.

Righter et al. [4] have shown that experimentally determined metal-silicate partition coefficients (D) may be related to thermodynamic intensive variables through the expression

$$\ln D = a\ln fO_2 + b/T + cP/T + d(nbo/t) + e\ln(1 - X_S) + f$$

where the b, c, and f terms result from the expansion of the free-energy term ($\Delta G° = \Delta H° - T\Delta S° + P\Delta V°$), and are related to $\Delta H°/R$, $\Delta V°/R$, and $\Delta S°/R$ respectively. The a term is related to the valence of the element in the silicate melt. The e term accounts for the S content of metallic liquid. The solubility of siderophile elements in silicate liquid can increase with decreasing melt polymerization, and the d term quantifies this dependency using the ratio of nonbridging oxygens divided by tetrahedrally coordinated cations (nbo/t) values.

Core formation may be modeled using the expression

$$C^i_{bulk} = x[C^i_{LS}[p + (1-p)D^i_{SS/LS}]] +$$

$$(1-x)[C^i_{LS}[mD^i_{LM/LS} + (1-m)D^i_{SM/LS}]]$$

where x = silicate fraction of the planet; p = fraction of the silicate that is molten; m = fraction of the metal that is molten; C^i_{sil}, C^i_{met}, and C^i_{bulk} are concentrations of siderophile elements in the silicate, metallic, and bulk portions of the planet; $D^i_{LM/LS}$ is the liquid metal/liquid silicate partition coefficient, $D^i_{SM/LS}$ is the solid metal/liquid silicate partition coefficient, and $D^i_{SS/LS}$ is the solid silicate/liquid silicate partition coefficient.

Newsom [5] has shown that the source region of the eucritic basalts must have been free of metal before the eucrites formed,

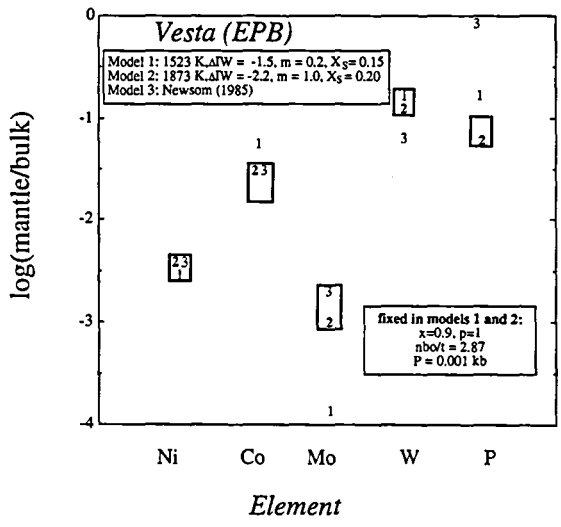

Fig. 1.

whether by partial melting or equilibrium crystallization [2,6]. The approach we take is to examine models for metal-silicate equilibrium under magma ocean conditions. For modeling metal-silicate equilibrium in Vesta in a magma ocean scenario, Vesta's mantle would be completely molten (p = 1) and the mantle composition reported by Jones (1984) has an nbo/t ratio of 2.87, both of which have been fixed in the calculations. The pressure at the center of Vesta is ~4 kbar, and we have set P = 0.001 kbar for these calculations; changes in P ≤ 4 kbar do not change the results of our calculations. The bulk abundances for Vesta were set at chondritic values, and the mantle abundances were those of Dreibus and Wänke [7] as tabulated in Newsom [8]. The prevailing O fugacity in Vesta has been constrained by experimental studies on eucrites by Stolper [6] and Jurewicz et al. [9] to be near or below $\Delta IW = -1$, and this parameter has been limited to values below $\Delta IW = -1.0$.

Temperature, X_S (mole fraction of S in the metal), x (fraction of silicate), and m (fraction of molten metal) have also been varied in order to model the siderophile-element abundances. A best fit to the mantle abundances is obtained with the following parameters: P = 0.001 kbar, T = 1873 K, $\Delta IW = -2.2$, $X_S = 0.20$, and nbo/t = 2.87 (model #2 in Fig. 1). We obtain a silicate fraction of 0.9, indicating the possibility of a smaller core size than that calculated by Newsom [5].

These results for Vesta indicate temperatures as high as 1873 K may have prevailed during metal-silicate segregation in the asteroid. These temperatures imply a magma ocean and are consistent with the heat budget associated with short-lived isotopes such as ^{26}Al.

References: [1] Binzel R. P. and Xu S. (1993) *Science, 260*, 186–191. [2] Consolmagno G. J. and Drake M. J. (1977) *GCA, 41*, 1271–1282. [3] Drake M. J. (1979) in *Asteroids* (T. Gehrels, ed.), pp. 765–782, Univ. of Arizona, Tucson, Arizona. [4] Righter K. et al. (1996) *Phys. Earth Planet. Inter.*, in press. [5] Newsom H. E. (1985) *Proc. LPSC 15th*, in *JGR, 90*, C613–C617. [6] Stolper E. M. (1977) *GCA, 41*, 587–611. [7] Dreibus G. and Wänke H. (1980) *Z. Naturforsch., 35a*, 204–216. [8] Newsom H. E. (1995) in *Global Earth Physics: A Handbook of Physical Constants: AGU Reference Shelf Vol. 1* (T. J. Ahrens, ed.), pp. 159–189, AGU, Washington, DC. [9] Jurewicz A. J. G. et al. (1991) *Science, 252*, 695–698.

ASTEROID 4 VESTA AS THE HED PARENT BODY: IMPLICATIONS FOR A METALLIC CORE AND MAGMA OCEAN CRYSTALLIZATION.

A. Ruzicka, G. A. Snyder, and L. A. Taylor, Planetary Geosciences Institute, Department of Geological Sciences, University of Tennessee, Knoxville TN 37996-1410, USA.

We have evaluated the size of a metallic core and the consequences of magma ocean crystallization in asteroid 4 Vesta, assuming that it is the howardite-eucrite-diogenite (HED) parent body. We assume for Vesta a density of 3.4 g/cm³ (±45% relative error) and a surface gravity of 2.53×10^{-4} m/s², based upon a mass of 2.78×10^{23} g [1] and diameter of 540 km [2,3].

Size of Metallic Core in Vesta: It has long been noted that the depletions of siderophile elements in HED samples are strongly suggestive of core formation in the HED parent body. Estimates of the amount of metal needed to cause the necessary depletions in the siderophile elements vary: 13% [4], 2–10% [5], 7–35% [6], 32–42% [7], 30–50%, and probably >20% [8]. Two independent estimates of the mineralogy (and hence density) of the silicate portion of the HED parent body (models 1 and 2) can be made based on data from HED meteorites. From these estimates, the size of a metallic core in Vesta can be determined by mass balance.

Model 1 assumes that the silicate portion of the HED parent body is identical to that inferred for the source region of the eucrites. Based on melting experiments and trace-element studies, Stolper [9] and Fukuoka et al. [10] suggested that the eucrite source region contains mainly olivine, orthopyroxene, and plagioclase. Using the mineral compositions inferred for the eucrite source region (Fo_{65}, En_{65}, and An_{94} [9]), and 12% partial melting of a source with 90% olivine, 8% orthopyroxene, and 2% plagioclase to produce the Sioux County eucrite [10], the density of the silicate fraction of the HED body is 3.6 g/cm³. With a probable upper limit density of 4.0 g/cm³ for Vesta, this implies a metal fraction (X_{metal}) of <5% for Vesta. Even with the extreme upper limit density of 4.9 g/cm³ for Vesta, X_{metal} <16%. If the density of Vesta is below 3.6 g/cm³, then olivine and orthopyroxene in the eucrite source region must be less ferrous than assumed. Model 2 uses the composition of the silicate portion of the HED asteroid, determined by Dreibus and Wänke [11], to calculate the following CIPW norm: 48.5 wt% olivine (Fo_{72}), 38.2% orthopyroxene (En_{79}), 9.5% plagioclase (An_{94}), 3.5% clinopyroxene ($Wo_{50}En_{39}$), and 0.3% ilmenite. Assuming this norm approximates the mineralogy of the silicate fraction of the HED asteroid, a density of 3.4 g/cm³ for the nonmetallic portion is implied. For the probable and extreme upper limit densities of 4.0 g/cm³ and 4.9 g/cm³ for Vesta, X_{metal} is <8% and <19% respectively. Models 1 and 2 give reasonably consistent results, suggesting that the size of a metal core, if any, on Vesta is probably less than a few mass percent. This is much smaller than typical estimates based on models of trace-siderophile-element depletions. We ascribe this difference to the preaccretionary loss of metal from Vesta in the planetesimals out of which Vesta was formed.

Mineral Assemblages in Magma Ocean Crystallization: If Vesta was initially molten, then it seems likely that differentiation would have occurred upon cooling. Using the estimated bulk composition of Dreibus and Wänke [11] for the HED parent body, we have calculated the fractional crystallization sequence of a Vesta-wide magma ocean based on phase equilibrium constraints (Table 1). Based upon these results, we would expect fractional crystallization of a molten HED parent body to result in a core-to-surface stratigraphy given approximately by assemblages (1) through (5) in Table 1, respectively. Such a stratigraphy, with olivine-rich cumu-

TABLE 1. Fractional crystallization sequence of a Vesta-wide magma ocean, determined with the program MAGFOX.*

1. 0–56% crystallization = olivine alone (Fo_{93} to Fo_{82})
2. 56–69% crystallization = 95% orthopyroxene (En_{84} to En_{74}) + 5% chromite
3. 69–78% crystallization = pigeonite alone (En_{74} to En_{56})
4. 78–92% crystallization = 61% plagioclase (An_{94} to An_{90}) + 23% pigeonite (En_{56} to En_{40}) + 14% fayalite (Fo_{53} to Fo_{25}) + 2% silica
5. 92–99.5% crystallization = 46% plagioclase (An_{90} to An_{73}) + 26% clinopyroxene ($Wo_{33}En_{22}$ to $Wo_{36}En_3$) + 20% fayalite (Fo_{25} to Fo_4) + 8% silica

* MAGFOX program developed by J. Longhi.

lates sequestered and unsampled in the lowermost mantle, and orthopyroxene- and pigeonite-rich cumulates forming the middle mantle, is at least consistent with the olivine-poor and pyroxene-rich nature of the diogenites. The uppermost one-fourth of the the mantle (assemblages 4 and 5 in Table 1) may then have crystallized relatively rapidly to form the source for the basaltic eucrites. However, olivine would crystallize both relatively early (as forsteritic olivine from 0% to 56% crystallization) and late (as fayalitic olivine from 78% crystallization onward). It is conceivable that the later olivine, with a much higher density than the earlier olivine, would have sunk or been convected into the lower mantle, disrupting the idealized stratigraphy. The proportion of plagioclase in assemblages (4) and (5) of Table 1 (61–46%) is somewhat greater than that seen in most eucrites (56–30%).

Efficiency of Magma Ocean Differentiation: The surface gravity of Vesta is nearly 5 orders of magnitude less than that on Earth and nearly 4 orders of magnitude less than that on the Moon. Thus, the separation of crystals from magma will be less efficient on Vesta than on either the Earth or Moon. The density of an HED/Vesta magma ocean near incipient crystallization is 2.82 g/cm^3 and after 78% crystallization is still only 2.87 g/cm^3. Magnesium-rich olivine and pyroxene have densities of 3.3–3.4 g/cm^3, and given a short amount of time (~10 k.y.), could settle in the magma ocean. Calcium-rich plagioclase has a density of 2.76 g/cm^3 and will tend to float. However, the relatively small density difference between magma ocean liquid and plagioclase, coupled with the higher viscosity of the magma ocean at the low temperatures at which plagioclase crystallizes, would serve to restrict the upward rise of plagioclase. In fact, *it would take plagioclase a million years to move upward just 4 km.* This suggests that the formation of an anorthositic flotation crust on Vesta would be inhibited. Thus, differentiation and stratification within a Vesta magma ocean would probably include only a pyroxene- and olivine-rich lower mantle and an upper mantle of roughly basaltic (eucritic) composition.

References: [1] Schubart J. and Matson D. L. (1979) in *Asteroids* (T. Gehrels, ed.), pp. 148–170. [2] Morrison D. (1977) *Icarus, 31*, 185–220. [3] Tedesco E. F. (1994) in *Asteroids, Comets, Meteors* (A. Milani et al., eds.), pp. 55–74. [4] Morgan J. W. et al. (1978) *GCA, 42*, 27–38. [5] Newsom H. and Drake M. J. (1982) *GCA, 46*, 2483–2489. [6] Newsom H. E. and Drake M. J. (1983) *GCA, 47*, 93–100. [7] Palme H. and Rammensee W. (1981) *Proc. LPS 12B*, pp. 949–964. [8] Newsom H. E. (1985) *Proc. LPSC 15th*, in *JGR, 90*, C613–C617. [9] Stolper E. (1977) *GCA 41*, 587–611. [10] Fukuoka T. et al. (1977) *Proc. LSC 8th*, pp. 187–210. [11] Dreibus G. and Wänke H. (1980) *Z. Natursforsch., 35a*, 204–216.

THE COMPOSITION OF THE EUCRITE PARENT BODY: IMPLICATIONS FOR THE ORIGIN OF THE MOON AND FOR PLANETARY ACCRETION.

A. Ruzicka, G. A. Snyder, and L. A. Taylor, Planetary Geosciences Institute, Department of Geological Sciences, University of Tennessee, Knoxville TN 37996-1410, USA.

Introduction: The composition of the eucrite parent body (EPB) has important implications for the the origin of the Moon and for the accretion of the terrestrial planets. We reexamine evidence pertaining to the composition of the EPB and the Moon by focusing on the abundances of incompatible elements in igneous samples of these objects. Theoretically, the ratios between highly incompatible elements in igneous rocks should be largely unaffected by magmatic processes and be diagnostic of the source area. The incompatible elements that we consider include the refractory lithophile elements La, Nd, Ba, and U, the volatile lithophile elements Na, K, Rb, Cs, and Tl, and the siderophile elements W, Ga, P, Mo, Ge, Au, Re, and Ir. Of these elements, all are typically highly incompatible in silicate systems, except for Na, which is compatible in plagioclase. In samples from the EPB and the Moon, volatile and siderophile elements are depleted relative to refractory lithophile elements when referenced to chondrite abundances. Thus, it is convenient to define a depletion factor that is simply the inverse of the CI-chondrite-normalized ratios of volatile/refractory or siderophile/refractory element pairs.

EPB vs. Moon: The calculated depletion patterns for the eucrite, lunar mare-basalt, and "pristine" lunar volcanic-glass source regions are similar (Fig. 1) and are consistent with metal and volatile loss. Comparing lunar glasses and mare basalts, there is a tendency for the glasses to be somewhat depleted in moderately volatile elements (Na, K, Rb, Cs, Ga, Ge) and in the highly volatile element Tl. Ringwood [1] argued on the basis of volatile-rich coatings on lunar glass beads that the deep interior of the Moon (volcanic-glass source region) was up to ~100× richer in volatile elements compared to the outer portion of the Moon (mare-basalt source region). However, Fig. 1 shows only a modest difference beween the derived depletion factors for mare basalts and volcanic glasses, so it appears that the Moon is indeed volatile-poor. For lunar samples, Na falls off the apparent volatility trend defined by other alkali elements (Fig. 1), possibly because both the mare-basalt and volcanic-glass source regions had previously undergone plagioclase fractionation. There is no comparable evidence for prior plagioclase fractionation in the eucrite source region.

Eucrites vs. Diogenites: Figure 2 shows depletion factors for

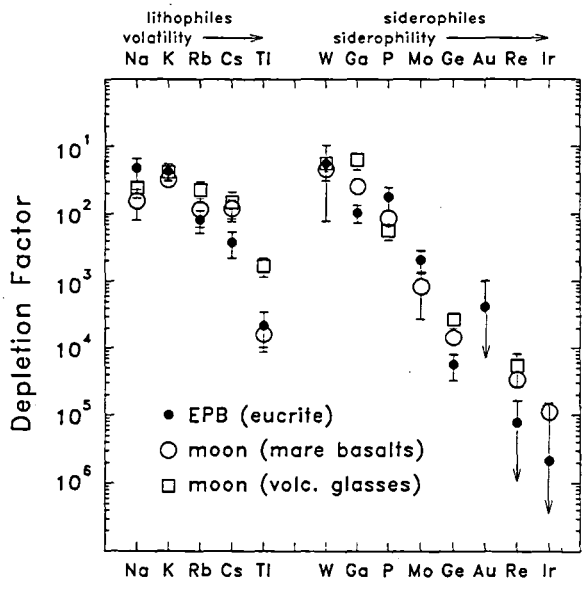

Fig. 1. Depletion factors for the EPB and the Moon. Data sources: eucrites [2, literature]; mare basalts [3, literature]; volcanic glasses [4].

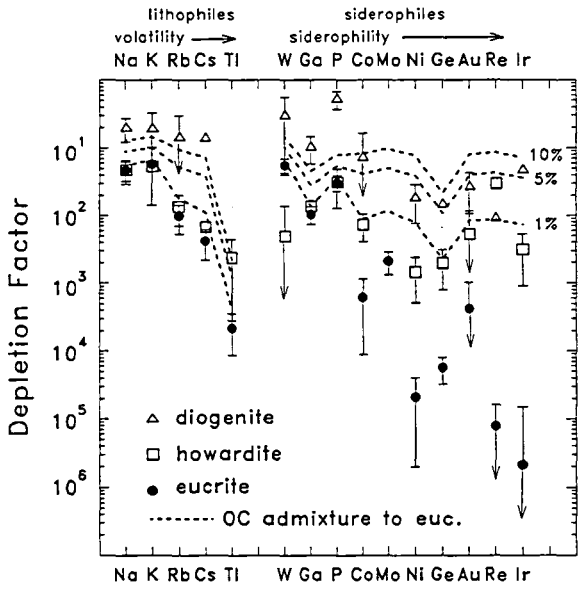

Fig. 2. Depletion factors for eucrites, howardites, and diogenites determined from literature data. "OC admixture to euc." refers to an admixture of average ordinary chondrite [9] to mean eucrite composition.

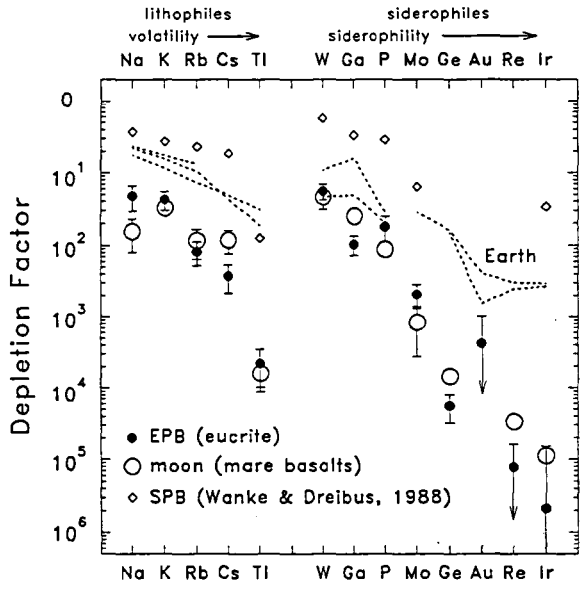

Fig. 3. Depletion factors for the EPB, Moon, Earth, and SPB. Data sources: eucrites and mare basalt same as for Fig. 1; Earth [5–7]; SPB [8].

the eucrites, howardites, and diogenites, all believed to have originated on the same body. Surprisingly, compared to eucrites, diogenites are consistently enriched in all incompatible lithophile and siderophile elements (and in the more compatible Co and Ni). Lower alkali and P abundances in eucrites relative to diogenites were previously noted by Mittlefehldt [2]. This was attributed to preferential loss of volatiles occurring from the eucrite source region because of its presumed proximity to the parent body surface. Howardites, which are polymict breccias composed primarily of eucrite and diogenite material, tend to have depletions intermediate to eucrites and diogenites (Fig. 2). The various depletion levels of diogenites, howardites, and eucrites are difficult to explain by magmatic processes alone, if all were derived from material of the same composition. Instead, it appears that an admixture of a small (~5%) amount of chondritic material to a mean eucrite composition can explain the incompatible-element abundances in diogenites of all the elements except for Na, Cs, P and Ga (Fig. 2).

Implications for Lunar Origin and Planetary Accretion: The depletion factors for the EPB and the Moon are compared to estimates for the silicate portions of the Earth and the shergottite parent body (SPB, probably Mars) in Fig. 3. The depletion patterns for all objects are similar although there are systematic differences, with the SPB being the least depleted in volatiles and siderophiles and the EPB and the Moon being the most depleted. These data suggest that (1) all the objects experienced broadly similar metal- and volatile-loss processes, and (2) the Moon more closely resembles the EPB than either the Earth or SPB. We conclude that *geochemical evidence for volatile and metal loss in the Moon does not favor a giant impact origin for the Moon.* It seems more likely that both the Moon and EPB accreted from the degassed mantles of differentiated planetesimals. The tendency for the mantle of the Earth and SPB (Mars) to be less depleted in siderophile and volatile elements than the EPB and the Moon may indicate that these objects preferentially accreted chondritic material, possibly owing to enhanced gravitational focusing caused by their large sizes compared to the Moon and EPB.

References: [1] Ringwood A. E. (1992) *EPSL, 111*, 537–555. [2] Mittlefehldt D. W. (1987) *GCA, 51*, 267–278. [3] BVSP (1981) *Basaltic Volcanism on the Terrestrial Planets*, pp. 239–253, Pergamon, New York. [4] Taylor G. J. et al. (1991) in *Lunar Sourcebook* (G. H. Heiken et al., eds.), pp. 183–284, Cambridge, New York. [5] Wänke H. (1981) *Philos. Trans. R. Soc. Lond., A303*, 287–302. [6] Taylor S. R. and McLennan S. M. (1985) *The Continental Crust: Its Composition and Evolution*, p. 264. [7] Anderson D. L. (1989) *Theory of the Earth*, p. 151. [8] Dreibus G. and Wänke H. (1988) *Philos. Trans. R. Soc. Lond., A325*, 545–557. [9] Wasson J. T. and Kallemeyn G. W. (1988) *Philos. Trans. R. Soc. Lond., A325*, 535–544.

REE PARTITION COEFFICIENTS FROM SYNTHETIC DIOGENITE-LIKE ENSTATITE AND THE IMPLICATIONS OF PETROGENETIC MODELING.

C. S. Schwandt and G. A. McKay, Mail Code SN4, NASA Johnson Space Center, Houston TX 77058, USA.

Determining the petrogenesis of eucrites (basaltic achondrites) and diogenites (orthopyroxenites) and the possible links between the meteorite types was initiated 30 years ago by Mason [1]. Since then, most investigators have worked on this question. A few contrasting theories have emerged, with the important distinction being whether or not there is a direct genetic link between eucrites and diogenites. One theory suggests that diogenites are cumulates resulting from the fractional crystallization of a parent magma with the eucrites crystallizing from the residual magma after separation from the diogenite cumulates [1–4]. Another model proposes that diogenites are cumulates formed from partial melts derived from a source region depleted by the prior generation of eucrite melts [5,6].

TABLE 1.

	Enstatite	Ibbenburen 3251	Glass	Eucrite Average
SiO_2	55.25	55.30	55.01	49.05
Al_2O_3	1.99	0.72	15.94	11.64
MgO	29.73	26.50	8.09	8.95
FeO	12.87	16.60	13.02	18.27
CaO	0.57	1.00	7.13	9.73
TiO_2	various	0.11	various	0.66
Cr_2O_3	various	0.30	various	—
	Low D		High D	
La	0.00031		0.00087	
Ce	0.00081		0.00141	
Nd	0.00294		0.00501	
Sm	0.00869		0.01424	
Eu	0.00333		0.00635	
Dy	0.03794		0.05582	
Er	0.06019		0.08636	
Yb	0.10646		0.15115	
Lu	0.12754		0.17701	

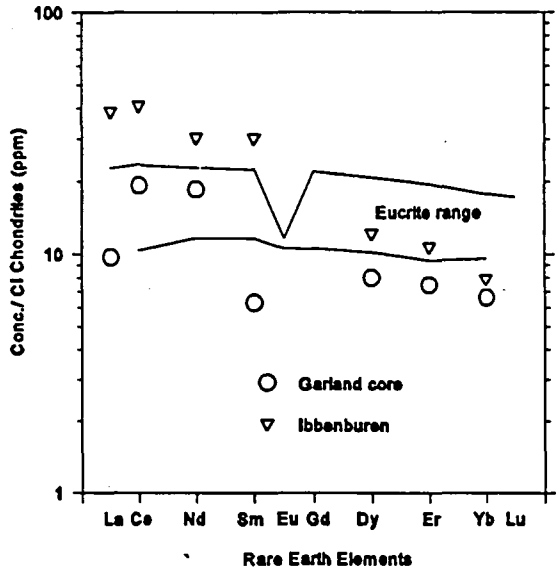

Fig. 1.

It has also been proposed that the diogenites may not be directly linked to the eucrites and that they are cumulates derived from melts that are more orthopyroxene normative than the eucrites [5,7]. This last theory has recently received more analytical and experimental support [8–12]. One of the difficulties with petrogenetic modeling is that it requires appropriate partition coefficients for modeling [13] because they are dependent on temperature, pressure, and composition [14,15]. For this reason, we set out to determine minor- and trace-element partition coefficients for diogenite-like orthopyroxene. We have accomplished this task and now have enstatite/melt partition coefficients for Al, Cr, Ti, La, Ce, Nd, Sm, Eu, Dy, Er, Yb, and La [16].

We have synthesized enstatites similar to diogenite enstatites from a melt made from reagent grade SiO_2, Al_2O_3, MgO, Fe_2O_3, and $CaCO_3$. Sodium and K were not included because of their very volatile nature in experimental apparatus. We don't perceive this as a problem as both are minor elements in diogenite pyroxenes. Additional Fe was added to the initial bulk glass composition to counteract the effect of Fe loss into the platinum crucible and wire loops during the experiments. Our goal was to achieve pyroxene compositions ($En_{80}Fs_{19}Wo_{01}$) that are like diogenite pyroxene compositions, not to worry about the fact that the melt composition was similar to eucrite composition. Though we started with an initial composition similar to the eucrite, Sioux County, the composition that we ended with is more hypersthene normative. Isothermal growth experiments conducted under O fugacity equivalent to Fe-wüstite conditions a few degrees below the liquidus temperature of about 1212°C produce crystals with dimensions of approximately 75 × 150 × ≥1000 μm. Enstatite is the only mineral on the liquidus at these temperatures. The amount of crystallization was kept to less than 5% of each experimental charge. As a result, glass composition remains nearly constant. Table 1 contains representative compositions of synthetic glass and enstatite and of natural eucrites and diogenite enstatites. The Mg/Mg + Fe values for the synthetic enstatites (0.80) match the diogenite enstatites (0.71–0.79).

Subsequently, we simultaneously doped our powdered glass with La, Ce, Nd, Sm, Eu, Dy, Er, and Yb oxides and $Lu(NO_3)_3$, and synthesized enstatite with nine REE. The REE were then measured in the glass and crystals using the UNM-SNL Cameca 4f ion microprobe. Natural basalt and pyroxene standards were used. The results were used to calculate the enstatite/melt partition coefficients for each of the nine REE in the enstatite. These are reported in Table 1 as taken from [16]. The table contains a low and a high D value, which is due to the presence of sector zoning in this enstatite. However, discussion of the sector zoning is beyond the scope of this forum but is discussed in detail in [17].

We complete this exercise by using our new enstatite Ds, which are similar though smaller than the Ds McKay derived for low-calcium pigeonite [18], to back-calculate REE signatures of the melts from which the diogenites crystallized. We use a few diogenite orthoenstatite REE compositions obtained by Fowler et al. [12] with an ion microprobe. It is assumed that enstatite is the only liquidus phase [cf. 11]. Therefore, knowing the partition coefficient and the concentration in the solid phase one can calculate the element concentration in the melt phase. A couple of these results using our high D values are shown in Fig. 1 compared with the range of published eucrite whole-rock REE patterns [6,19–21]. It is immediately evident without further modeling that the eucrites are not the crystallized remnant melts after fractional crystallization of orthopyroxene, because the eucrite patterns are basically flat and modeled melts are LREE enriched. Therefore, diogenites apparently crystallized from more hypersthene normative melts than the eucrites, and as such the rock types may not share a direct genetic link.

References: [1] Mason B. (1962) *Meteorites*, Wiley. [2] Warren P. H. (1985) *GCA, 49*, 577–586. [3] Bartels K. S. and Grove T. L. (1991) *Proc. LPS, Vol. 21*, pp. 351–365. [4] Grove T. L. and Bartels K. S. (1992) *Proc. LPS, Vol. 22*, pp. 437–445. [5] Stolper E. (1977) *GCA, 41*, 587–611. [6] Consolmagno G. J. and Drake M. J. (1977) *GCA, 41*, 1271–1282. [7] Jones J. H.(1984) *GCA, 48*, 641–648. [8] Jurewicz A. J. G. et al. (1991) *Science, 252*, 695–698. [9] Jure-

wicz A. J. G. et al. (1993) *GCA, 57*, 2123–2139. [10] Jurewicz A. J. G. et al. (1995) *GCA, 59*, 391–408. [11] Mittlefehldt D. W. (1994) *GCA, 58*, 1537–1552. [12] Fowler G. W. et al. (1995) *GCA, 59*, 3071–3084. [13] Treiman A. H. (1996) *GCA, 60*, 147–155. [14] McKay G. A. (1986) *GCA, 50*, 69–79. [15] Colson R. O. et al. (1989) *GCA, 53*, 643–648. [16] Schwandt C. S. and McKay G. A., in preparation. [17] Schwandt C. S. and McKay G. A., in preparation. [18] McKay G. A. (1989) *Rev. Mineral., 21*, 45–77. [19] Schnetzler and Philpotts (1969) *Meteorite Research*, pp. 206–216. [20] Shimizu N. and Masuda (1986) *GCA, 50*, 2453–2460. [21] Warren P. H. and Jerde (1987) *GCA, 51*, 713–725.

METAMORPHISM OF EUCRITES AND EUCRITE-RELATED METEORITES AND IMPLICATIONS FOR PARENT BODY SOURCES.

D. W. G. Sears, S. J. K. Symes, and P. H. Benoit, Cosmochemistry Group, Department of Chemistry and Biochemistry, University of Arkansas, Fayetteville AR 72701, USA.

Introduction: Exsolution structures in pyroxene [1] and induced thermoluminescence (TL) data [2,3] suggest that eucrite and related meteorites have experienced significant levels of metamorphism on their parent bodies. In this respect, they are quite different from otherwise mineralogically and chemically similar lunar samples [4]. Eight petrologic types of eucrite have been defined on the basis of the heterogeneity and presence of exsolution structures in the pyroxenes and TL sensitivity. On the basis of pyroxene compositions and lamellae widths, metamorphic temperatures and cooling rates of, typically, 850°–900°C and 40°C/10^4 yr have been proposed [1,5,6]. Identifying the physical conditions under which metamorphism occurred, and the relative timing of metamorphism and brecciation, would provide insights into the parent body and eucrite history.

Evidence: Whole-rock-induced TL data are shown in Figs. 1 and 2. We have interpreted the peak temperature data with the help of heating experiments (Fig. 3) [2,3]. We find that heating the samples at temperatures above 800°C causes the TL peak temperature to increase from 120° to 220°C. We have performed these experiments with a wide variety of feldspar-bearing samples, and all plagioclase feldspars (including the most anorthitic) show this behavior. We have not identified the cause of this increase, but a similar change in peak temperatures occurs in terrestrial feldspars (Fig. 4) where it is associated with an increase in the $\Delta 2\theta$ parameter, suggesting that it is related to structural disordering [7]. However, the effect is indirect since the activation energy for the TL change is 10–20 kcal/mol [8] compared with ~70 kcal/mol for disordering [9]. Taken at the simplest empirical level of interpretation, the TL data suggest that most eucrites experienced metamorphism at temperatures below 800°C, broadly consistent with geothermometry based on mineral pairs. The TL data also provide a quantitative means of assigning the eucrites to petrologic types that are otherwise fairly qualitative.

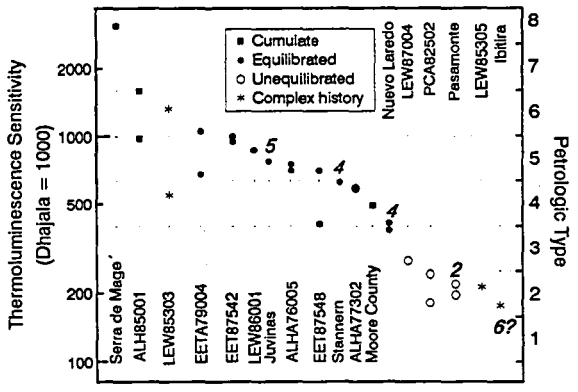

Fig. 1. Induced TL sensitivities for eucrites showing the petrologic types. We have suggested that the TL sensitivity increases with metamorphism as Fe diffuses out of the feldspar and into the pyroxenes.

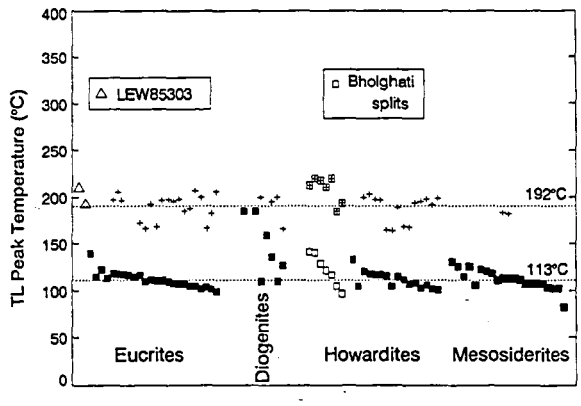

Fig. 2. Induced TL peak temperatures for eucrite, howardite, and mesosiderite meteorites. Minor peaks are indicated by a cross.

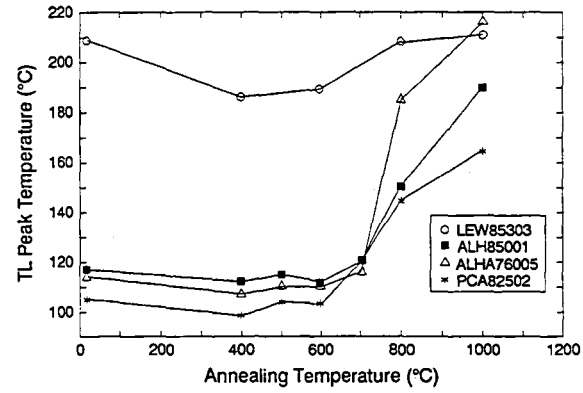

Fig. 3. Induced TL data for four eucrites as a function of heating temperature. The four eucrites were annealed for 96 hr.

An exceptional eucrite is LEW 85300 and its many pairings [10]. These meteorites have TL glow curves with a broad high-temperature peak very similar to that of normal eucrites heated >1000°C and lunar samples. We suggested that these meteorites had been severely shock heated, a conclusion that was borne out by petrographic observations [11].

Data for Clasts and Matrix Samples: All the clast and matrix separates from the LEW 85300 group have the same unusual

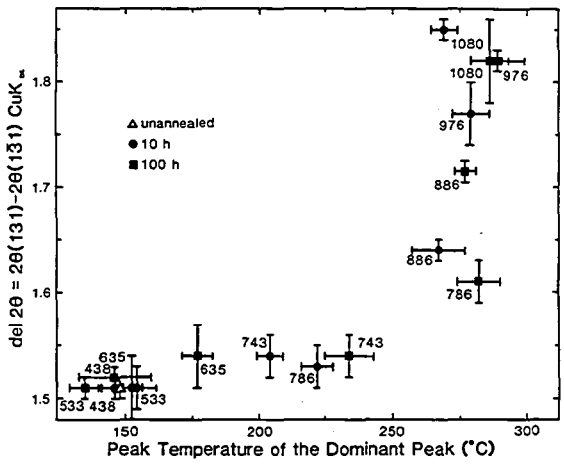

Fig. 4. Increases in peak temperature upon heating compared with the Δ2θ parameter, a measurement of the degree of structural disordering in a terrestrial oligoclase. The numbers alongside the data points refer to temperatures in °C. We suggest that the change in peak temperature is associated with disordering; however, the activation energy for the TL changes is considerably less than that required for disordering, so the effect must be indirect. Pasternak [22] suggested that the TL was reflecting defect production that preceded structural disordering.

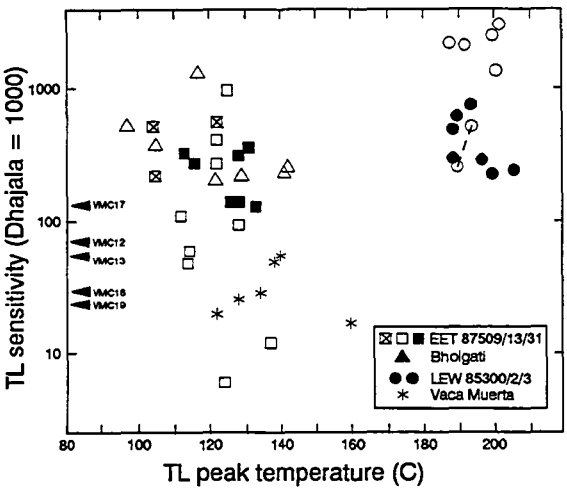

Fig. 5. TL sensitivity against TL peak temperature for the dominant peak (or the low-temperature peak when both peaks are of approximately equal intensity) in clasts (open symbols), matrix samples (filled symbols), and bulk samples (symbol with cross) of two howardites (EET 87509/13/31 and Bholgati), an atypical eucrite (LEW 85300/2/3), and a mesosiderite (Vaca Muerta). Peak-temperature data are not available for five Vaca Muerta clasts but their TL sensitivities are indicated by arrows.

glow curve shapes dominated by a high-temperature TL peak, while all the separates from the other three meteorites have normal low-temperature peaks consistent with a prolonged low-temperature episode (Fig. 5). Thus to a first approximation the clasts of a given meteorite have very similar thermal histories. The spread of TL sensitivity values for samples from the two howardites and the mesosiderite, and the differences in TL sensitivity between the howardites and the mesosiderites, largely reflect differences in mineralogy [12,13], but for the LEW 85300 shocked eucrite reflect the effects of shock and perhaps multiple impact events [10].

Implications: The bottom line of the induced TL work is that the eucrite association meteorites have suffered a prolonged period of low-temperature (<800°C) metamorphism. This has generated the strong low-temperature peak that is easily destroyed by even short-term heating above 800°C. In most cases, TL sensitivity variations reflect differences in mineralogy, but in a suite of mineralogically similar eucrites this too signals variations in metamorphic alteration and provides a quantitative estimate of petrologic type.

The main question is where and how the metamorphism occurred. A reasonable working idea is that these meteorites formed in a regolith on a large parent body. Recent theoretical treatments [15,16] and satellite observations of Gaspra, Ida, and Phobos [17,18] suggest that there are substantial regoliths on even small asteroids. We can reasonably assume that heat was deposited in that regolith by one or many impact events, while the bottom and top of the layer were maintained at a temperature of essentially zero. One can use the appropriate heat conduction equations [14] to investigate possible regolith temperature depth profiles as a function of time [3,6]. For a permeability of about 3×10^{-8} cm^2 s^{-1}, the most metamorphosed eucrites would have to be buried ~350 m in the regolith while the least metamorphosed eucrites would come from regoliths only ~50 m deep. The permeability chosen for these calculations might be rather high and smaller values would decrease regolith depths. However, the conclusion of significant burial seems hard to avoid.

References: [1] Takeda H. et al. (1983) *Mem. NIPR, Spec. Issue 30*, 181–205. [2] Batchelor J. D. and Sears D. W. G. (1991) *Nature, 349*, 516–519. [3] Batchelor J. D. and Sears D. W. G. (1991) *GCA, 55*, 3831–3844. [4] Symes S. et al. (1995) *Meteoritics, 30*, 585. [5] Miyamoto M. and Takeda H. (1977) *Geochem. J., 11*, 161–169. [6] Miyamoto M. et al. (1985) *Proc. LPSC 15th*, in *JGR, 90*, C629–C635. [7] Hartmetz C. P. and Sears D. W. G. (1987) *LPS XVII*, pp. 397–398. [8] Guimon R. K. et al. (1985) *GCA, 19*, 1515–1524. [9] McKie D. and McConnell J. D. C. (1963) *Mineral. Mag., 33*, 581–588. [10] Batchelor J. D. and Sears D. W. G. (1991) *LPS XXI*, pp. 63–64. [11] Hewins R. H. (1990) *LPS XIX*, pp. 509–510. [12] Reid A. M. et al. (1990) *GCA, 54*, 2162–2166. [13] Rubin A. E. and Mittlefehldt D. W. (1992) *GCA, 56*, 817–840. [14] Carslaw H. S. and Jaeger J. C. (1959) *Heat Conduction Through Solids*. [15] Carr M. et al. (1994) *Icarus, 107*, 61–71. [16] Asphaug E. and Melosh H. J. (1993) *Icarus, 101*, 144–164. [17] Housen K. R. (1992) *LPS XXIII*, pp. 555–556. [18] Asphaug E. and Nolan M. C. (1992) *LPS XXIII*, pp. 43–44. [19] Pasternak E. S. (1978) Ph.D. thesis, Univ. of Pennsylvania.

PETROGENETIC MODELS FOR THE ORIGIN OF DIOGENITES AND THEIR RELATIONSHIP TO BASALTIC MAGMATISM ON THE HED PARENT BODY.

C. K. Shearer, G. Fowler, and J. J. Papike, Institute of Meteoritics, Department of Earth and Planetary Sciences, University of New Mexico, Albuquerque NM 87131-1126, USA.

Introduction: Diogenites have long been recognized as a major constituent of the HED meteorite group. Yet their remarkable monotonous mineralogy [1–4] has limited the extent to which

diogenites have been used to reconstruct HED parent body (HEDPB) magmatism. Several papers exploring the trace-element characteristics of diogenites [2–4] have identified trace-element systematics that appeared to mimic simple magmatic processes involving large degrees of fractional crystallization (60% to >90%). However, based on reasonable basaltic magma compositions, changes in temperature during orthopyroxene crystallization [5], and observations in terrestrial layered intrusions [6], it is highly unlikely that extensive degrees of fractionation of a single basaltic magma (60–90%) should be the primary process linking all the diogenites. Recent chondrite partial melting experiments also question a simple relationship between eucrites and diogenites [7,8]. Our purpose is to explore other potential processes for the chemical variability observed in diogenites and the petrogenetic relationship of diogenites to other HED lithologies. We are using two different and complementary approaches. First, we are using thermodynamic calculations (MELTS) [9] to model partial melting of both measured chondrite compositions and calculated HEDPB mantle compositions. A total of 20 different bulk compositions have been used. Initial calculations were made at the IW buffer and evaluate both batch and fractional melting processes. Second, we are using these predicted phase relationships and melt compositions to calculate trace-element characteristics of primary and secondary melts produced by partial melting.

Data: Preliminary partial melting calculations (at IW) for a series of chondrites (LL6, H6) and calculated HEDPB mantle compositions [10,11] are summarized in Fig. 1. These initial calculations show that the different potential bulk compositions of the HEDPB mantle are capable of yielding a fairly wide range of melt compositions (i.e., Mg# and percent normative orthopyroxene) and residuum mineralogy-mineral chemistry (i.e., percent melting required to remove plagioclase from the residuum and Mg# of the residuum at that point). Calculations also show that fractional melting will produce a sequence of melts with progressively higher Mg#. Diogenitic melt compositions from Fowler et al. [4] and melt and residuum trajectories calculated from MELTS residuum mineral assemblages, trace-element compilations for the HEDPB [10],

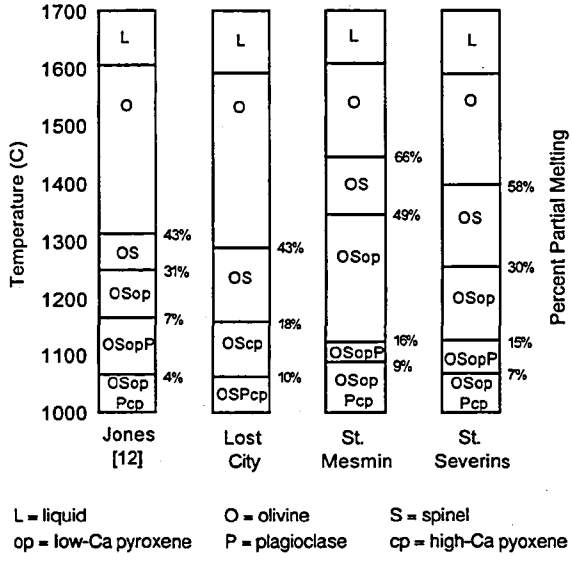

Fig. 1.

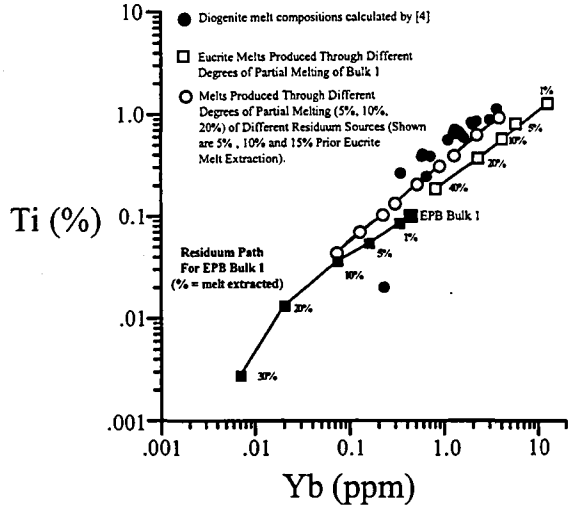

Fig. 2.

and trace-element modeling equations are illustrated in a plot of Yb vs. Ti (Fig. 2). The models assume extraction of a series of eucritic melts. Following the extraction of these eucritic liquids, the residuum is remelted at a higher temperature producing magmas that are perhaps parental to the intrusions containing the diogenite lithologies. Trajectories for these "diogenitic" melts that are produced through the remelting of residue with prior eucrite melt extraction are shown. The Mg# of the calculated diogenitic melts increase moderately with increasing degrees of partial melting of a single residuum and increase slightly at the same degrees of partial remelting of residue that experienced higher degrees of prior melt extraction. The calculated diogenitic magmas have Mg#s that are higher than the calculated eucritic magmas.

Discussion: Our calculations show that distinctive HEDPB compositions that had experienced varying degrees of prior melting and melt extraction provide the best sources for parental diogenitic magmas. Without calling upon extensive and unrealistic degrees of partial melting or fractional crystallization, our initial models produce the range of incompatible trace elements exhibited by the diogenitic magmas as calculated by [4]. Based on our initial calculations, models such as those previously proposed by Stolper [12] appear to best fit the previously generated data for the diogenites. Our initial models do have some problems. For example, although melting of residuum hollowing "eucrite melt extraction" will produce melts with higher Mg# and higher normative orthopyroxene, the Mg# is still not as high as suggested by diogenites. This may be partially due to the conditions under which these calculations were made (≥IW).

References: [1] Bowman L. E. et al. (1995) *LPS XXVII*, pp. 147–148. [2] Mittlefehldt D. W. (1994) *GCA, 58*, 1537–1552. [3] Fowler G. W. et al. (1994) *GCA, 58*, 3921–3929. [4] Fowler G. W. et al. (1995) *GCA, 59*, 3071–3084. [5] Grove T. L. and Bartels K. S. (1992) *Proc. LPS, Vol. 22*, pp. 437–445. [6] Papike J. J. (1996) *Am. Mineral., 81*, 525–544. [7] Jones J. H. et al. (1994) *LPS XXV*, pp. 639–640. [8] Jurewicz A. J. G. et al. (1995) *GCA, 59*. [9] Ghiorso M. S. et al. (1994) *Eos, 75*, 571–576. [10] Newsom H. E. (1995) *Global Earth Physics*, 159–189. [11] Jones J. H. (1984) *GCA, 48*, 641–648. [12] Stolper E. (1977) *GCA, 41*, 587–611.

IS THERE ANOTHER LINK IN THE CHAIN? LOOKING FOR STREAMS OF HED METEORITES. T. D. Swindle[1,2], R. Lippse[2], and I. Scott[2], [1]Lunar and Planetary Laboratory, University of Arizona, Tucson AZ 85721, USA, [2]UA/NASA Space Grant, University of Arizona, Tucson AZ 85721, USA.

In recent years, a chain of evidence has been built that links the asteroid 4 Vesta with the basaltic achondrite or HED (howardite, eucrite, and diogenite) meteorites. That chain is at the heart of this conference, but it is reasonable to ask how many links there are in the chain. In particular, we are curious about the most recent astronomical source of these meteorites. There have been at least two suggestions that there might be "streams" of these meteorites [1,2], which we wish to test.

One suggestion of a stream comes from looking for streams among the meteorite-dropping fireballs of the Prairie Network and MORP network [3] or among known near-Earth asteroids (NEAs) [1]. These searches were done by using the D' criterion, which is a somewhat arbitrary measure of how similar two sets of orbital elements are. In each group of orbits, there seem to be three or four clusters of objects. In fact, both studies defined the same clusters [1], which is either an intriguing coincidence or a suggestion that the clusters are somehow significant. Since one of the near-Earth asteroid clusters contains two V-type (Vesta-like) asteroids, it seems possible that this stream, identified by both Halliday et al. [3] and Drummond [1], is a stream of HED meteorites.

The other suggestion comes from observing that HED meteorites have preferentially fallen on or near certain days of the year, and searching for the asteroids that can come closest to the Earth on the days at the center of those peaks [2]. Using this approach, Wood [2] identified two potential streams that could account for approximately two-thirds of the witnessed HED falls. It should be noted that neither of these two streams is consistent with the Drummond-Halliday stream, and that orbital dynamics calculations predict that streams should disperse in much less than the exposure ages of the HED meteorites [4].

We have taken three approaches to testing these streams. First, we have looked at NEAs discovered since the Drummond- Halliday suggestion of a stream. We find that there are indeed several asteroids whose orbits match the potential HED stream. The same is true of their other proposed streams. It turns out that these streams encompass a majority of the asteroids with perihelion of 0.95–1.15 AU, inclination less than 15°, and semimajor axis of 1.8–2.52 AU, the most common values of each of these parameters. The stream orbits are all very similar in shape, and differ primarily in orientation (e.g., location of perihelion). This could be a sign that the "streams" merely represent the mostly densely packed region of phase space, but are not genetically related. If that is the case, however, we are at a loss to explain why two analyses of independent sets of objects gave the same clusters (i.e., the same orientations in space). Thus, we consider the results of this test somewhat ambiguous.

Second, we used dates of fall to identify potential stream members, then looked for distinctive cosmic-ray-exposure histories. We find no significant differences in the distributions for any of the proposed streams from HED meteorites as a whole.

As a third approach, we apply not just dates of fall of meteorites, but also times, locations, and directions. If all these are known, it is possible to rule out many orbits that could cross the Earth's on a particular day. Although times and locations are easily found [5], directions are not usually recorded in catalogs. We are pursuing these data from original sources, but at this time, we have found the directions for only a few of the HED meteorites. However, we can make some tentative conclusions.

First, there is no strong increase in the number of falls during the days that would be expected for the Drummond-Halliday stream. However, there is at least one meteorite, Serra de Magé, for which the direction and time of fall is consistent with membership in that stream.

Second, one of Wood's two streams includes Ibitira, for which many visual observations of the fireball were collected [6]. The direction of the fall of Ibitira appears to be consistent with the orbit of the proposed source asteroid, 1988XB. However, many of the other proposed members of the streams could not be stream members, because objects along the orbit of 1988XB could not have hit at those locations at those times.

In conclusion, the question is not yet answered. There are some pieces of data that are consistent with one or more streams of HED meteorites, but there are problems with any of the proposed streams. Further work on fall histories may enable us to resolve whether any significant fraction of HED meteorites could come from streams.

References: [1] Drummond J. (1991) *Icarus, 89*, 14–25. [2] Wood C. et al. (1995) *LPS XXVI*, pp. 1515–1516. [3] Halliday I. et al. (1990) *Meteoritics, 25*, 93–99. [4] Wetherill G. (1988) *Icarus, 76*, 1–18. [5] Graham A. et al. (1985) *Catalogue of Meteorites*, 4th edition. [6] Menezes V. (1957) *Sky and Telescope, 17*, 10.

MINERALOGICAL RECORDS OF EARLY PLANETARY PROCESSES OF THE HED PARENT BODY. H. Takeda, Research Institute, Chiba Institute of Technology, Tsudanuma, Narashino City, Chiba 275, and Mineralogical Institute, Graduate School of Science, University of Tokyo, Hongo, Tokyo 113, Japan.

A group of achondrites in the howardite-eucrite-diogenite series is called HED [1] because they form a continuous series of mineralogical, crystallographic, and chemical variations of minerals, especially of pyroxenes. The key samples filling a gap between diogenites and eucrites [2] and howardites and polymict eucrites [3] have been found in the Antarctic meteorite collections. They often have been ignored in some discussions on the partial melting (PM) models [4] vs. crystal fractionation (CF) models for the formation of the HED parent body.

There have been two approaches to deciphering the crystallization trend of the HED parent body: (1) Arrangements of individual monomict or crystalline samples in the order of crystallization and cooling; and (2) Reconstruction of the original crust before cratering events from polymict breccias such as howardites and polymict eucrites [5]. Difficulties in these approaches are due to cratering mixing of and metamorphic overprints on the original crustal materials. Combined chronological and mineralogical studies of metamorphosed monomict eucrites (often called ordinary eucrites) revealed that they experienced extensive thermal metamorphic events in the early history of the crustal evolution [6], and that impact craterings are later events ranging from 4.1 to 3.4 Ga ago [7]. In this paper, several important observational facts and new results are given, then a total picture in agreement with these items are envisioned subsequently.

Observational Facts and Results: 1. *Total conversion of the primitive materials into differentiated products.* In comparison with other differentiated meteorites (e.g., ureilites, lodranites-acapulcoites, winonaites-IAB irons, aubrites-E-chondrites), we have not observed any remnant or metamorphosed primitive materials in the HED collections, neither as an individual specimen nor components in the breccias. There are some clasts of carbonaceous chondrite affinity, but they are clasts introduced into the regoliths as fragments of projectiles.

2. *Two differentiation trends in the* mg *number of pyroxene vs. the An of plagioclase.* A trend of the An variation (91–73) with nearly constant *mg* numbers (65–69), which is vertical to the known lunar ferroan anorthosite trend, has been reconstructed from the interstitial plagioclases in diogenites with cumulate eucrite affinity [8]. The starting point of the trend is the same as that of the normal covariation trend.

3. *No gap between diogenites and cumulate eucrites.* In the beginning of the HED studies, Binda and Moore County were known cumulate eucrites, and howardites had been interpreted as mechanical mixtures of diogenites and eucrites [9]. Subsequently, many cumulate eucrites have been found as individual specimens or clasts in the polymict breccias [8]. Yamato 75032-type meteorites in particular contain components very difficult to identify as diogenites or cumulate eucrites [2].

4. *Systematic variations of inversion and exsolution textures with a chemical differentiation trend.* Mineralogical and crystallographic studies of terrestrial layered intrusions show systematic variation of the pyroxene textures [5]. Pyroxenes in magnesian members of cumulate eucrites close to diogenite show blebby inclusions of augites of the Kintokisan-type orthopyroxene inverted from low-Ca pigeonite [2] and those in the Fe-rich members show thick exsolution lamellae on (001). Some exceptions have been found in newly found specimens, but they can be explained as excavation in the middle of cooling, metamorphic events, mixtures of cumulate and trapped liquid. Because 4 Vesta is a large body, lateral variation of cumulate eucrites is possible. The *mg* number where crystallization of orthopyroxene changes to low-Ca pigeonite is always constant (*mg* number little larger than 67 of Binda).

5. *Relative amounts of the diogenitic orthopyroxene, cumulate eucrite, and ordinary eucrite in the polymict breccias.* Such amounts in howardites, polymict eucrites, and an intermediate member can be explained by impacts into a layered crust [5].

6. *Most of the eucrites are metamorphosed products of initially quickly cooled lavas.* No individual crystalline eucrite, which preserved the texture and chemistry of a quickly cooled basalt, has been found. A clast in polymict eucrites Y 75011,84 and the nearly monomict breccia Pasamonte nearly preserved such a pristine nature [10]. All crystalline eucrites found to date can be interpreted as extensively metamorphosed breccias. Asuka 881388 and A 881394 are such examples found recently.

Discussions: New observational facts are interpreted as evidence either in support of the PM or CF models. Some PM models ignore the existence of cumulate eucrites in the HED crust. Any PM model has difficulty in converting all primitive crust into totally differentiated materials. This model is contrary to fact 1. Successive lava eruptions on the surface of primitive crust and subsequent extensive global metamorphism still leaves some primitive materials between the metamorphosed crust and residues of partial melting. No model has been proposed to convert all primitive materials into the differentiated products. The remnants of the primitive materials will be mixed with differentiated products as breccia components. We have no such meteorite in the HED collections.

Eucrites with inverted pigeonites with augite has been designated as a type 7 eucrite by Yamaguchi et al. [6]. The preservation of the recrystallized matrix texture with secondary augite in A 87272 [1,11] suggests that this specimen did not experience a detectable impact brecciation event after metamorphism. The presence of inverted pigeonite with coarse exsolution lamellae in A 87272 (type 7) resembling some cumulate eucrites indicates that the metamorphism of the eucritic crust is comparable to the cooling environment of cumulate eucrites [12] on the HED parent body. These are the final products of lavas of the PM model, which fails to explain facts 1 and 2. Some cumulate eucrites were excavated in the middle of cooling [12]. Therefore, diversity of cumulate eucrites is not surprising.

Despite these complex histories, observational facts 3 and 4 suggest that crystal fractionation of the HED crust can be taken as one event in a magma, presumably one assumed in the CF model. The temperature of the first pigeonite crystallization is above 1100°C. Fact 2 indicates differentiation of trapped liquid in the cumulate-diogenite pile, and fact 5 suggests a layered crust and cratering events of different sizes.

Fact 6 indicates that they are the final product of the original lavas and are not cumulate eucrites produced in the CF model.

Acknowledgments: We acknowledge the Antarctic Meteorite Working Group and NIPR for supplying us with the samples.

References: [1] Takeda H. et al. (1983) *Mem. NIPR, Spec. Issue 30,* 181–205. [2] Takeda H. and Mori H. (1985) *Proc. LPSC 15th,* in *JGR, 90,* C626–C648. [3] Delaney J. S. (1983) *Meteoritics, 18,* 103–101. [4] Stolper E. M. (1977) *GCA, 41,* 587–611. [5] Takeda H. (1979) *Icarus, 40,* 455–470. [6] Yamaguchi A. et al. (1996) *Icarus,* in press. [7] Bogard D. D. (1995) *Meteoritics, 30,* 244–268. [8] Takeda H. (1991) *GCA, 55,* 35–47. [9] McCarthy T. S. et al. (1972) *EPSL, 15,* 86–93. [10] Takeda H. and Graham A. L. (1992) *Meteoritics, 26,* 129–134. [11] Yanai K. (1993) *Proc. NIPR Symp. Antarct. Meteorites, 6,* 148–170. [12] Miyamoto M. and Takeda H. (1995) *EPSL, 122,* 343–349.

EUCRITES, TERRESTRIAL BASALTS, AND VOLCANIC PROCESSES ON VESTA.

G. J. Taylor, R. C. Friedman, and A. Yamaguchi, Hawai'i Institute of Geophysics and Planetology, University of Hawai'i, Honolulu HI 96822, USA.

Basaltic eucrites contain information about volcanic processes that occurred under conditions different from those on the terrestrial planets and the Moon: lower gravity (0.03 *g*), no atmosphere, and low volatile contents (water free, much like the Moon). Vestan volcanism is thus an end member in studies of planetary volcanism. The eucritic crust of Vesta is between 10 km [1] and 25 km [2] thick, which comprises a volume between 0.85 and 2.0×10^7 km^3. The decay products of short-lived nuclides in basaltic eucrites [3] suggests volcanism lasted no longer than several million years; if 2 m.y., the estimated crustal volumes imply eruption rates of 4.5–10 km^3/yr. These volumes and emplacement times and rates are comparable to large igneous provinces on Earth [4], presenting the opportunity to study the formation of a large igneous province on a small planet with different heat sources, mantle dynamics, gravity, and tectonics.

Theoretical studies of volcanic processes on asteroids are important [5], but the only direct record we have at present of the nature of eruptive processes on Vesta are the original igneous textures of eucrites. To understand those textures and lava flow dynamics in general, we have been studying the textures of Hawai'ian and other terrestrial lava flows. Our preliminary results suggest that most eucrites crystallized in pahoehoelike flows, one cannot use grain sizes to deduce definitive flow thicknesses, but modeling suggests eruptions on Vesta generally formed wide flows a few meters thick.

Terrestrial Basalts: The textures of terrestrial a'a and pahoehoe lavas are distinctive. A'a flows have more and finer grains. For example, the interior (1.4 m down into the massive zone beneath the clinkery top) of the Keamoku a'a flow on Mauna Loa contains 55 plagioclase grains/mm^2, not counting the 30–40% of the rock that is extremely fine-grained groundmass (<10 μm). In contrast, an inflated pahoehoe flow near Kamoamoa on Kilauea, sampled at about the same depth in the flow (1.5 m), contains 38 plagioclase grains/mm^2 and little groundmass. In addition, the width of the largest plagioclase crystal (which in experiments [6] is correlated with cooling rate) differs significantly: 0.07 mm in the a'a flow and 0.12 mm in the pahoehoe flow. These differences are consistent from flow to flow. Furthermore, there is no systematic difference in grain size with depth in a'a flows. For example, the largest plagioclase width in the 1907 a'a flow from Mauna Loa is 60 μm at the top of the massive interior zone and 70 μm at 2.3 m below that. In pahoehoe flows, below the top 20 cm of crust, there is a slight variation with depth, but far less than suggested from simple cooling models of lava flows.

The textural differences between a'a and pahoehoe are caused by the mechanics of flow emplacement. Emplacement dynamics control the thermal environment of the lava, which determines the density of crystal nuclei, which in turn dominates the final textures of basaltic rocks [7]. A'a flows form at relatively high effusion rates (>5 m^3/s in Hawai'i [8]) in open, turbulent channels in which a significant amount of the exposed lava is incandescent. This results in many opportunities for supercooling and production of crystal nuclei before a given packet of lava comes to rest. The interiors of a'a flows are cooler than pahoehoe flows and teem with crystal nuclei, which limits crystal size growth. The turbulent emplacement process also makes for a well-mixed flow, with little crystal size variation with depth.

In contrast, pahoehoe flows are emplaced at lower effusion rates (<5 m^3/s [8]), form an external insulating crust and internal tube system, and thus remain hot as they advance. This leads to fewer crystal nuclei and a generally hotter environment favoring crystal size growth. However, pahoehoe thermal history is much more complex than simple conductive cooling models of an emplaced sheet of initially hot lava with a uniform temperature throughout. Pahoehoe flows have complicated internal dynamics involving inflation of small lobes initially only a few tens of centimeters thick [9]. As the flow inflates, the new lava injected is insulated by previously formed crust and the liquid core becomes thicker. But the solid crust also thickens as crystallization continues at the top of the growing liquid core. Thus, the final textures and grain sizes we see throughout the flow interior are surprisingly more uniform than might be expected.

Implications for Vesta: Our preliminary examinations suggest that eucrites are much more like pahoehoe flows than a'a in texture and thus, perhaps, in emplacement. Eucrite basalts have crystal number densities like those in pahoehoe flows (e.g., 20 plagioclase grains/mm^2 in Pasamonte), with little groundmass. A dominance of pahoehoelike flows on Vesta is consistent with theory and empirical data. In Hawai'ian eruptions, pahoehoe dominates when eruption rates are <5 m^3/s [8]; assuming vents are typically 10 m long for most of an eruption, this eruption rate corresponds to <0.5 m^3/s/m of fissure. Vestan eruption rates of 0.1–3 m^3/s/m of fissure [5], then, indicate that the dominant lava type could be either pahoehoe or a'a. However, the type of flow generated also involves factors such as viscosity, strain rate, and flow velocity [10]. Eucrite viscosities are not greatly different from terrestrial basalts (if anything, eucrites would be more fluid), so it seems likely that these eruption rates on Vesta would favor formation of pahoehoe because lava would flow slower in the low gravity on Vesta.

If flows were mostly pahoehoe on Vesta, we can use observations of Hon et al. [9] and the calculations of Wilson and Keil [5] to estimate the size of a typical pahoehoe field on Vesta. Using a radial spreading model applied by [9], an eruption rate of 1 m^3/s/m of fissure, a fissure length of 1000 m, a duration of 40 hr [5], and spreading in all directions from the fissure, we calculate that the flow field would have a radius of 12 km and a thickness of 1.9 m. A 200-hr eruption would generate a larger flow field with a thickness of 3 m.

Such flow fields might resemble low, broad shields with surrounding flows, like those on the Snake River plains, such as Hell's Half Acre, which Greeley [11] dubbed "plains volcanism." If calculations by Wilson and Keil [5] are correct, the Vesta cases would be smaller, 1–4 km^3 vs. 12–15 km^3 for the Snake River type. Alternatively, if topography confines the flows, they might resemble elongate lava flows such as the 75-km-long Carrizozo flow in New Mexico [12], which has a volume of 4.3 km^3. Ponding of flows in impact craters is also possible. Whatever the precise shape of the flow fields, we envision the crust of Vesta being constructed from countless overlapping lava flow fields dominated by pahoehoelike emplacement. Impacts brecciated the flows, erasing the most direct evidence for their existence.

References: [1] Miyamoto M. and Takeda H. (1994) *EPSL, 122*, 343–349. [2] Delany J. S. (1995) *LPS XXVI*, pp. 329–330. [3] Shukolyukov A. and Lugmair G. W. (1993) *Science, 259*, 1138–1141. [4] Coffin M. F. and Eldholm O. (1994) *Rev. Geophys., 32*, 1–36. [5] Wilson L. and Keil K. (1996) *JGR*, in press; also this volume. [6] Walker D. et al. (1978) *Proc. LPSC 9th*, pp. 1369–1391. [7] Lofgren G. E. (1983) *J. Petrol., 24*, 229–255. [8] Rowland S. K. and Walker G. P. L. (1990) *Bull. Volcanol., 52*, 615–628. [9] Hon K. et al (1994) *GSA Bull., 106*, 351–370. [10] Peterson D. W. and Tilling R. I. (1980) *J. Volc. Geotherm. Res., 7*, 271–293. [11] Greeley R. (1982) *JGR, 87*, 2705–2712. [12] Keszthelyi L. P. and Pieri D. C. (1993) *J. Volc. Geotherm. Res., 59*, 59–75.

VESTA: SPIN POLE, SIZE, AND SHAPE FROM HST IMAGES. P. C. Thomas[1], R. P. Binzel[2], M. J. Gaffey[3], B. H. Zellner[4], A. D. Storrs[5], and E. Wells[5], [1]Center for Radiophysics and Space Research, Cornell University, Ithaca NY 14853, USA, [2]Department of Earth, Atmospheric, and Planetary Sciences, Massachusetts Institute of Technology, Cambridge MA 02139, USA, [3]Department of Geology, West Hall, Rensselaer Polytechnic Institute, Troy NY 12181, USA, [4]Department of Physics, Georgia Southern

University, Statesboro GA 30460, USA, [5]Space Telescope Science Institute, 3700 San Martin Drive, Baltimore MD 21218, USA.

HST images obtained at scales of 52 km/pixel in 1994 have been used to determine the spin pole, size, and shape of Vesta. Several surface bright and dark features allow control-point stereogrammetric measurement of spin-pole orientation. An independent solution of the spin pole and shape can be made from the limb and terminator coordinates. A combined control point and limb solution for Vesta's rotation pole is at $\alpha_0 = 308° \pm 10°$, $\delta_0 = 48° \pm 10°$; J2000. Its shape can be fit by an ellipsoid of radii 280, 272, 227 (±12) km. The mean density of Vesta from the mass reported by Schubart and Matson [1] is 3.8 ± 0.6 g/cm^3. For this density Vesta's shape is close to that of a Maclaurin spheroid with superposed variations of ~15 km. The departures from an ellipsoidal shape are well within the sizes expected of cratering events responsible for ejection of the HED meteorites. HST data from 1996 will allow substantial refinement of the shape and topography of Vesta.

References: [1] Schubart J. and Matson D. L. (1979) in *Asteroids*, pp. 84–97, Univ. of Arizona, Tucson.

THE CUMULATE EUCRITE SERRA DE MAGÉ: NEW INAA DATA AND THE COMPOSITION OF ITS PARENT MAGMA.

A. H. Treiman[1] and D. W. Mittlefehldt[2], [1]Lunar and Planetary Institute, 3600 Bay Area Boulevard, Houston TX 77058-1113, USA, [2]Lockheed Martin, Houston TX 77058, USA.

Trace-element abundances have been obtained by INAA for a USNM sample of the cumulate eucrite Serra de Magé [1]. The USNM sample has more Al and Eu and less Mg, Fe, and Sc than does only other completely analyzed sample [2]. Compositions of both samples are consistent with being cumulates from basalt magma like the Nuevo Laredo eucrite, but with different proportions of magma, pigeonite, and plagioclase: 3.5%, 37.5%, and 59% respectively for the former [1], and 11%, 52.5%, and 36.5% for the latter [2]. Thus, there is no need to invoke unusual magmas or complex petrogenetic processes in the formation of Serra de Magé.

Sampling and Instrumental Neutron Activation Analysis (INAA): Trace- and minor-element abundances were determined by INAA [3] for powder USNM 5963, which was homogenized from a ~5-g bulk sample of Serra de Magé. A subsample of 53.45 mg was carefully split from the 113-mg aliquot of <100 mesh powder provided by E. Jarosewich. Results (Table 1) are qualitatively consistent with other analyses of Serra de Magé [2,4]. Abundances of Co, Ta, and W are high and may reflect contamination from the W carbide mortar used in powdering the sample.

From these and literature analyses [2,4,5], it is clear that Serra de Magé is chemically heterogeneous (Table 2), e.g., the USNM sample has high Al_2O_3 [1], yielding 59% normative plagioclase content, while other analyses imply as little as 35% normative plagioclase. Trace-element abundances follow major-element abundances, e.g., Eu tracks Al_2O_3 and normative plagioclase content, and Sc tracks MgO and normative pigeonite content. Abundances of highly incompatible elements also vary widely: La ranges from 0.26 to 0.58 ppm [5].

Parent Magma Composition: Identification of parent magmas for the cumulate eucrites has engendered "frank exchanges of views." On one hand, application of mineral/magma distribution coefficients suggests highly fractionated parent magmas (La to 5000× CI), currently unknown among the basaltic eucrite meteorites [6–8]. On the other hand, application of mass balance suggests that known eucrite magmas types are adequate as parental magmas [9–11].

TABLE 1. INAA chemical analysis of Serra de Magé, USNM powder, this work.

Cr_2O_3 (%)	0.316 ± 0.004
FeO (%)	10.15 ± 0.11
CaO (%)	12.2 ± 0.5
Na_2O (%)	0.345 ± 0.004
K_2O (%)	<0.021
Sc (ppm)	14.39 ± 0.16
Co (ppm)	(94.7) ± 1.1
Zn (ppm)	17 ± 4
As (ppm)	0.154 ± 0.006
Se (ppm)	0.462 ± 0.009
Sr (ppm)	65 ± 10
Sb (ppm)	0.035 ± 0.007
La (ppm)	0.324 ± 0.012
Ce (ppm)	0.73 ± 0.19
Nd (ppm)	<6
Sm (ppm)	0.154 ± 0.006
Eu (ppm)	0.462 ± 0.009
Tb (ppm)	0.035 ± 0.007
Yb (ppm)	0.166 ± 0.022
Lu (ppm)	0.034 ± 0.005
Hf (ppm)	0.112 ± 0.022
Ta (ppb)	(28) ± 5
W (ppb)	(770) ± 9
Ir (ppb)	0.166 ± 0.022
Au (ppb)	2.9 ± 0.08

Sample = 53.45 mg, 1σ analytical uncertainties. Values in parentheses judged to reflect contamination.

TABLE 2. Major-element analyses of Serra de Magé and calculated model cumulates of Nuevo Laredo magma + equilibrium plagioclase + equilibrium pigeonite.

	Serra de Magé [1]	Model Cumulate	Serra de Magé [2]	Model Cumulate
SiO_2	46.69	47.81	48.45	49.07
TiO_2	0.11	0.11	0.13	0.21
Al_2O_3	20.89	20.99	14.77	14.29
Cr_2O_3	0.33	0.16	0.63	0.24
FeO	9.97	9.86	14.40	14.75
MnO	0.36	0.35	0.48	0.52
MgO	7.52	7.42	10.66	10.55
CaO	13.09	12.55	9.75	9.81
Na_2O	0.3	0.52	0.25	0.37
K_2O	0	0.014	0.012	0.013
P_2O_5	0.05	0.004	0.028	0.012
Total	99.31	99.78	99.56	99.84
X^{magma}		0.035		0.11
$X^{pig.}$		0.375		0.525
$X^{plag.}$		0.59		0.365

X = mass fraction in the model cumulate. Magma is Nuevo Laredo eucrite, "pig." and "plag." are pigeonite and plagioclase respectively, both in chemical equilibrium with Nuevo Laredo magma.

For Serra de Magé, the composition of the Mainz sample [2] can be reproduced closely as Nuevo Laredo eucrite magma plus equilibrium plagioclase and pigeonite (Table 2 [9,10]). The combined bulk and INAA data on the USNM powder of Serra de Magé (Tables 1 and 2) permit a test of this inference [9–11]; the USNM sample should also be consistent with formation from Nuevo Laredo eucrite magma. In fact, the composition of the USNM sample composition *is* consistent with formation from a Nuevo Laredo eucrite magma (Table 2), but not from Main Group (e.g., Juvinas, Sioux County) or Stannern Trend (e.g., Stannern, Bouvante) eucrites.

Thus, the compositions of two different samples of Serra de Magé are consistent with having formed from the same parent magma, although with different proportions of cumulus pyroxene, plagioclase, and intercumulus magma (Table 2). This consistency is not proof that Serra de Magé did form from Nuevo Laredo-type eucrite magma, but implies that unusual magma types are not necessarily required in the petrogenesis of Serra de Magé.

Geology of Eucrite Parent Body (EPB) = Vesta? 1. Samples of the Serra de Magé cumulate contain surprisingly little intercumulus magma: 3.5–11% (Table 2). Can these low proportions be induced by gravity alone, or must one invoke other processes such as adcumulus mineral growth [12] or compaction in a thermal gradient [13]?

2. The cumulate eucrites Serra de Magé, Moore County, and Moama all have compositions consistent with formation from a Nuevo Laredo-type magma [11]. Is possible that these meteorites are samples from a single magmatic systems on EPB?

3. This work and [10,11] suggest that known eucrite basalts are adequate as parent magmas for the cumulate eucrites. Whether the known eucrite basalts represent fractional crystallization and/or partial melting, the compositions of the cumulate eucrites require no additional geochemical complexities in the EPB mantle, particularly not the complexities involved in production of significant volumes of LREE-rich basalts.

Acknowledgments: We are grateful to R. Jarosewich of the Smithsonian Institution for the sample of Serra de Magé.

References: [1] Jarosewich E. (1990) *Meteoritics, 25*, 323–337. [2] Palme H. et al. (1978) *Proc. LPSC 9th*, pp. 25–57. [3] Mittlefehldt D. W (1994) *GCA, 58*, 1537–1552. [4] Schnetzler C. C. and Philpotts J. A. (1969) in *Meteorite Research*, pp. 206–216. [5] Morgan J. W. et al. (1976) *GCA, 40*, 861–888. [6] Warren P. and Jerde E. (1987) *GCA, 51*, 713–725. [6] Ma M.-S. and Schmitt R. (1979) *Meteoritics, 14*, 81–88. [7] Hsu W. and Crozaz G. (1995) *Meteoritics, 30*, 522. [8] Pun A. and Papike J. (1995) *GCA, 59*, 2279–2289. [9] Treiman A. H. (1996) *GCA, 60*, 147–155. [10] Treiman A. H. (1996) *LPS XXVII*, pp. 1337–1338. [11] Treiman A. H. (1996) *Meteoritics*, submitted. [12] Wadsworth W. (1985) *Geol. Mag., 122*, 549–554. [13] Lesher C. and Walker D. (1988) *JGR, 93*, 10295–10311.

MASTER: AN ORBITER FOR THE DETAILED STUDY OF VESTA.

J. Veverka[1], G. L. Adams[2], R. P. Binzel[3], R. H. Brown[4], D. Carpenter[4], L. Evans[5], M. J. Gaffey[6], K. Klaasen[4], H. McSween[7], L. Miller[4], S. Squyres[1], P. C. Thomas[1], J. Trombka[5], and D. K. Yeomans[4], [1]Cornell University, Ithaca NY, USA, [2]Lockheed Martin Corporation, USA, [3]Massachusetts Institute of Technology, Cambridge MA, USA, [4]Jet Propulsion Laboratory, Pasadena CA, USA, [5]NASA Goddard Space Flight Center, Greenbelt MD, USA, [6]Rensselaer Polytechnic Institute, Troy NY, USA, [7]University of Tennessee, Knoxville TN, USA.

MASTER (Mainbelt Asteroid Exploration/Rendezvous), a Discovery-class orbiter, will carry out a global geological and geochemical survey of Vesta. Primary goals include (1) determining Vesta's mean density and interior structure through detailed mapping of the gravity field, (2) imaging surface morphology at 3-m resolution, (3) mapping mineralogy between 0.4 and 2.5 μm, and (4) determining abundances of key elements through X-ray and γ-ray spectroscopy.

Spectroscopic evidence indicates the presence of basaltic lava flows on Vesta and suggests that impact basins may have exposed mantle materials. These possibilities, combined with the likelihood that Vesta is the ultimate source of HED meteorites, makes this asteroid an important target for a comprehensive orbiter mission. MASTER's global survey, combined with ongoing studies of HED meteorites, will be a major step in understanding the chemical, thermal, and geological evolution of Vesta.

A particularly attractive opportunity involves a launch in June 2003 with arrival at Vesta in November 2009. The orbital phase of the mission is scheduled to last one year. A flyby of another mainbelt asteroid enroute to Vesta may be possible.

HED PETROGENESIS: ARE ORTHOPYROXENITIC MAGMAS PLAUSIBLE?

P. H. Warren, Institute of Geophysics and Planetary Physics, University of California, Los Angeles CA 90095-1567, USA.

The acronym HED is appropriate because an abundance of evidence indicates that howardites, eucrites, and diogenites formed on a single parent asteroid. Howardites are clearly mixtures of eucrites and diogenites, with very little else. Eucrites are basalts and compositionally basaltic (gabbroic) cumulates. Diogenites are orthopyroxenites, and are also widely assumed to be igneous cumulates. A popular although unproven hypothesis is that asteroid 4 Vesta is the HED source, based on spectroscopic detection of a number of apparently howarditic, eucritic, and diogenitic smaller asteroids in the vicinity of Vesta and the 3:1 resonance [1]. The relationship between diogenites and eucrites is still highly controversial, however.

Several compositionally and mineralogically typical howardites are our only regolith breccias (with such regolith features as impact spherules [2] and solar wind noble gas enrichments) from the parent asteroid. Eucrites greatly outnumber diogenites, but the numbers of meteorites probably reflect vagaries of the delivery process, and are not a reliable indicator of the relative abundances on the parent asteroid. Howardite compositions indicate that impact gardening contributed roughly equal proportions of eucrite and diogenite to the asteroid's surface regolith despite the strong likelihood, based on textural evidence, that diogenites are of systematically deeper origin.

Two contrasting models have been proposed for the origin of diogenites. One model assumes that the parent melts were basaltic to *mildly* ultramafic in composition, in which case the products of fractional crystallization must have included a considerable fraction of residual basalt and gabbro (RBG), resembling (at least approximately) eucrites. Another model, which coincidentally has recently

been viewed with favor by both of the conveners of this meeting [3,4], suggests that the parent magmas were of orthopyroxenitic composition, little different from the average composition of the diogenites themselves. The key difference between these models is in the normative feldspar, i.e., Al, content of the parent magma. Assuming (based on the howardite evidence) that the total amount of diogenite in the asteroid is at least nearly the same as the total amount of eucrite, mass balance for Al [5] implies either (1) the parent melts formed by radically higher degree of melting (or from a radically Al-depleted source) compared to primary eucritic melts, or (2) the parent melts were moderately Al-rich, and thus should have engendered enough RBG to account for more than half the total basaltic-gabbroic material in the asteroid.

One objection to the orthopyroxenitic magma hypothesis [5] is physical implausibility. Melting would have to proceed to a degree several times greater than involved in genesis of any of the primary eucritic melts, unless the source was partially melted a second time after removal of its original basaltic component. Neither seems likely. A leading candidate heat source, ^{26}Al, would be gone with the basalt. An early superluminous Sun would melt overlying basalt together with the ultramafic matter. Impact heating would be inefficient on a small, low-gravity body, and would have engendered lots of compositionally intermediate melt (and thus lots of RBG). Of the more plausible heat sources, only electromagnetic induction seems credible for the specific task of generating ultramafic magmas on a small asteroid where otherwise all primary magmas were basaltic.

Here I raise a second weighty objection: mass balance for MgO and FeO. Diogenites are consistently MgO-rich, with orthopyroxene mg# (MgO/[MgO + FeO], mol%) = 68–78, and bulk-rock mg# averaging 74 (there could be a bias in favor of shallow-formed, low-mg# samples). Eucrites traditionally classed as noncumulates have low mg#, virtually all ≤42. Assuming the parent melts produced diogenite + RBG, that the diogenite formed with average mg# = 74, and that the RBG had (MgO + FeO) concentration two-thirds that of the diogenite, a mass balance can be constructed for MgO and FeO in the parent melts as a function of the proportion of RBG and its assumed average mg# (results are shown in Fig. 1). This is straightforward mass balance. No partition coefficient is involved. Unless most of the melt product is RBG, and preferably RBG with a low average mg#, the initial bulk melt composition is required to have an implausibly high mg#. For example, assuming the RBG mg# = 50 (for comparison, most of the eucrites traditionally classed as cumulates have average mg# ≈60), in order for the yield of RBG to be less than the yield of diogenite the initial melt mg# is required to be >65. This mg# is implausibly high in relation to the consistently low mg# of the eucrites. An mg# of ≈67 is required for the source of the primary noncumulate eucrites [6]. Even assuming remelting after mg# enhancement by removal of a plausible proportion (not ⩾25 wt%) of eucritic basalt, melts produced from the same mantle that formed noncumulate eucrite melts could never have mg# ⩾50. Diogenites did not form from orthopyroxenitic, RBG-poor magmas.

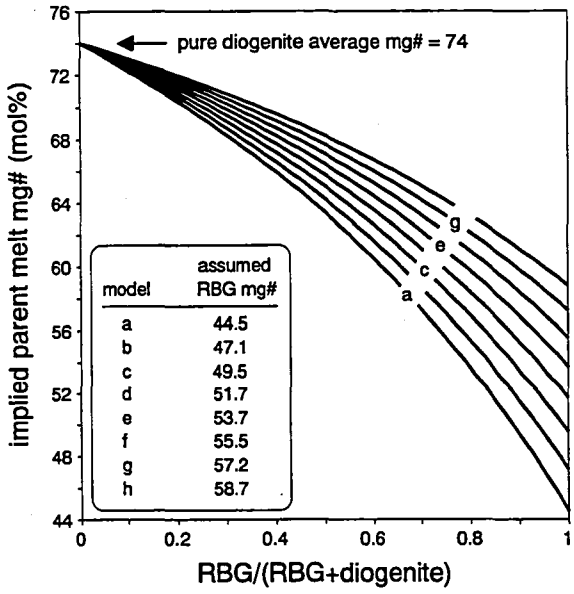

Fig. 1.

References: [1] Binzel R. P. and Xu X. (1993) *Science, 260,* 186–191. [2] Olsen E. J. et al. (1990) *Meteoritics, 25,* 187–194. [3] Mittlefehldt D. W. (1994) *GCA, 58,* 1537–1552. [4] Fowler G. W. et al. (1995) *GCA, 59,* 3071–3084. [5] Warren P. H. (1985) *GCA, 49,* 577–586; also (1996) *GCA, 60,* 539–542. [6] Warren P. H. and Jerde E. A. (1987) *GCA, 51,* 713–725.

COMPOSITIONAL-PETROLOGIC INVESTIGATION OF QUENCH-TEXTURED EUCRITES: MICROPORPHYRITIC ALH 81001 AND VESICULAR PCA 91007.

P. H. Warren[1,2], G. W. Kallemeyn[2], and T. Arai[1], [1]Mineralogical Institute, University of Tokyo, Hongo, Tokyo 113, Japan, [2]Institute of Geophysics and Planetary Physics, University of California–Los Angeles, Los Angeles CA 90095-1567, USA.

We have studied bulk compositions and mineralogy of several unusual eucrites. Bulk compositions were determined using standard UCLA methods: INAA, RNAA (Ni, Zn, Ge, Cd, Re, Os, Ir, and Au), and fused-bead EPMA (major elements + Ti). Mineral compositions were studied using EPMA at the University of Tokyo. Samples for which RNAA data have been acquired include ALH 81001, EET 87548, LEW 86002, LEW 87010, RKP 80204, RKP 80224, Y 791186, Y 791195, and Y 82037, and also the polymict eucrites EET 79005, LEW 87004, LEW 87026, and LEW 87295.

Polymict (?) Eucrites: Except for the above-mentioned polymict eucrites, all the eucrites studied feature extremely low siderophile concentrations, even compared to previous data for monomict eucrites (Fig. 1, showing new data from [1]). The 0.003× CI reference lines show levels below which the vast majority of lunar basalts are distributed; lunar impact-modified compositions tend to contain higher levels of Ir and Os. In the cases of ALH 81001 and LEW 87010, these new data are difficult to reconcile with previous classification of these eucrites as polymict [2]. The textures are not obviously polymict; both are essentially unbrecciated. ALH 81001 is porphyritic, with small, acicular pyroxene phenocrysts set in a very fine-grained groundmass [3,4]. ALH 81001 and LEW 87010 were apparently deemed polymict in the sense of being impact melts. They should be reclassified as more likely normal igneous (compositionally "pristine") eucrites.

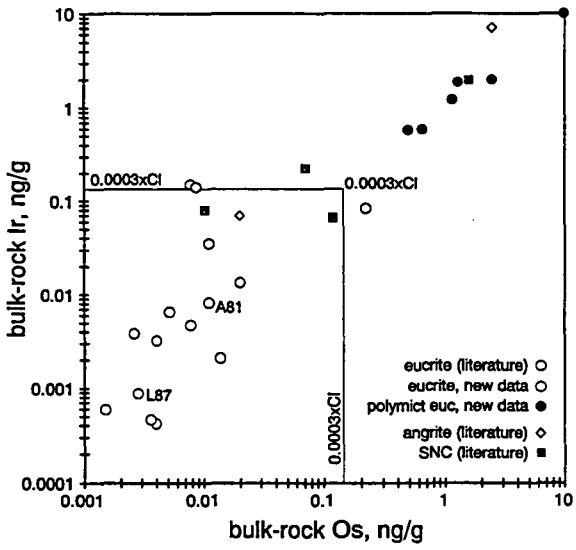

Fig. 1.

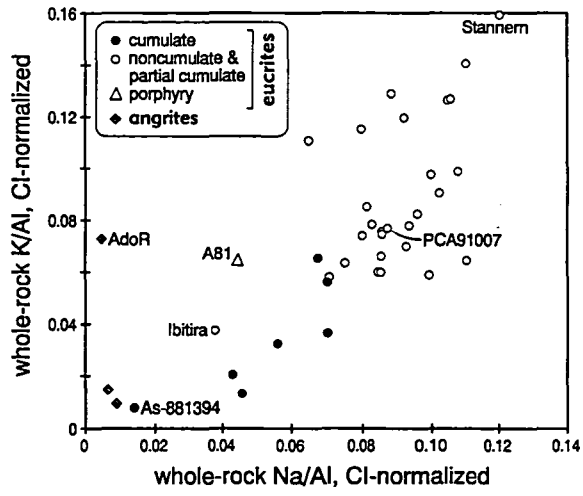

Fig. 2.

TABLE 1. ALH 81001 is *not* an uncommonly Al-rich eucrite.

Oxides (wt%)	Na_2O	MgO	Al_2O_3	SiO_2	CaO	TiO_2	Cr_2O_3	MnO	FeO
DBA correction factors (calculated)	[1.0]	1.07	0.82	[1.0]	0.94	1.29*	[1.0]	[1.0]	1.12
Warren and Jerde [ref. 4]	0.23	8.0	11.5	49.6	9.1	0.98	0.45	0.56	19.0
Warren and Jerde [ref. 4]	0.26	7.8	11.5	49.4	10.2	0.97	0.45	0.56	19.3
Uncorrected DBA-1	0.20	6.7	14.0	49.0	10.0	0.90	0.60	0.70	18.0
Uncorrected DBA-2	0.18	6.8	14.0	50.9	10.6	0.74	0.39	0.58	17.0
Corrected DBA-1	0.20	7.2	11.4	49.0	9.4	1.16	0.60	0.70	20.1
Corrected DBA-2	0.18	7.3	11.4	50.9	10.0	0.96	0.39	0.58	19.0

* TiO_2 is nearly evenly distributed among several different phases. The factor shown was derived empirically for mare basalts by Dowty et al. [ref. 5].

ALH 81001 has been discussed as an uncommonly Al-rich eucrite [3]. An unusually Al-rich composition is difficult to reconcile with the observation that the sole phenocryst phase is pyroxene—more feldspar than pyroxene would be expected. In any case, the two analyses discussed by [3] are both based on the defocused beam analysis (DBA) electron probe technique, with no mention of how the analyses were corrected for density effects in a polyphase electron probe analysis. When multiple phases are in the area exposed to electron bombardment, the analysis becomes distorted in proportion to the densities of the various phases. High-density phases are areally underrepresented; low-density phases are overrepresented. We have thus calculated density-correction factors for DBA of ALH 81001 based on a roughly estimated mode. These factors agree well with factors derived for a similar rock type, lunar mare basalt, by Dowty et al. [5], based on a purely empirical method. When correction factors are applied to the two DBA analyses discussed by [3], the results (Table 1) agree well with the two direct analyses of [4]. Compared to other noncumulate eucrites, the bulk composition of ALH 81001 features a low Na/Al ratio (Fig. 2), an uncommonly high mg# (42 mol%), and relatively high contents of incompatible elements (an interesting combination), but its Al content is quite ordinary.

PCA 91007 (we have not yet completed RNAA) is only the second nearly unbrecciated eucrite found to contain vesicles. The only precedent, discounting cavities of uncertain origin in heavily brecciated samples, was Ibitira. Interpretation of Ibitira is complicated by its unusually intense metamorphic history. PCA 91007 is not as vesicular as Ibitira, but the roughly 5-mm^2 thin section we studied features at least five (possibly eight or more) approximately spherical cavities, with diameters of 50–150 (–300?) μm. The section is extremely irregular in shape, so possibly a few larger vesicles are present but not identifiable. Unlike Ibitira [6], PCA 91007 has been only moderately metamorphosed. Pyroxene compositions are fairly well equilibrated, with exsolution lamellae typically about 1 μm wide, but the original texture is essentially preserved. This texture is more uniformly fine grained (typically 0.05–0.1 mm; the longest grain is an acicular pyroxene, 500 × 30 μm) than in any other known eucrite. ALH 81001 has an even more fine-grained groundmass, but also features a major proportion of relatively coarse, phenocryst-like pyroxene grains. Thus, PCA

91007 represents the best case for a large (224 g) eucrite that has been quenched to preserve the composition of a former HED-asteroidal melt. However, the bulk composition is not highly unusual. Unlike Ibitira, PCA 91007 shows no significant depletion of alkalis relative to typical eucrites (Fig. 2). Incompatible elements are also at typical noncumulate eucrite concentrations. The mg# (37 mol%) is significantly lower than those of ALH 81001 and Ibitira (both 42 mol%).

References: [1] Warren P. H. et al. (1996) *Abstracts NIPR Symp., 21*, 195–197. [2] Grossman J. N. (1994) *Meteoritics, 29*, 100–143. [3] Delaney J. S. et al. (1984) *LPS XV*, pp. 212–213. [4] Warren P. H. and Jerde E. A. (1987) *GCA, 51*, 713–725. [5] Dowty E. et al. (1973) *Proc. LSC 4th*, pp. 423–444. [6] Steele I. M. and Smith J. V. (1976) *EPSL, 33*, 67–78.

CUMULATE EUCRITES: VOLATILE-DEPLETED ASUKA 881394, CHROMIUM-LOADED EET 87548, AND CUMULATE VS. NONCUMULATE RELATIONSHIPS. P. H. Warren[1,2], G. W. Kallemeyn[2], and K. Kaneda[1], [1]Mineralogical Institute, University of Tokyo, Hongo, Tokyo 113, Japan, [2]Institute of Geophysics and Planetary Physics, University of California–Los Angeles, Los Angeles CA 90095-1567, USA.

Among several eucrites we have been studying by our usual methods [1,2], two stand out as extraordinary cumulates: Asuka 881394, a volatile-depleted cumulate eucrite, and EET 87548, an extraordinarily pyroxene- and chromite-rich cumulate eucrite.

The medium-grained granular texture of Asuka 881394 [3] is possibly altered from the original igneous texture, and difficult to categorize in terms of cumulate vs. noncumulate origin. Based on low incompatible-element contents and (+) Eu anomaly (Sm = 0.29 µg/g, Eu = 0.27 µg/g [1]) and high mg# (56.6 mol%), we infer it is a cumulate. Even so, its extremely low concentrations of volatile elements (Fig. 2 of [2]) seem remarkable. The Ga/Al ratio (0.010× CI) is also exceptionally low. This sample tends to blur the distinction between eucrites and angrites. However, many significant differences vs. angrites remain. For example, the Fe/Mn ratio (34) is typical for eucrites, and only 0.4× the lowest Fe/Mn among angrites.

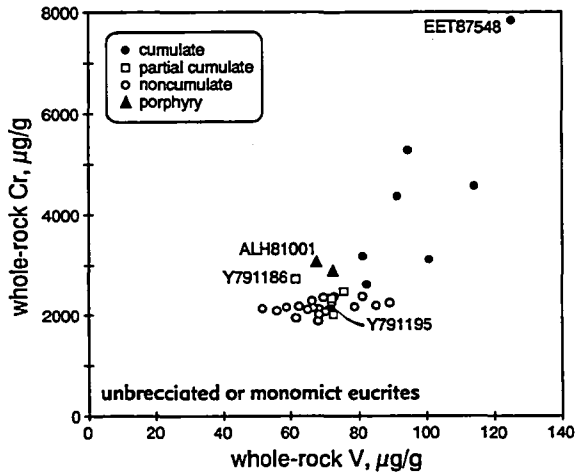

Fig. 1.

EET 87548, an Extraordinarily Pyroxene- and Chromite-rich Cumulate Eucrite: PTS EET 87548,11 contains 67.9 vol% pyroxene (px), 29.3 vol% plagioclase (pl), 1.1 vol% chromite (cm), and 1.7 vol% other phases (mainly silica and Fe-metal). This mode features more than twice the cm content of any other eucrite, and ties with Binda for the highest px/pl ratio among eucrites. The high cm content is reflected in exceptionally high bulk-rock contents of Cr and V (Fig. 1). Augite exsolution lamellae in px are up to 35 µm wide. Three of the chromites contain bands of ilmenite, up to about 4 µm wide. These bands probably formed by exsolution, because they are unusually Cr-rich for eucritic ilmenites, their host cm's are compositionally distinctive (vs. band-free cm), and in one case a crack that crosses the cm grain disappears as it crosses the ilmenite band (implying that the band formed after brecciation of the cm).

The high cm content of EET 87548 strongly confirms previous conjectures [e.g., 4] that cm may be a cumulus phase in some eucrites. The extremely low incompatible-element contents of this rock (e.g., Sm = 0.137–0.140 µg/g [1]) imply that if it formed by any reasonably simple cumulus process from any conceivable eucrite-related magma, only about 4 wt% can have come from trapped liquid. In such a case, there is practically no way to generate a rock with twice the cm content of normal eucrites, unless the cm is at least partly cumulus in origin.

Stolper [5] argued long ago that some cumulate eucrites probably formed from parent melts more ferroan (low mg#) than any known eucrite. This conclusion has been supported by further cumulate eucrite discoveries [6]. Recently, however, Treiman [4] has criticized this conclusion, arguing that most cumulate eucrites crystallized from "normal eucritic" magmas, not significantly more ferroan than Nuevo Laredo, which has bulk-rock mg# = 33 mol%. Specifically, Treiman's model primarily addressed Serra de Magé. As a historical aside, Treiman [4] included [6] among a set of five papers criticized for "flawed" modeling "from mineral analyses" and "without consideration of magma trapped among the crystals." Actually, the modeling approach of [6], first used to model Pomozdino by [7], is basically identical to (i.e., anticipated) that later adopted by Treiman [4], and agrees in predicting that such a sample (Serra de Magé) must have formed with 11 wt% trapped liquid (TL) from a parent melt with mg# (32 mol%), assuming the melt's Sm content was roughly 2–3 µg/g—a close match to Nuevo Laredo (33 mol% and 2.3 mg/g).

However, the same modeling approach predicts that EET 87548 formed with only 3.6–3.7 wt% TL (very definitely ⩽10 wt%), and its parent melt had mg# = 28–29 mol%. This model includes a slight adjustment for diminution of the bulk-rock mg# associated with the cumulus cm. The parent melts of Y 791195 and RKPA 80224, modeled by the same technique (in these cases the TL contents are much higher), require even lower mg#. For Moama and Medanitos (both accumulates like EET 87548, with very low TL) the implied parent melts are similar to that implied for Serra de Magé. All the known cumulate eucrites except Binda appear to have crystallized from melts with mg# as low as, or considerably lower than, the extreme low-mg# end of the noncumulate eucrite compositional range. The cause of this systematic offset remains one of the outstanding enigmas of HED petrology.

References: [1] Warren P. H. et al. (1996) *Abstracts NIPR Symp., 21*, 195–197. [2] Warren P. H. et al., this volume. [3] Yanai

K. et al. (1995) *Catalog of the Antarctic Meteorites.* [4] Treiman A. H. (1996) *LPS XXVII*, pp. 1337–1338. [5] Stolper E. (1977) *GCA, 41*, 587–611. [6] Warren P. H. and Kallemeyn G. W. (1992) *Meteoritics, 27*, 303–304. [7] Warren P. H. et al. (1990) *Proc. LPSC 20th*, pp. 281–297.

SPACE WEATHERING OF BASALT-COVERED ASTEROIDS: VESTA AN UNLIKELY SOURCE OF THE HED METEORITES. J. T. Wasson[1] and C. R. Chapman[2], [1]University of California, Los Angeles CA 90095, USA, [2]Southwest Research Institute, Boulder CO 80302, USA

Space weathering has exerted a dramatic effect on the surfaces of some or most large asteroids. As discussed by Wasson [1] and in detail by Chapman [2], space weathering has altered the reflection spectra of all large ordinary-chondrite (OC) asteroids. No asteroid with D > 40 km shows an OC (Q-type) reflection spectra even though ordinary chondrites are the most abundant meteorites to fall and, based on time-of-fall data, are largely exiting the asteroid belt at the 3:1 period resonance with Jupiter corresponding to an orbital semimajor axis of 2.50 AU [3].

Only one large asteroid, 4 Vesta, shows a reflection spectrum having the low-Ca pyroxene absorption near 900 nm and neutral colors in the 500–750-nm range characteristic of freshly ground basalts (and, with minor differences, of orthopyroxenites). Vesta's spectrum is remarkably well defined, so sharp in fact that Pieters and Binzel [4] speculated that the regolith might be young and Wasson et al. [5] used Galileo observations of variable degrees of weathering of impact features on the S asteroid Ida to estimate that the resurfacing event occurred roughly 10 m.y. ago.

It has been common practice in the years since the basaltlike spectrum of Vesta was reported by McCord et al. [6] to attribute the igneous-clan, HED meteorites to Vesta. As discussed by several authors including Wasson and Wetherill [7], the chief problem with this idea is the implausibly high launch velocity that this requires in order to transfer impact debris from Vesta to a resonance that would increase the orbital eccentricity enough to make the orbit Earth-crossing. The high escape velocity (360 m s^{-1}) and the velocity necessary to transfer debris from Vesta's orbit at 2.36 AU to the nearest resonance at 2.50 AU both contribute to this velocity; Binzel and Xu [8] showed that the most probable minimum launch velocity is about 1000 m s^{-1}. If the projectile velocity were 5000 m s^{-1}, the yield of meteorite-sized debris having an ejection velocity of 1000 m s^{-1} would be trivial. The many smaller bodies having lower escape velocities and occupying orbits nearer to resonances contribute a higher time-averaged flux of debris to Earth-crossing orbits.

To assess the source of the HED meteorites we need to know what fraction of these other asteroids are differentiated (the maximum mass fraction that any differentiated asteroid with a chondritic bulk composition can be basaltic is roughly 10%). The time-averaged flux of differentiated meteorites to Earth offers some information. Unfortunately, given our minimal understanding of the effects of space weathering, the large number of reflection spectra available offers very little help.

How does space weathering affect the spectra of basalt-covered bodies? We suggest that the answer is that the effects are quite similar to those affecting lunar and ordinary chondrite materials. In the case of the Moon the process is the formation of submicroscopic metal through reduction of Fe^{+2} in the process of agglutinitic-glass formation following particle impacts. The chief elements in this scenario are the trapping of solar-wind H and the heating of materials by the impacts of micrometeorites. Because the same dominant mineral—FeO-rich low-Ca pyroxene—is involved, it follows that the space weathering of basalts should be very similar to ordinary chondrites: The 900-nm absorption band becomes shallower, the region between 750 and 500 nm is reddened, and the resulting spectrum falls somewhere within the broad limits of the S type. Chapman [2] summarized Galileo observations on Ida that show an age-related progression from OC spectra to S-type spectra. Many S-type spectra would also be consistent with analogous space weathering of differentiated silicate assemblages including HED meteorites.

A key past argument in support of a Vesta-HED connection is that one parent body contributes most (or, more correctly, igneous) achondrites, and that only one asteroid shows a basaltic reflection spectrum, and 1 = 1. The basaltic spectrum argument clearly collapses if the fraction of degraded spectra among basaltic asteroids is similar to that among OC asteroids. If ≥5% of the ~110 large (D > 40 km) asteroids in the inner (a < 2.6 AU) belt are basaltic it is highly likely that one of these is much closer to a resonance than is Vesta. Note that, although the 5% is an assumption, the large fraction of basaltic bodies with degraded spectra is not, but a logical consequence of the fact that every large OC asteroid has a degraded spectrum and that the same minerals contribute to the characteristic spectral features.

It is quite unlikely that, for the past 4 G.y., the HED parent body has continuously been the main source of differentiated stony meteorites. During short (10-m.y.) periods, the most common groups of meteorites are coming from a relatively small set of asteroids. Because the injection of new meteoroids into resonances is a stochastic process, the large asteroids whose impact ejecta populated the resonance regions in the recent past may not be the ones that were dominant 100 (or 200 or 300) m.y. ago. The near-Earth asteroids that are the immediate sources of many meteorites are also removed on a timescale of several tens of millions of years, and replenished on that timescale from a new set of large asteroids. Because of the stochastic nature of these processes one cannot argue that the HED parent asteroid has been the only major provider of basaltic meteorites throughout the history of the solar system.

Wasson [1] estimates that at least 60 bodies are required to account for the iron meteorites that formed in cores, and that it is likely that all these bodies had basalts on their surface immediately after differentiation. In addition to those bodies that provided iron meteorites there must be a set similar in size that have not yet been fragmented and others that are fragmented but whose core fragments have not been introduced into resonant orbits during the last 10 m.y. Some of these basaltic surface regions have been destroyed by impacts, but modeling calculations [e.g., 9] indicate that roughly half the initial set of bodies with D > 40 km are still present today. Thus it seems improbable that Vesta is the only large asteroid inside 2.6 AU that had basalt on its surface and that has surviving basaltic materials capable of providing meteorites to the Earth.

Binzel and Xu [8] discovered that a sizable fraction of the small asteroids in the Vesta dynamic family have spectra that are similar to basalts or orthopyroxenites. These small (4 < D < 10 km) "vestoids" occupy orbits having semimajor axes extending from 2.31 to 2.47 AU. Because the 2.47 AU is close to the 2.50 AU resonance,

an appreciable fraction of the impact ejecta from such an asteroid could enter this resonance and evolve into Earth-crossing orbits; however, the relative contribution to the terrestrial meteoroid flux would be small.

The common interpretation of the Binzel-Xu observations is that the vestoids are fragments spalled off Vesta's crust. Farinella et al. [10] were so convinced of this that they altered the standard equations of impact mechanics to increase by a large factor the fraction of high-velocity ejecta from cratering events, and removed the constraint that the higher the velocity, the smaller the size of the ejecta.

In fact, the observations of Vickery (1986, 1987) of secondary craters on the Moon and other airless bodies show that there is a strong negative relationship between ejecta size and velocity, and that the ejection velocities of fragments with diameters of ≥3 km do not exceed 600 m s^{-1}. Note that these are direct observations against which the equations of impact mechanics must be calibrated. They will not be changed by future revisions in somebody's hydrocode.

There is an alternative to denying the validity of past studies of impact mechanics. The vestoids may have formed in an oblique impact, and thus largely consist of fragments of the projectile. Their basaltic or orthopyroxenitic surfaces can then be explained in either of two ways: (1) The projectile was a differentiated asteroid; or (2) the impact generated an enormous cloud of dust, and some of the projectile fragments became coated with this dust while still near Vesta.

In summary, because low-Ca pyroxene is the dominant absorber in OC and HED, it is probable that space weathering of the basaltic asteroids converts their reflection spectra to S-type spectra. Because all the large OC asteroids have been space weathered, it follows that nearly all basaltic asteroids have also been space weathered. Iron-meteorite data show that many asteroids were differentiated; most probably had basaltic surfaces immediately after differentiation. A sizable fraction of these bodies were fragmented to produce iron meteorites, but many intact basalt-containing bodies should remain. It is likely that a number of these survive with degraded spectra and that one is the source of the HED meteorites.

References: [1] Wasson J. T. (1996) *Icarus*, rejected. [2] Chapman C. R. (1996) *Meteoritics & Planet. Sci.*, in press. [3] Wetherill G. W. and Chapman C. R. (1988) in *Meteorites and the Early Solar System* (J. F. Kerridge and M. S. Matthews, eds.), pp. 35–70, Univ. of Arizona, Tucson. [4] Pieters C. M. and Binzel R. P. (1994) *LPS XXV*, pp. 1083–1084. [5] Wasson J. T. et al. (1996) *LPS XXVII*, pp. 1387–1388. [6] McCord T. B. et al. (1970) *Science, 168*, 1445–1447. [7] Wasson J. T. and Wetherill G. W. (1979) in *Asteroids* (T. Gehrels, ed.), pp. 926–974, Univ. of Arizona, Tucson. [8] Binzel R. P. and Xu S. (1993) *Science, 260*, 186–191. [9] Davis D. R. et al. (1979) in *Asteroids* (T. Gehrels, ed.), pp. 528–557, Univ. of Arizona, Tucson. [10] Farinella P. et al. (1993) *Icarus, 101*, 174–187.

COSMIC-RAY-EXPOSURE AGES OF DIOGENITES AND THE COLLISIONAL HISTORY OF THE HED PARENT BODY OR BODIES. K. C. Welten[1], L. Lindner[2], K. van der Borg[2], Th. Loeken[3], P. Scherer[3], and L. Schultz[3], [1]Mail Code SN4, NASA Johnson Space Center, Houston TX 77058, USA, [2]Department of Subatomic Physics, Utrecht University, 3508 TA Utrecht, The Netherlands, [3]Max-Planck-Institut für Chemie, P.O. Box 3060, 55020 Mainz, Germany.

Cosmic-ray-exposure ages of meteorites provide information on the collisional history of their parent bodies and the delivery mechanism of meteorites to Earth. The exposure-age distributions of ordinary chondrites show distinct patterns for H, L, and LL types, consistent with their origin on different parent bodies [1]. The exposure-age distributions of howardites, eucrites, and diogenites (HEDs) show a common pattern with major peaks at 22 Ma and 38 Ma [2–4]. This provides additional evidence for a common origin of the HED meteorites, possibly 4 Vesta [5], although orbital dynamics calculations showed that the delivery of meteorites from Vesta to Earth is difficult [6]. However, the discovery of several kilometer-sized Vesta-like asteroids in the region between Vesta and the 3:1 resonance suggested that these seem more likely parent bodies of the HEDs than Vesta itself [7]. This implies that the exposure-age clusters may represent samples of several parent bodies. Therefore, the near-absence of diogenites with ages <20 Ma might be of interest for the composition of these kilometer-sized fragments of Vesta. Here we present cosmic-ray-exposure ages of 20 diogenites, including 9 new meteorites [8]. In addition, we calculate the probability for each peak to occur by chance, assuming a constant production rate of HED fragments.

Our diogenite exposure ages are based on He, Ne, and Ar isotopic compositions in 25 Antarctic and non-Antarctic diogenite samples [8]. We applied shielding corrections for the ^{3}He, ^{21}Ne, and ^{38}Ar production rates based on the cosmogenic $^{22}Ne/^{21}Ne$ ratio and the equations derived for ordinary chondrites [9]. On the basis of chemical analyses (XRF and ICP) we applied corrections for differences in composition [9]. For the ^{38}Ar production rate (P^{38}) in diogenites [8] we used P^{38} (10^{-10} cm^3/g Ma) = 1.63[Ca] + 2.64[K] + 0.32[Ti + Cr + Mn] + 0.083[Fe + Ni], which gives 12–14% lower P^{38} values than used in [3] and results in concordant ^{3}He, ^{21}Ne, and ^{38}Ar exposure ages and an overall precision of 4–5% for most samples.

Ten out of 20 diogenites have exposure ages between 20 and 25 Ma, averaging 23.0 ± 1.4 Ma. Since the width of this peak is comparable to the 10–15% analytical resolution obtained for multiple analyses of St. Severin [10], the 23-Ma peak is consistent with a single event. A cluster of four diogenites with ages between 36 and 45 Ma and a resolution of 18% may hint at a second major event. In order to compare the exposure-age distribution of diogenites with those of eucrites and howardites, we only used eucrite and howardite exposure ages with uncertainties ≤10%. In addition to 18 well-determined ^{81}Kr-Kr ages for eucrites [3,4], this leaves 11 useful ^{21}Ne-^{38}Ar ages for howardites and 10 for eucrites.

Next, we assumed a "continuous" exposure-age distribution based on a constant production of collisional debris (N_0) and mean orbital lifetimes ($\tau 1$) of 10–20 Ma [10], and added a term that accounts for mean "transfer" times ($\tau 2$) of 0–10 Ma before fragments are perturbed into Earth-crossing orbits. This gives the expression for the number of meteorites, N, with exposure age, T, $N(T) = f \times N_0 \times \exp^{-T/\tau 1} \times (1 - \exp^{-T/\tau 2})$, where f is the fraction of fragments that eventually collide with Earth. We fitted this function to the exposure age distribution of all ordinary chondrites [1,10], after omitting 70–90% of the H chondrites with ages between 6 and 9 Ma, since the H-chondrite distribution is strongly dominated by a single event at ~7.5 Ma. We obtained best fits with $\tau 1$ = 16 Ma and $\tau 2$ = 5 Ma. These values give probabilities of 10% and 7% for meteorites to show exposure ages between 20 and 25 Ma and 35 and 45 Ma respectively.

With the use of a random number generator we calculated that the random probability (P) of the 20–25-Ma peak is 0.01% for 20 diogenites and is even 1000× smaller for the overall HED distribution (23 out of 59 cases). The 35–45-Ma peak for diogenites is only significant (P < 5%) if we assume that all cases in the 20–25-Ma peak are produced in one single event and thus excluded from the background population. The 35–45-Ma peak is more significant in the exposure-age distribution of all HEDs: P < 0.5% if we exclude more than 80% of the 20–25-Ma cases. We thus conclude that the 20–25-Ma and 35–45-Ma peaks represent two major impact events on one or two parent bodies.

With the new diogenite results, the fraction of exposure ages below 20 Ma increased to 20 ± 10%, overlapping the range of 36 ± 10% for 11 howardites and 28 eucrites. Two of these diogenite ages coincide with the 12–14-Ma peak of eucrites and one coincides with the 6–7-Ma peak. Although the peaks at 6–7 and 12–14 Ma are not (yet) statistically significant, our results contribute to the growing consensus that most HEDs reaching Earth are produced in several large impact events [3,4].

The near-absence of exposure ages below 8 Ma (7%) may either indicate that the transfer times of HED meteorites into Earth-crossing orbits are longer than for ordinary chondrites or that few recent impacts occurred on the HED parent bodies. If we assume that the HEDs were ejected from the kilometer-sized Vesta fragments very close to the 3:1 resonance [7], then large transfer times seem less likely than the lack of recent impacts. Interestingly enough, a similar deficit of short exposure ages was also observed for LL chondrites [10].

References: [1] Marti K. and Graf Th. (1992) *Annu. Rev. Earth Planet. Sci., 20,* 221–243. [2] Welten K. C. et al. (1993) *Meteoritics, 28,* 459. [3] Eugster O. and Michel Th. (1995) *GCA, 59,* 177–199. [4] Shukolyukov A. and Begemann F. (1996) *Meteoritics & Planet. Sci., 31,* 60–72. [5] Consolmagno G. J. and Drake M. J. (1977) *GCA, 41,* 1271–1282. [6] Wetherill G. (1987) *Philos. Trans. R. Soc. London, A323,* 323–337. [7] Binzel R. P. and Xu S. (1993) *Science, 260,* 186–191. [8] Welten K. C. (1995) Ph.D. thesis, Utrecht University. [9] Eugster O. (1988) *GCA, 52,* 1649–1662. [10] Graf Th. and Marti K. (1994) *Meteoritics, 29,* 643–648.

THE NATURE OF VOLCANIC ERUPTIONS ON 4 VESTA.

L. Wilson[1,2] and K. Keil[1], [1]Hawai'i Institute of Geophysics and Planetology, School of Ocean and Earth Science and Technology, University of Hawai'i, Honolulu HI 96822, USA, [2]Environmental Science Division, Institute of Environmental and Biological Sciences, Lancaster University, Lancaster LA1 4YQ, UK.

Partial melting in asteroid mantles produces basaltic melts that percolate along grain boundaries and collect into veins. Veins of sufficient size, overpressured by volume expansion caused by melting, grow by cracking the rocks at their tips and scavenge melt from intersecting smaller veins. Buoyancy and excess pressure combined allows them to migrate as isolated dikes, cracking open at the upper end while pinching shut at the lower end. The dike sizes depend on the physical and rheological properties of the magmas, the gravitational acceleration, and the country rock elastic properties, especially the apparent fracture toughness, K_f. Small amounts of gas

TABLE 1. Properties of dikes reaching the surface of Vesta for likely apparent fracture toughnesses of crustal rocks.

K_f	P_d	Z	W	U	V/L
150	0.60	31.0	3.7	0.89	3.29
100	0.46	23.6	2.1	0.29	0.61
70	0.36	18.6	1.3	0.11	0.14

K_f is the fracture toughness in MPa $m^{1/2}$; P_d is the driving pressure in MPa holding the dike open; Z is the vertical length of the dike in kilometers; W is its mean thickness in meters; U is the mean rise speed of magma in the dike in m s^{-1}; V/L is the erupted mass flux per unit dike length along strike in m^3 s^{-1} m^{-1}. Values are calculated using a magma density less than that of the surrounding rocks by $\Delta\rho$ = 300 kg m^{-3} and the acceleration due to gravity is g = 0.26 m s^{-2}.

TABLE 2. Sizes (in mm) of the largest magma droplets that can be transported in a steady flow from the magma disruption level as a function of magma gas content, n, in ppm and depth of origin of the magma, Y, in km in a dike 23.7 km high (middle line of Table 1).

	n = 10	n = 30	n = 100	n = 300	n = 1000	n = 3000
Y = 5.9	0.63	0.67	0.77	0.91	4.7	25.0
Y = 11.8	0.62	0.64	0.71	0.82	3.4	19.0
Y = 23.7	0.61	0.62	0.67	0.76	2.2	13.5

TABLE 3. Magma gas contents.

	P_v	u_v	u_∞	u_{30}	u_{100}	u_{300}	u_{1500}	u_{4000}	R	L
n = 30	23.0	6.4	12.5	12.3	12.3	12.2	10.3	!	0.58	1
n = 100	13.8	7.9	20.1	19.6	19.6	19.5	17.6	5.8	1.48	5
n = 300	1.33	12.1	33.9	32.9	32.9	32.8	31.0	19.1	4.18	30
n = 1000	0.23	21.7	61.6	59.9	59.9	59.8	57.9	46.1	13.84	165
n = 3000	0.14	36.7	106.0	103.4	103.4	103.3	101.4	89.6	41.28	830

Values are given for the pressure in the choked flow in the vent, P_v, in kPa; the mean eruption speed in the vent, u_v, in m s^{-1}; the final speed of the expanding gas, u_∞, in m s^{-1}; the launch speeds of droplets with diameters 30, 100, 300, 1500, and 4000 μm, u_{30} to u_{4000}, respectively; the maximum range of the clasts, R, in km; and the size of the zone at the outer edge of the deposit, L, in m, within which droplets can experience cooling. The symbol ! indicates that this droplet size fails to be lifted as far as the surface.

accumulating in dike tips greatly increase K_f over laboratory values. Calculations of sizes and rise speeds of dikes in a Vesta-sized asteroid for a wide range of conditions (Table 1) show that if K_f is too small the magma will cool excessively before the dike can reach the surface. Since eucritic meteorites do appear to be the products of surface eruptions we infer a lower limit for the K_f value controlling the feeder dikes.

As a dike opens to the surface of an asteroid with no atmosphere, an expansion wave propagates down into the magma at a large fraction of the local speed of sound in the fluid and initiates decompression as magmatic gas expands and accelerates magma upward. Expansion of the gas provides the work done against gravity and against wall friction and the magma kinetic energy. Eventually gas bubbles expand to the point where the magma disrupts into a spray of liquid droplets entrained in the gas flow. The sizes of the droplets produced depend on the pressure history of the gas bubbles and range from ~30 μm to ~4 mm. The largest droplets produced at the magma disruption level may not be transported upward by the gas flow. Table 2 shows the largest eruptable sizes as a function of magma gas content and depth of origin in a dike 23.7 km high, corresponding to an apparent fracture toughness of 100 MPa $m^{1/2}$ in Table 1.

Above the magma disruption level the spray of gas and droplets accelerates under a pressure gradient maximizing the mass flux, achieved when the pressure at the vent, P_v, is such that the mean speed of the erupting mixture, u_v, is equal to the local speed of sound, i.e., the flow is choked. Above the vent the gas expands adiabatically and accelerates upward and sideways, becoming supersonic. Within a distance of a few times the dike width the velocity approaches a limit u_∞ at which all the internal energy of the gas is converted to kinetic energy. The gas-droplet spray spreads out to a maximum angle from the vertical determined by the changing local Mach number. Vertical droplet speeds are always less than the gas speed by an amount equal to the droplet terminal velocities, and together the vertical and horizontal droplet speeds determine the height and width of the lava fountain they form. Table 3 gives values for P_v, u_v, and u_∞ for several magma gas contents, n, and also the vertical launch speeds of droplets with diameters ϕ = 30, 100, and 300 μm and 1.5 and 4 mm, and the maximum ranges, R, that they can reach.

Magma droplets cool by radiation after ejection from a vent, but only if they can "see" their surroundings. If the number density of droplets in a fountain is large, only those within a critical distance L of the outer edge can lose heat, the rest reaching the ground at magmatic temperatures to coalesce into a lava pond feeding lava flows. L depends on the erupted volume flux, the mean droplet size, and the launch velocity: Values are given as a function of n in the last column of Table 3. Note that L is $\ll$R: Only a *very* narrow strip around the outer edge of the deposit, representing much less than 1% of the erupted material at low gas contents, survives to form a layer of recognizable pyroclastic droplets; the rest coalesces into lava flows that, by analogy with flows on Earth having the volume fluxes given in Table 1, have lengths from a few kilometers to a few tens of kilometers, widths up to a few kilometers, and thicknesses from 5 to 20 m. These predictions agree well with findings from studies of the HED meteorites: No pyroclastic droplets have yet been identified in searches carried out by A. Yamaguchi (personal communication), but the sizes of plagioclase crystals in eucrites are consistent with their having cooled in lava flows ~10 m thick.

SIGNIFICANCE OF THE MOST METAMORPHOSED EUCRITES.

A. Yamaguchi, G. J. Taylor, and K. Keil, Hawai'i Institute of Geophysics and Planetology, School of Ocean and Earth Science and Technology, University of Hawai'i at Mānoa, Honolulu HI 96822, USA.

Eucrites formed as basaltic lavas that erupted on the surface of an asteroid, presumably 4 Vesta [1]. This volcanic epoch, which consisted of lava flows, fire fountains, and intrusions of narrow dikes [2], lasted only several million years, as shown by the presence of the decay product of short-lived nuclides in eucrites [e.g., 3]. In spite of the production of vast quantities of volcanic products, a striking feature of eucrites is that almost all of them are metamorphosed [e.g., 4,5]. This suggests a metamorphic event of global proportions, perhaps caused by burial as the thick (20 km) crust was constructed by a succession of lava flows [4]. We have been studying the metamorphic record in basaltic eucrites to understand the geologic evolution of the crust of Vesta. We report here our observations on four of the most metamorphosed basaltic eucrites.

Clasts in Millbillillie and RKPA 80205: A detailed description of a fine-grained clast in Millbillillie was given by [6]. The clast has a subophitic texture composed of lathy plagioclase (~600 × 50 μm) and anhedral pyroxene (~700 μm in size). The texture of the RKPA 80205 clast is quite similar to that of the fine-grained clast in Millbillillie, but its mean grain size is somewhat finer (i.e., plagioclase laths ~300 × 50 μm; anhedral to granular pyroxene ~600 μm). Recrystallized mesostasis occurs interstitially between the plagioclase laths, similar to the location of mesostasis in unequilibrated basaltic clasts in Pasamonte. Plagioclases in these clasts show normal chemical zoning. However, pyroxene crystals in both meteorites are well equilibrated and have no remnant Ca zoning. In addition, some pigeonites in the rocks are partly inverted to orthopyroxene in which there are thin (a few micrometers thick) (001) augite lamellae (~10-μm spacing) and very fine ($\ll$1 μm) (100) augite lamellae between them.

EET 90020 and Ibitira: A portion of EET 90020,18 displays a subophitic texture consisting of lath-shaped plagioclase with curved edges (900 × 400 μm) and anhedral pigeonite [7]. Ibitira is a strongly recrystallized, unbrecciated eucrite, but it has a ghostlike igneous (variolitic?) texture [8]. In contrast to the clasts in Millbillillie and RKPA 80205, silica minerals (tridymite) are distributed heterogeneously. In EET 90020 and Ibitira, there are several large elongated laths of tridymites (<780 × 90 μm). We found a large (<1.2 × 3 mm) pyroxene-plagioclase-silica assemblage in which granular to rectangular plagioclases (~60 × 100 μm) are set in a tridymite matrix in EET 90020. The pigeonites in Ibitira and EET 90020 contain homogeneously distributed fine, closely spaced (~5–10 μm) (001) augite lamellae, but they are not inverted to orthopyroxene. The opaque minerals generally occur as large grains (several tens of micrometers in size). In both meteorites, compositional ranges of the plagioclases are very small (EET 90020: An_{87-91}; Ibitira: An_{94-97}), suggesting partial equilibration.

Discussion: The fine-grained igneous textures of the clasts in RKPA 80205 and Millbillillie, distributions of the (recrystallized) mesostasis areas, and the chemical zoning trends in the plagioclases are essentially identical to those observed in unequilibrated eucrites, such as basaltic clasts in Pasamonte. Thus, these basalts cooled rapidly from melts (~0.1–1 K/hr [9], although we show elsewhere that textures are not reliable indicators of the cooling

rates of lava flows). The textures show that the clasts are fragments of rock crystallized in thin surface lava flows or small dikes intruded into the shallow crust. Yet, surprisingly, the pyroxenes in these fine-grained basaltic eucrites are equilibrated chemically; furthermore, parts of the pigeonites show inversion textures to orthopyroxene, features generally observed in plutonic rocks. The igneous textures of EET 90020 and Ibitira are not so clear, but careful inspection reveals that the rocks contained lathy plagioclases before recrystallization. In contrast to the clasts in RKPA 80205 and Millbillillie, the mesostasis areas are not well defined but the silica minerals occur as euhedral tridymite crystals that frequently occupy relatively large areas (a few millimeters in size in EET 90020). No such textures are observed in unequilibrated eucrites, implying that the large tridymite crystals formed during metamorphism. However, solid-state processes are probably too slow to form large crystals. Thus, it seems plausible that the low-temperature assemblages (mesostasis) were partially melted during the metamorphism. If so, the peak metamorphic temperatures exceeded or were close to the melting temperature of eucrites (~1060°C). Such silica-rich partial melts would have had very high viscosities, which would have prevented melt segregation from these areas.

Pigeonites record subsolidus thermal histories. The mechanisms of the exsolution and inversion of pigeonites in eucrites have been described in detail [10]. If primary pigeonites of basaltic eucrites cooled very slowly in the subsolidus, they would transform into orthopyroxene in a complex way, resulting in Stillwater-type pyroxene [10]. Pigeonites in the clasts in RKPA 80205 and Millbillillie are partially inverted to orthopyroxene, as are those observed in the Moore County cumulate eucrites. Compared to Moore County, the inverted pigeonites in the basaltic eucrites have much more closely spaced and finer (001) lamellae. However, this may not have been caused simply by differences in the cooling rates. For example, bulk Mg/(Mg + Fe) of the pyroxene in Moore County is higher; the inversion and exsolution phenomena of pyroxenes in this cumulate eucrite may thus have taken place at a higher temperature [10] with consequent faster diffusion, so exsolution and inversion might have occurred more effectively. The cooling rates of some eucrites might therefore have been similar to those of cumulate eucrites. This implies that eucrites like Millbillillie were buried at similar depths in the hot crust as were cumulate eucrites.

EET 90020 and Ibitira pyroxenes, on the other hand, are not inverted to orthopyroxene, even though these eucrites experienced high peak metamorphic temperatures (~1060°C) that were higher than those in Millbillillie and RKPA 80205. One possible explanation is that they were excavated by impact during slow cooling before the inversion from piegeonite to orthopyroxene, as proposed by [11] for the Moore County cumulate eucrite. Considering this high temperature, they must have been located quite deep in the crust, perhaps near its center to base ~10–25 km beneath the surface. This implies that an early, very large impact occurred to quench the rocks and, at least in the case of Ibitira, preserve its old age of 4.495 Ga [12].

Many eucrites cooled very slowly in the subsolidus, implying that they resided in hot environments, yet they formed initially by rapid cooling in lava flows. Other eucrites seem to have experienced metamorphic temperatures so hot that they partially melted. What geological history led to the extensive metamorphism of a series of lava flows? The rocks are extensively brecciated and shocked as well, so one might argue that the metamorphism could have been caused by impact heating. However, the metamorphism is ubiquitous among eucrites and it lasted thousands to millions of years, implying that the metamorphism was very widespread, probably affecting the entire crust of Vesta. Such global metamorphism is impossible to achieve by impact processes [13]. In fact, if anything, impacts probably cooled the crust by excavating hot rocks buried at depth. The most likely source of the heat for metamorphism is simple burial of a succession of lava flows as the crust grew by volcanism and intrusions. Heat diffusing from the hot interior caused the temperature to rise in the crust, leading to widespread metamorphism [4].

References: [1] Binzel R. P. and Xu S. (1993) *Science, 260*, 186–191. [2] Wilson L. and Keil K. (1996) *JGR Planets*, in press. [3] Shukolyukov A. and Lugmair G. W. (1993) *Science, 259*, 1138–1141. [4] Yamaguchi A. et al. (1996) *Icarus*, submitted. [5] Takeda H. and Graham A. L. (1991) *Meteoritics, 26*, 129. [6] Yamaguchi A. et al. (1994) *Meteoritics, 29*, 237. [7] Yamaguchi A. et al. (1996) *LPS XXVII*, pp. 1469–1470. [8] Steele I. M. and Smith J. V. (1976) *EPSL, 33*, 67–78. [9] Walker D. et al. (1978) *Proc. LPSC 9th*, pp. 1369–1391. [10] Ishii T. and Takeda H. (1974) *Mem. Geol. Soc. Japan, 11*, 47–36. [11] Miyamoto M. and Takeda H. (1994) *EPSL, 122*, 343–349. [12] Bogard D. D. and Garrison D. H. (1995) *GCA, 59*, 4317–4322. [13] Keil K. et al. (1996) *Meteoritics & Planet. Sci.*, submitted.

COOLING RATES OF DIOGENITES: A STUDY OF Fe^{2+}-Mg ORDERING IN ORTHOPYROXENE BY X-RAY SINGLE-CRYSTAL DIFFRACTION.

M. Zema[1], M. C. Domeneghetti[2], G. Molin[3], and V. Tazzoli[1], [1]Dipartimento di Scienze della Terra, Università di Pavia, 27100 Pavia, Italy, [2]CNR, C.S. Cristallochimica e Cristallografia, 27100 Pavia, Italy, [3]Dipartimento di Mineralogia e Petrologia, Università di Padova, 35100 Padova, Italy.

Diogenites are either breccias [1] or recrystallized breccias [2] consisting almost entirely of orthopyroxene, sometimes with minor olivine and chromite and traces of silica, plagioclase, troilite, metal, and phosphates [3]. A remarkable feature is the very homogeneous major-element composition of diogenite orthopyroxenes (~Wo_2 $En_{74}Fs_{24}$) [4,5]. Diogenites, together with howardites and eucrites, are assumed to come from a single parent body (HED), probably asteroid 4 Vesta [6,7], that consists of a diogenitic mantle and an eucritic crust whose thickness has been estimated to be not less than 10 km [8].

The purpose of this work was to use single-crystal X-ray diffraction (XRD) and kinetic analysis of Fe^{2+}-Mg ordering in orthopyroxene to obtain additional information on the thermal history of the HED parent body. The ordering of Fe^{2+} and Mg between the two crystallographic M1 and M2 sites is temperature, time, and composition dependent and provides a means of determining cooling rates.

Several orthopyroxene single-crystals from seven different diogenites, PCA 91077, LAP 91900, LEW 88008, ALHA 77256, Shalka, Roda, and Johnstown, were selected for XRD. Structure refinements were carried out in space group Pbca. For some crystals from Johnstown, Roda, PCA 91077, and LAP 91900 samples, the presence of reflections 0kl with $k = 2n + 1$, in violation of the systematic absence for the b-glide plane in the Pbca space group, was observed. For these crystals the structure refinement procedure

TABLE 1. Closure temperatures and cooling rates.

Sample	K_D	T_c(°C)	Cooling Rate (°C/y) at $T = T_c$
OPX LAP 91900 N.1	0.0204(35)	344 ± 20	0.01
OPX LAP 91900 N.3	0.0252(44)	350 ± 25	0.01
OPX PCA 91077 N.2	0.0259(42)	355 ± 23	0.02
OPX PCA 91077 N.11	0.0296(45)	375 ± 22	0.08
OPX LEW 88088 N.9	0.0317(43)	373 ± 22	0.22
OPX LEW 88088 N.11	0.0317(43)	385 ± 22	0.17
OPX ALHA 77256 N.12	0.0283(35)	368 ± 19	0.05
OPX Roda N.2	0.0353(27)	403 ± 13	0.58
OPX Roda N.3	0.0362(22)	408 ± 10	0.82
OPX Shalka N.7	0.0293(24)	374 ± 13	0.07
OPX Shalka N.8	0.0283(28)	368 ± 15	0.05
OPX Johnstown N.11	0.0260(39)	355 ± 22	0.02
OPX Johnstown N.15	0.0297(33)	375 ± 17	0.08
OPX Johnstown N.16	0.0265(42)	358 ± 23	0.02

of Domeneghetti et al. [9] for a Pbca phase coexisting with a C2/c exsolved phase was adopted. This allowed us to determine the fraction of the exsolved phase (1%) and obtain a more correct determination of M1 and M2 site populations. The final discrepancy indexes R_{obs} ranged between 1.24% and 2.78%. Microprobe analysis was carried out in WDS mode on the same crystals used for XRD. The mean orthopyroxene composition was $Wo_2En_{74}Fs_{24}$, which is in perfect agreement with Mittlefehldt's data [4]. For each crystal, cation distribution coefficient K_D ($K_D = [X_{Fe}^{M1}(1 - X_{Fe}^{M2})]/[X_{Fe}^{M2}(1 - X_{Fe}^{M1})]$) was calculated. The Fe^{2+}-Mg ordering closure temperatures, determined by the equation $\ln K_D = -2739.5/T(K) + 0.7048$ [10], ranged from 344° ± 20°C in LAP 91900 to 408° ± 10°C in Roda. The range of closure temperatures defined by diogenites also includes the cumulite eucrite Serra de Magé (398° ± 9°C) [9], suggesting a common origin. Higher closure temperatures were measured, using the same method, for achondrites from the A-L parent body. In particular, closure temperatures measured for Acapulco and ALHA 81261 acapulcoites [11] and for FRO 90011 [12] and Gibson [13] lodranites ranged between 465° ± 43° and 530° ± 20°C. The lowest closure temperatures are exhibited by the orthopyroxenes from a silicate inclusion of Landes IAB iron meteorite (195°C, Stimpfl and Molin, personal communication) and from Estherville and Bondoc mesosiderites (~250°C) [14].

Cooling time constants η ($K^{-1}t^{-1}$) were calculated using the numerical method developed by Ganguly [15] on the basis of Mueller's theoretical model [16,17]. An asymptotic cooling law $1/T = 1/T_O + \eta t$ and the disordering rate constant from Ganguly and Tazzoli [18] were adopted with O fugacity $f_{O_2} = 10^{-32}$, as defined by the WI buffer for highly reducing conditions. As reported in Table 1, for six of the seven diogenites the cooling rates ranged between 0.01° and 0.22°C/yr, while the Roda orthopyroxene crystals showed slightly faster cooling rates (0.58° and 0.82°C/yr, near their T_c), close to the value of 0.74°C/yr calculated for the Serra de Magé cumulite eucrite [9].

References: [1] Mason B. (1963) *Am. Museum Novit. 2155.* [2] Takeda H. et al. (1981) *Mem. NIPR, Spec. Issue 20,* 81–99. [3] Berkley J. L. and Boynton N. J. (1992) *Meteoritics, 27,* 387–394. [4] Mittlefehldt D. W. (1994) *GCA, 58,* 1537–1552. [5] Fredriksson K. et al. (1976) *Meteoritics, 11,* 278–280. [6] McCord T. B. et al. (1970) *Science, 168,* 1445–1447. [7] Chapman C. R. (1976) *GCA, 40,* 701–719. [8] Binzel R. P. and Xu S. (1993) *Science, 260,* 186–191. [9] Domeneghetti M. C. et al. (1996) *Am. Mineral., 81,* 842–846. [10] Ganguly J. and Domeneghetti M. C. (1996) *Contrib. Mineral. Petrol., 122,* 359–367. [11] Zema M. et al., *EPSL,* submitted. [12] Molin G. M. et al. (1994) *EPSL, 128,* 479–487. [13] Zema M. et al. (1996) *Meteoritics & Planet. Sci., 31,* in press. [14] Ganguly J. et al. (1994) *GCA, 58,* 2711–2723. [15] Ganguly J. (1982) in *Advanced Physical Geochemistry, Vol. 2* (S. K. Saxena, ed.), pp. 58–99, Springer. [16] Mueller R. F. (1967) *J. Phys. Chem. Solids, 28,* 2239–2243. [17] Mueller R. F. (1969) *MSA, Spec. Paper 2,* 83–93. [18] Ganguly J. and Tazzoli V. (1994) *Am. Mineral., 79,* 930–937.

CARBONACEOUS CHONDRITE CLASTS IN HED ACHONDRITES.

M. E. Zolensky[1], M. K. Weisberg[2], P. C. Buchanan[3], and D. W. Mittlefehldt[4], [1]Mail Code SN2, NASA Johnson Space Center, Houston TX 77058, USA, [2]Department of Earth and Planetary Sciences, American Museum of Natural History, New York NY 10024, USA, [3]Department of Geology, University of Witwatersrand, Johannesburg, South Africa, [4]Lockheed Martin, 2400 NASA Road 1, Houston TX 77058, USA.

Introduction: Since carbonaceous chondrite planetesimals are attractive candidates for the progenitors of HED asteroid(s) [1–3], we have performed a survey of HED meteorites in order to locate and characterize the mineralogy, chemistry, and petrography of the oft-reported carbonaceous chondrite clasts by microprobe, SEM-EDX, and TEM techniques. We examined samples of all HEDs we could lay our gloved hands on, and found carbonaceous chondrite clasts in the howardites Kapoeta, Jodzie, EET 87513, Y 793497, LEW 85441, LEW 87015, and G'Day, the polymict eucrites LEW 87295 and LEW 85300, and the diogenite Ellemeet. We verified previous suggestions that the majority (~80%) of these clasts are CM2 material, but we discovered that a significant proportion are CR2 (~20%) and other rare types are present. We conclude that chondritic compounds of mixed CM2 and CR2 materials should be investigated in future geochemical modeling of the origin of the HED asteroid(s).

CM2 Clasts: The CM2 clasts, found in all investigated HED meteorites *that contained clasts*, were matrix-supported mixtures of olivine-pyroxene-phyllosilicate-sulfide-bearing aggregates, loose olivines and pyroxenes, sulfides, carbonates, and sinuous spinel-phyllosilicate-diopside CAIs. Magnetite and metal are rare. Some aggregates have fine-grained rims of material resembling matrix. The opaque, fine-grained matrix consists predominantly of serpentine of extremely variable composition and sulfides; tochilinite is occasionally present. The trace-element data for one Jodzie clast from this study, and the average of similar clasts from Kapoeta, support a classification as CM: Volatiles are depleted relative to CI and enriched relative to CR.

CR2 Clasts: The CR2 clasts are found (in small numbers) in four of the investigated howardites: Bholghati, Jodzie, Kapoeta, and Y 793497. Petrographically, they are matrix-supported mixtures of olivine aggregates (sometimes containing sulfides), loose olivines, pyrrhotite, pentlandite, low-Ca pyroxene (minor), hedenbergite (rare), kamacite (rare and only found within olivine), Ca carbonates, and abundant magnetite framboids and plaquets.

Phyllosilicates are fine grained and largely confined to matrix; they are mixtures of serpentine and saponite. The matrix of CR2 clasts also contains pyrrhotite, pentlandite, chromite, and a significant fraction of poorly crystalline material with the same bulk composition as matrix phyllosilicate.

Other Clast Types: Other clasts types are rare, and are well described by Zolensky et al. [4].

Heating of Clasts: There is evidence of heating in a substantial number of clasts, both CM2 and CR2, including (1) corrugated serpentine flakes, (2) pseudomorphs of anhydrous ferromagnesian material after flaky phyllosilicates, and (3) hedenbergite rim calcite. While the timing of the hedenbergite rims is debatable, the destruction of phyllosilicates clearly occurred at a late stage, plausibly during impact onto the HED asteroid(s), and required peak-heating temperatures on the order of 400°C.

Discussion: CM2 material was apparently the most common carbonaceous chondrite lithology encountering the HED asteroids, as it is for the Earth today. This result is consistent with those from previous mineralogical studies [5–14] as well as published siderophile- and volatile-element data [15]. The ratio of CR/CM clasts in HEDs is essentially the same as for modern falls at Earth. This may indicate that the ratio of disaggregated CM2 to CR2 asteroidal material has been approximately constant through the history of the solar system.

At the time of carbonaceous chondrite incorporation into the HED asteroid(s) the CM2 and CR2 lithology-carrying asteroids might have been in near proximity to the HED asteroid(s), with orbits that crossed one another, but at the very least debris from the carbonaceous asteroids had to cross the orbit of the HED asteroid(s). Various scenarios that satisfy this condition can be imagined as follows: (1) The CM2 and CR2 parent asteroids were feeding material to the HEDs before the disruption of the other carbonaceous chondrite parent bodies. Therefore only the CM2 and CR2 lithologies made major contributions to the HED asteroid(s). (2) The carbonaceous chondrite parent bodies were all disrupted at approximately the same time, but only the CM2 and CR2 materials were placed into HED-crossing orbital pathways. (3) CM2 and CR2 lithologies were located on the outside of carbonaceous chondrite parent bodies (lying stratigraphically above the other carbonaceous chondrite lithologies), were stripped off earlier by impact erosion, and were therefore preferentially available for incorporation into the HED asteroid(s). Our results are compatible with type 2 carbonaceous chondrites being equivalent to or from the same source as the material that originally accreted to form the HED asteroid(s). We therefore suggest that models of *mixed* CM2 and CR2 materials (rather than merely CM2 or CV3) should be investigated in future geochemical modeling of the origin of the HED asteroid(s).

Acknowledgments: We thank A. Pun, H. McSween, L. Browning, F. Hörz, D. Bogard, G. Wetherill, J. Jones, G. Ryder, G. MacPherson, A. Krot, G. Kurat, and P. Warren for critical discussions and/or information. Samples were contributed by E. King, T. Bunch, I. Casanova, G. MacPherson, L. Schramm, M. Prinz, K. Yanai, H. Kojima, the Meteorite Working Group, and J. Wood. This research was supported by NASA through the Planetary Materials and Geochemistry and Origins of Solar Systems Programs (both to M.E.Z.).

References: [1] Stolper (1977) *GCA, 41*, 587–611. [2] Jurewicz et al. (1993) *GCA, 57*, 2123–2139. [3] Boesenberg and Delaney (1994) *Meteoritics, 29*, 445–446. [4] Zolensky et al. (1996) *Meteoritics & Planet. Sci., 31*, in press. [5] Wilkening (1973) *GCA, 37*, 1985–1989. [6] Pun (1992) Unpublished Masters thesis, Univ. of New Mexico, Albuquerque, 171 pp. [7] Brearley (1993) *LPS XXIV*, pp. 183–184. [8] Buchanan et al. (1993) *Meteoritics, 28*, 659–669. [9] Smith (1982) Unpublished Ph.D. dissertation, Univ. of Oregon, 193 pp. [10] Pedroni (1989) Unpublished Ph.D. dissertation, Eidgenoessischen Technischen Hochschule Zuerick. [11] Bunch (1975) *Proc. LSC 6th*, pp. 469–492. [12] Kozul and Hewins (1988) *LPS XIX*, pp. 647–648 [13] Hewins and Klein (1978) *Proc. LPSC 9th*, pp. 1137–1156. [14] Labotka and Papike (1980) *Proc. LPSC 11th*, pp. 1103–1130. [15] Chou et al. (1976) *Proc. LSC 7th*, pp. 3501–3518.

End of Document